USZ Universitäts Spital Zürich

Jubiläums-veranstaltung

Sonderprogramm

20th Day of Clinical Research

# COVID 19-Symposium – Klinik und Forschung am USZ

Donnerstag, 15. April 2021, 8.00 – 14.45 Uhr
Online-Veranstaltung

**Wir wissen weiter.**

# COVID 19-Symposium – Klinik und Forschung am USZ

**08.00 Uhr** **Begrüssung durch den Vorsitzenden der Spitaldirektion**
Gregor Zünd, Prof. Dr. med.

**08.05 Uhr** **1. COVID-19 Block: Einweisung mit Corona Infektion**
Moderation Philipp Bosshard, PD Dr. sc. nat.

Einführung durch Prof. Dr. med. Gabriela Senti, Direktorin Forschung und Lehre und Prof. Dr. med. Annelies Zinkernagel (Programmleitung)

**08.10 Uhr** **Aus der Notfallstation: Diagnostik, Abklärung und Entwicklung**
Ksenija Slankamenac, PD Dr. med.

**08.20 Uhr** **Aus der Infektologie: Klinik, Verlauf, Therapie**
Dominique Braun, PD Dr. med.

**08.30 Uhr** **Aus der Diagnostik: Serologie, PCR, Varianten, Klinik**
Irene Abela, Dr. med. Dr. sc. nat.

**08.40 Uhr** **Aus der Forschung Diagnostik – Serotracking**
Marc Emmenegger, Dr. sc. nat.

**08.50 Uhr** **Diskussion mit Fragen aus dem Chat durch den Moderator**

**09.20 Uhr** **2. COVID-19 Block: Verlauf im Spital**
Moderation Mira Katan Kahles, PD Dr. med.

Einführung durch Prof. Dr. med. Gabriela Senti, Direktorin Forschung und Lehre und Prof. Dr. med. Annelies Zinkernagel (Programmleitung)

**09.25 Uhr** **Aus der Intensivstation: ICU Registry und Prognose**
Matthias Hilty, PD Dr. med.

**09.35 Uhr** **Aus der Intensivstation: Lungenprotektive Beatmung**
Philipp Bühler, Dr. med.

**09.45 Uhr** **Radiologische Diagnostik: Bedeutung der Bildgebung**
Thomas Frauenfelder, Prof. Dr. med.

**09.55 Uhr** **Komplikationen, Superinfektionen und Resistenzen**
Silvio Brugger, Dr. med.

**10.05 Uhr** **Diskussion mit Fragen aus dem Chat durch die Moderatorin**

**10.35 Uhr** **3. COVID-19 Block: Interdisziplinäre Herausforderung**
Moderation Silvia Ulrich, Prof. Dr. med.

Einführung durch Prof. Dr. med. Gabriela Senti, Direktorin Forschung und Lehre und Prof. Dr. med. Annelies Zinkernagel (Programmleitung)

**10.40 Uhr** **Pneumo COVID**
Christian Clarenbach, PD Dr. med.

**10.50 Uhr** **Cardio COVID**
Andreas Flammer, Prof. Dr. med.

**11.00 Uhr** **Neuro COVID**
Ilijas Jelcic, Dr. med.

**11.10 Uhr** **Angio COVID**
Stefano Barco, Dr.

**11.20 Uhr** **Patho COVID**
Zsuzsanna Varga, Prof. Dr. med.

**11.30 Uhr** **Diskussion mit Fragen aus dem Chat durch die Moderatorin**

**12.00 Uhr** **Pause**

**12.35 Uhr** **4. COVID-19 Block: Wie geht es weiter nach dem Austritt?**
Moderation Johannes Nemeth, Dr. med. univ.

Einführung durch Prof. Dr. med. Gabriela Senti, Direktorin Forschung und Lehre und Prof. Dr. med. Annelies Zinkernagel (Programmleitung)

**12.40 Uhr** **Impfungen: Klinik Impfung und Produkte**
Barbara Hasse, PD Dr. med.

**12.50 Uhr** **mRNA Impfstoff-Forschung am USZ**
Steve Pascolo, PD Dr. med.

**13.00 Uhr** **Spitalhygiene: Was hat sich nach COVID verändert?**
Walter Zingg, PD Dr. med.

**13.10 Uhr** **Für Long-Covid Kräfte bündeln mit Philanthropie**
Corinna Adler, USZ Foundation

**13.20 Uhr** **Diskussion mit Fragen aus dem Chat durch den Moderator**

**13.50 Uhr** **5. Block: Preisverleihung des Day of Clinical Research**
Moderation Gabriela Senti, Prof. Dr. med., Direktorin Forschung und Lehre und Rainer Weber, Prof. Dr. med., Dekan der Medizinischen Fakultät

**14.00 Uhr** Kardiologie-Preis: Yustina Maria Puspitasari, M.D., M.Sc.
**14.10 Uhr** Onkologie-Preis: Chiara F. Magnani, PhD
**14.20 Uhr** Neurologie-Preis: Lena Hänsch, PhD student
**14.30 Uhr** Immunologie-Preis: Zuzanna Kotkowska, PhD student

**14.40 Uhr** Verabschiedung und Ende der Veranstaltung

## Committee Day of Clinical Research

Aguzzi Adriano, Prof. Dr.
Cinelli Paolo, PD Dr.
Distler Oliver, Prof. Dr.
Katan Kahles Mira, PD Dr.
Moch Holger, Prof. Dr.
Schneider Robin, MBA
Senti Gabriela, Prof. Dr.
Speck Roberto, Prof. Dr.
von Eckardstein Arnold, Prof. Dr.
Weller Michael, Prof. Dr.
Zinkernagel Annelies, Prof. Dr.

## Table of contents



**Cover Figure**: Collage - Participants of the 20th Day of Clinical Research

## Cardiovascular / Metabolism / Endocrinology

### Basic Research

**232**
S. Ambrosini, F. Montecucco, D. Pedicino, A. Akhmedov, S. Mohammed, G. Liuzzo, A. Beltrami, F. Crea, T. Lüscher, S. Costantino, F. Paneni
The methyltransferase SETD7 drives myocardial ischemic injury by modulating the Hippo pathway: a study in mice and humans

**238**
S. Saeedi Saravi, N. Bonetti, A. Vukolic, L. Liberale, T. Lüscher, G. Camici, J. Beer
Dietary omega-3 fatty acid reverses age-linked heart failure with preserved ejection fraction

**241**
C. Diaz-Canestro, Y. Puspitasari, L. Liberale, T. Guzik, A. Flammer, N. Bonetti, P. Wüst, S. Constantino, F. Paneni, A. Akhmedov, JH. Beer, F. Ruschitzka, M. Hermann, TF. Lüscher, I. Sudano, G. Camici
Therapeutic MMP-2 knockdown blunts age-dependent carotid stiffness by decreasing elastin degradation and augmenting eNOS activation

**259**
L. Liberale, A. Akhmedov, Y. Puspitasari, A. Vukolic, F. Montecucco, J. Beer, T. Luscher, J. Jin, G. Camici
JCAD enhances arterial thrombosis by regulating endothelial plasminogen activator inhibitor-1 and tissue factor expression

**270**
I. Martinez Lopez, M. Kirschner, F. Schläpfer, V. Orlowski, S. Ulrich, I. Opitz
Establishment of in vitro models for the study of chronic thromboembolic pulmonary hypertension

### Clinical Trials

**221**
B. Kovacs, S. Winnik, A. Medeiros-Domingo, S. Costa, G. Fu, S. Biskup, F. Ruschitzka, A. Flammer, F. Tanner, F. Duru, A. Saguner
Novel Heterozygous TRPM4 Variant in a Family with Cardiomyopathy, Conduction Disorders and Sudden Cardiac Death

**223**
B. Kovacs, U. Graf, I. Magyar, L. Baehr, A. Maspoli, F. Duru, W. Berger, A. Saguner
Two novel variants in the SLC4A3 gene in two families with Short QT Syndrome: the role of cascade screening

**224**
S. Barco
Age-sex specific pulmonary embolism-related mortality in the USA and Canada, 2000-18: an analysis of the WHO Mortality Database and of the CDC Multiple Cause of Death database

**248**
K. Slankamenac, F. Mathis, DI. Keller
Gender-specific differences in hypertensive crisis and the need for hospitalization

## Hematology / Oncology

### Basic Research

**225**
M. Raeber, R. Rosalia, D. Schmid, U. Karakus, O. Boyman
Interleukin-2 signals converge in a lymphoid–dendritic cell pathway that promotes anticancer immunity

**239**
R. Werner, M. Kirschner, I. Opitz
Establishment and validation of primary non-small cell lung cancer organoids as in vitro lung cancer models

**243**
L. Volta, R. Myburgh, C. Catalano, C. Pellegrino, J. Müller, C.M. Wilk, D. Neri, M.G. Manz
Universal on-off switchable anti-FITC CAR T-Cells for Tumor Therapy

**246**
A. Kraft, M. Meerang, M. Kirschner, V. Boeva, I. Opitz
Screening for extracellular vesicle-derived biomarkers for early detection of malignant pleural mesothelioma

**249**
A. Fischer, S. Hiltbrunner, L. Bankel, C. Britschgi, M. Rechsteiner, J. Rüschoff, E. Rushing, A. Laure, S. Kasser, A. Curioni-Fontecedro
Targeted treatments should be offered to patients with advanced non-small cell lung cancer harboring MET aberrations, despite abundance of co-mutations.

**250**
L. Bankel, R. Wegmann, K. Dedes, D. Franzen, K. Bode, H. Moch, M. Manz, C. Britschgi, B. Snijder
Early results of a single-cell ex vivo drug response testing platform on fluid samples from patients with solid tumors

**251**
C. Magnani, R. Myburgh, N. Russkamp, S. Pascolo, A. Müller, D. Neri, M. Manz
anti-CD117 CAR T cells demonstrate potent anti-leukemic activity against acute myeloid leukemia and ablate human normal hemopoiesis in vivo

**253**
M. Meerang, J. Kreienbühl, V. Orlowski, S. Müller, M. Kirschner, I. Opitz
Importance of Cullin4 Ubiquitin Ligase in Malignant Pleural Mesothelioma

**254**
S. Fazio, S. Isringhausen, M. Chambovey, B. Ludewig, C. Nombela-Arrieta
Unraveling the role of a novel subtype of bone marrow mesenchymal stromal cell in healthy and pathological hematopoiesis

**256**
J. Jang, M. Haberecker, A. Curioni-Fontecedro, A. Soltermann, I. Gil-Bazo, F. Janker, I. Hwang, K. Kwon, W. Weder, W. Jungraithmayr
CD26/DPP4 - a novel prognostic marker for lung adenocarcinoma

**258**
Y. Zhang, F. Schläpfer, V. Orlowski, I. Opitz, M. Kirschner
Evaluating the role of microRNAs in chemotherapy response of malignant pleural mesothelioma

**261**
F. Lehner, S. Salemi, C. Millan, C. Kündig, T. Sulser, D. Eberli
Anti-tumor effect of a recombinant protease inhibitor targeting human kallikrein-related peptidase 2 in prostate cancer

**263**
M. Wipplinger, A. Abukar, A. Hariharan, M. Ronner, E. Felley-Bosco
RNA binding motif protein 8a, a novel RNA editing target in mesothelioma

**265**
S. Sun, F. Frontini, W. Qi, A. Hariharan, M. Ronner, M. Wipplinger, C. Blanquart, H. Rehrauer, J. Fonteneau, E. Felley-Bosco1
Endogenous Retrovirus expression activates type-I interferon signaling in an experimental mouse model of mesothelioma development

**272**
S. Salemi, B. Kranzbühler, L. Prause, V. Baumgartner, D. Eberli
Apalutamide and autophagy inhibition in xenograft mouse model of human prostate cancer

**277**
M. Hirt, A. Barukcic, V. Haunerdinger, T. Albert, A. Bosch, M. Hauri-Hohl
Novel Phenotypic and Functional Characterization of CD34-Positive Cells in Steady-State Peripheral Blood

**279**
F. Caiado, L. Kovtonyuk, M. Manz
Contribution of IL-1 Mediated Inflamm-ageing to Clonal Hematopoiesis Progression in Murine Models

**281**
F. Meier-Abt, J. Lu, L. Kunz, B. Collins, P. Xue, M. Gwerder, M. Roiss, J. Hüllein, S. Scheinost, S. Dietrich, W. Huber, R. Aebersold, T. Zenz
The Proteome Landscape of Chronic Lymphocytic Leukemia (CLL)

**287**
H. Lakshminarayanan, D. Rutishauser, S. Pfammatter, P. Schraml, H. Bolck, H. Moch
Liquid biopsy as a tool for disease monitoring in renal cell carcinoma

**289**
C. Pellegrino, N. Favalli, S. Michael, L. Volta, G. Bassi, J. Millul, S. Cazzamalli, M. Matasci, A. Villa, R. Myburgh, M. Manz, D. Neri
Impact of Ligand Size and Conjugation Chemistry on the Performance of Universal Chimeric Antigen Receptor T-Cells for Tumor Killing

**290**
A. Kahraman, T. Karakulak, D. Szklarczyk, C. von Mering
Pathogenic impact of transcript isoform switching in 1209 cancer samples covering 27 cancer types using an isoform-specific interaction network

**291**
L. Isenegger, P. Bode, C. Pauli, U. Camenisch, C. Matter, H. Moch, C. Britschgi
Phenotypic and Functional Validation of an in vitro Candidate Kinase Inhibitor Screen in Clear Cell Sarcoma

**294**
F. Arnold, A. Kahraman, J. Hanimann, M. Nowak, C. Pauli, B. Sobottka-Brillout, T. Karakulak, D. Aguilera, H. Moch, M. Zoche
MTPpilot: An Interactive Software-Tool for NGS Result Analyses for Molecular Tumor Boards

**298**
A. La Greca Saint-Esteven, M. Bogowicz, S. Tanadini-Lang, E. Konukoglu, J. van Timmeren
HPV Prediction in OPC patients by means of Deep Learning

**Clinical Trials**

**234**
O. Verhoek, O. Lauk, I. Opitz, T. Frauenfelder, K. Martini
Sarcopenia, tumor volume and mediastinal fat as outcome predictors in surgically treated malignant pleural mesothelioma.

**240**
T. Thavayogarajah, G. Nair, D. Müller, U. Schanz
Fludarabine pharmacokinetics: a new tool for reduction of conditioning regimen toxicity?

**244**
N. Miglino, R. Dummer, V. Heinzelmann, A. Theocharides, M. Manz, A. Wicki
Tumor Profiler (TuPro): a multi-omics tumor profiling platform to enable molecularly matched therapy prediction beyond genomics

**276**
G. Treichler, D. Akhoundova, S. Höller, M. Rechsteiner, S. Freiberger, M. Zoche, H. Moch, F. Lisy, C. Britschgi, A. Curioni-Fontecedro
An efficient algorithm for molecular testing of advanced lung cancer

**286**
M. Hilbers, F. Dimitriou, P. Lau, G. McArthur, L. Zimmer, K. Kudura, C. Gerard, O. Michielin, M. Levesque, R. Dummer, J. Mangana, P. Cheng
Real-life data for first-line combination immune-checkpoint inhibition and targeted therapy in patients with melanoma brain metastases

**288**
S. Ludwig, L. Schmid, A. Kahraman, M. Rechsteiner, M. Zoche, A. Curioni-Fontecedro, A. Siebenhüner, K. Dedes, M. Kiessling, R. Fritsch, A. Wicki, H. Moch, A. Weber, C. Britschgi
Impact of molecular testing and molecular tumor board decisions on clinical outcome of patients with solid tumors: A single center, retrospective analysis

**292**
F. Dimitriou, R. Staeger, M. Ak, M. Maissen, K. Kudura, MJ. Barysch, M. Levesque, R. Dummer, J. Mangana, PF. Cheng
Frequency, treatment and outcome of immune-related toxicities in patients with immune-checkpoint inhibitors for advanced melanoma: results form an institutional database analysis

## Head Region / Neuroscience

### Basic Research

**247**
L. Hänsch, M. Peipp, R. Myburgh, T. Weiss, F. Vasella, M. Manz, M. Weller, P. Roth
Characterizing CD317 as a novel target for chimeric antigen receptor (CAR) T cell therapy in glioblastoma

**278**
N. Jarzebska, S. Pascolo, M. Tusup
Optimization of RNA-based formulations for targeted cancer therapy

### Clinical Trials

**271**
K. Burelo, M. Sharifshazileh, J. Sarnthein, G. Indiveri
Detecting High-frequency Oscillations in scalp EEG recordings using a Spiking Neural Network

## Infection / Immunity / Inflammation / Systemic Diseases

### Basic Research

**245**
Z. Kotkowska, P. Schineis, I. Kolm, Y. Waeckerle-Men, C. Halin, P. Johansen
Photochemical internalization (PCI): a novel vaccination method for induction of cytotoxic CD8 T-cell responses

**266**
B. Schmid, A. Künstner, A. Fähnrich, E. Bersuch, P. Schmid-Grendelmeier, H. Busch, M. Glatz, P. Bosshard
Characterization of the skin microbiome in patients with atopic dermatitis versus healthy controls

**269**
P. Frey, J. Baer, J. Bergada-Pijuan, C. Lawless, P. Bühler, R. Kouyos, K. Lemon, A. Zinkernagel, S. Brugger
Quantifying variation in bacterial reproductive fitness: a high-throughput method

**273**
T. Schweizer, F. Andreoni, C. Acevedo, E. Marques Maggio, I. Heggli, N. Eberhard, S. Dudli, A. Zinkernagel
Intervertebral disc cells undergo chondroptosis and elicit strong immune response upon Staphylococcus aureus challenge

**274**
T. Schweizer, S. Mairpady Shambat, V. Dengler Haunreiter, C. Mestres, A. Weber, A. Zinkernagel, B. Hasse
Polyester Vascular Graft Material and Risk for Intracavitary Thoracic Vascular Graft Infection

**275**
J. Bär, M. Boumasmoud, S. Mairpady Shambat, C. Vulin, M. Huemer, T. Schweizer, A. Gómez-Meja, N. Eberhard, Y. Achermann, S. Brugger, R. Schüpbach, R. Kouyos, B. Hasse, A. Zinkernagel
Clinical factors affecting within-patient persister levels during Staphylococcus aureus infections

**293**
V. Haunerdinger, M. Maria Domenica, L. Opitz, S. Vavassori, H. Dave, M. Hauri-Hohl
Comprehensive Identification and Quantitation of Human Thymic Epithelial Cells by Flow Cytometry.

### Clinical Trials

**226**
D. Braun, M. Zeeb, B. Hampel, C. Grube, S. Burkhard, H. Kuster, K. Metzner, J. Böni, R. Kouyos, H. Günthard
Sustained viral suppression with dolutegravir monotherapy during 12'212 patient weeks of follow-up in individuals starting combination antiretroviral therapy during primary HIV infection: a randomized, controlled, multi-site, non-inferiority trial

**237**
J. Prinz, I. Waldmann, T. Schmid, B. Mühleisen, R. Zbinden, I. Laurence, Y. Achermann
Photodynamic therapy improves skin antisepsis as a prevention strategy in arthroplasty procedures: A pilot study

## Mixed Topics

### Basic Research

**222**
P. Wolint, N. Näf, S. Schibler, N. Hild, W. Stark, P. Giovanoli, M. Calcagni, J. Buschmann
Suspension of amorphous calcium phosphate nanoparticles impact commitment of human adipose-derived stem cells in vitro

**228**
D. Spiess, V.F. Abegg, A. Chauveau, E. Duong, O. Potterat, M. Hamburger, A.P. Simões-Wüst
Phytomedicines for mental diseases and the placental barrier: an ex vivo study

**229**
D. Schäfle, P. Selchow, B. Borer, M. Meuli, A. Rominski, B. Schulthess, P. Sander
Mycobacterium abscessus Arr confers Rifabutin resistance

**230**
M. Sutter, S. Samodelov, GA. Kullak-Ublick, M. Visentin
Cholesterol recognition and interaction in OCT2 – a tough nut to CRAC (and CARC)

**231**
G. Bortoli, D. Canepa, H. Pape, Y. Neldner, S. Märsmann, E. Casanova, P. Cinelli
Identification of New Markers Characterizing Adipose-Derived Mesenchymal Stromal Cells with Enhanced Osteogenic Potential

**235**
N. Karavasiloglou, E. Michalopoulou, M. Limam, D. Korol, M. Wanner, S. Rohrmann
Net survival of women diagnosed with breast cancers: a population-based study in Switzerland

**236**
N. Alijaj, B. Pavlovic, P. Oechslin, K. Saba, P. Poyet, T. Hermanns, P. Martel, L. Derré, M. Valerio, N. Rupp, D. Eberli, I. Banzola
Novel Urine Biomarkers for the Early Detection of Prostate Cancer

**242**
L. Roth, L. Russo, C. Pauli, E. Breuer, PA. Clavien, A. Gupta, K. Lehmann
The impact of locoregional treatment on the anticancer immune response against peritoneal metastasis from colon cancer

**252**
S. Dudli, I. Heggli, L. Guidici, R. Schüpbach, N. Farshad-Amacker, N. Herger, A. Juengel, M. Betz, J. Spirig, F. Wanivenhaus, N. Ulrich, F. Brunner, M. Farshad, O. Distler
Type III collagen is a hallmark of the fibrotic pathomechanism in Modic type 1 changes and is linked to myofibroblast differentiation

**255**
O. Eichhoff, P. Cheng, N. Yumi, P. Turko, S. Freiberger, C. Stoffel, J. Käsler, R. Dummer, M. Levesque
Establishment of primary melanoma cell cultures with c-Kit mutations enables the development of novel pharmacological treatment options for patients with ALM

**260**
S.L. Samodelov, K. Becker, K. Haldimann, Z. Gai, S.N. Hobbie, M. Visentin, GA. Kullak-Ublick
Reduction of colistin-induced kidney injury by the vitamin-like compound L-carnitine in mice

**262**
A. Hariharan, M. Sculco, M. Ronner, E. Felley-Bosco
Oncogenic effect of RNA editing enzyme Adar2 in mesothelioma

**264**
L. Russo, L. Roth, A. Gupta, K. Lehmann
Improving loco-regional treatment of peritoneal metastasis

**280**
I. Heggli, R. Schüpbach, N. Herger, T.A. Schweizer, N. Farshad-Amacker, M. Betz, J.M. Spirig, F. Wanivenhaus, N. Ulrich, F. Brunner, M. Farshad, O. Distler, S. Dudli
Infectious and autoinflammatory Modic type 1 changes have different pathomechanisms

**282**
S. Mohammed, M. Alberio, K. Gergely, S. Ambrosini, T. Lüscher, S. Costantino, F. Gian Paolo, F. Paneni
The BET protein inhibitor Apabetalone (RVX-208) restores angiogenic response in type 1 and type 2 diabetes by transcriptional regulation of Thrombospondin-1

**284**
J. Barranco Garcia, R. Braun, S. Tanadini-Lang
On the Use of AI-based Diagnosis Tools in Dermatology

**285**
S. Angori, H. Bolck, T. Karakulak, A. Kahraman, K. Mühlbauer, P. Schraml, H. Moch
Addressing the medical need for treatment of patients with papillary Renal Cell Carcinoma (pRCC)

**296**
D. Vuong, M. Bogowicz, J. Unkelbach, S. Hillinger, S. Thierstein, E.I. Eboulet, S. Peters, M. Pless, M. Guckenberger, S. Tanadini-Lang
A new voxel-based approach to study the relation of tumor location and overall survival in locally advanced NSCLC

**299**
H. Gabrys, L. Basler, S. Hogan, M. Pavic, M. Bogowicz, D. Vuong, S. Tanadini-Lang, R. Förster, M. Huellner, R. Dummer, M. Guckenberger, M. Levesque
Radiomics for prediction of metastatic melanoma patient survival after immunotherapy

**Clinical Trials**

**220**
S. Halvachizadeh, L. Gröbli, T. Berk, K. Jensen, C. Hierholzer, H. Bischoff-Ferrari, R. Pfeifer, HC. Pape
The effect of Geriatric Comanagement (GC) on geriatric trauma Patients in a Level 1 Trauma Setting: A comparison of data prior and after the implementation of GC

**283**
J. Prange, D. Mohr-Haralampieva, N. Steinke, N. Hensky, F. Schmid, D. Eberli
Challenging milestones for a phase I clinical trial for incontinence treatment between GMP and GCP

**300**
J. van Timmeren, M. Bogowicz, M. Chamberlain, S. Ehrbar, R. Dal Bello, H. Garcia Schüler, J. Krayenbuehl, L. Wilke, N. Andratschke, M. Guckenberger, S. Tanadini-Lang, P. Balermpas
Adaptive radiotherapy for head and neck cancer – evaluation of volume changes and migration of salivary glands

**220**

S. Halvachizadeh[1, 2], L. Gröbli[2], T. Berk[1], K. Jensen[1], C. Hierholzer[1], H. Bischoff-Ferrari[1, 2], R. Pfeifer[1, 2], HC. Pape[1, 2]

**The effect of Geriatric Comanagement (GC) on geriatric trauma Patients in a Level 1 Trauma Setting: A comparison of data prior and after the implementation of GC**

*University Hospital Zurich[1], University of Zurich[2]*

**Introduction:**
Improvements in life-expectancy are associated with a rise in geriatric trauma patients. These patients require special attention due to their multiple comorbidities and osteoporosis issues. The aim of this study was to assess the impact of the implementation of geriatric comanagement (GC) on the allocation and clinical outcome of geriatric trauma patients.

**Methods:**
This observational cohort study compared the demographic development and the clinical outcome of geriatric trauma patients (aged 70 years and older) prior and after the implementation of GC. Geriatric trauma patients were admitted between 1 January 2010 and 31 December 2010 were stratified to group pre-GC and admissions between 1 January 2018 and 31 December 2018 to Group post-GC. We excluded patients that require end-of-life treatment and patients who died within 24 h due to severe traumatic brain injury. Outcome parameter included demographic changes, medical complexity, measured by American Society of Anaesthesiology Score (ASA) and Charlson Comorbidity Index (CCI) and in-hospital mortality and length of hospitalization.

**Results:**
This study included 626 in Group pre-GC (mean age 80.3 ± 6.7 years) and 841 in Group post-GC (mean age 81.1 ± 7.3 years). Group pre-GC included 244 (39.0%) males, Group post-GC included 361 (42.9%) males. The mean CCI was 4.7 (± 1.8) points in pre-GC and 5.1 (± 2.0) points in post-GC ($p < 0.001$). In Group pre-GC 100 patients (16.0%) were stratified as ASA 1 compared with 47 patients (5.6%) in Group post-GC ($p < 0.001$). Group pre-GC had significantly less patients stratified as ASA 3 or higher (n = 235, 37.5%) compared with Group post-GC (n = 389, 46.3%, $p < 0.001$). Length of stay (LOS) decreased significantly from 10.4 (± 20.3) days in Group pre-GC to 7.9 (±22.9) days in Group post-GC ($p = 0.011$). The 30-day mortality rate was comparable amongst these groups (pre-GC 8.8% vs. post-GC 8.9%).

**Conclusion:**
According to our data, there were improvements associated with the implementation of a geriatric service as follows: Despite a higher CCI and an increased number of patients with higher ASA classifications, there was a similar LOS and the mortality rate remained comparable. The increase in the case numbers exceeded the trend expected by the general trend of ageing. We feel that further study is warranted to assess long term outcome and effects.

**221**

B. Kovacs[3], S. Winnik[3], A. Medeiros-Domingo[5], S. Costa[3], G. Fu[2, 3], S. Biskup[4], F. Ruschitzka[3], A. Flammer[3], F. Tanner[3], F. Duru[1, 3], A. Saguner[3]

**Novel Heterozygous TRPM4 Variant in a Family with Cardiomyopathy, Conduction Disorders and Sudden Cardiac Death**

*Center for Integrative Human Physiology, University of Zurich, Zurich, Switzerland[1], Department of Cardiology, Capital Medical University affiliated Beijing Shijitan Hospital, Beijing, China[2], Department of Cardiology, University Hospital Zurich, Switzerland[3], Praxis für Humangenetik, Tübingen, Germany[4], Swiss DNAlysis, Dubendorf, Switzerland[5]*

**Introduction:**
Transient Receptor Melastatin 4 channel (*TRPM4*) encodes a calcium-activated, non-selective cation channel that mediates membrane potential depolarization of cardiomyocytes. Loss-of-function models were associated with conduction abnormalities and left ventricular dilation. Human gene variants in this gene have been associated with cardiomyopathy and conduction disease. We report a novel pathogenic heterozygous stop variant in *TRPM4* in a family with sudden cardiac death (SCD), conduction disease, and cardiomyopathy.

**Methods:**
We performed clinical and genetic characterization of the family of a 40-year old male patient, who was newly diagnosed with non-ischemic dilated cardiomyopathy with severely reduced left-ventricular ejection fraction and a complete left bundle branch block (LBBB). He had received six cycles of chemotherapy (doxorubicin, bleomycin, vinblastin, dacarbazin) for thoracic Hodgkin lymphoma, with the last cycle given seven months prior to first diagnosis of DCM. A 12-lead ECG prior to initiation of chemotherapy had already shown a complete LBBB indicating pre-existing cardiopathy.

**Results:**
Family history and cardiac and genetic cascade screening of family members over four generations revealed SCD, conduction disease and/or cardiomyopathy associated with a novel heterozygous variant in *TRPM4* (c.448G>T; p.Gly150*) co-segregating with the phenotype in this family suggesting a Mendelian autosomal-dominant inheritance with variable penetrance. Genetic cascade screening detected this variant in our patient as well. In silico analysis of this novel *TRPM4* variant predicted the loss of a neighboring splice site, resulting in aberrant transcript splicing, leading to a truncated protein or nonsense-mediated mRNA-decay. Current guidelines suggest likely pathogenicity (class IV) of this variant. We hypothesize that the presence of this novel *TRPM4* variant may have increased the susceptibility of our patient to aggravate DCM after potentially cardiotoxic chemotherapy.

**Conclusion:**
We identified a novel likely pathogenic heterozygous point variant in *TRPM4* in a patient with DCM and in his family presenting with SCD, cardiac conduction disease, and cardiomyopathy. Co-segregation analysis suggested autosomal-dominant inheritance with a variable penetrance and phenotypic expression. Functional studies are needed to further characterize the pathologic effects of this variant.

**222**

P. Wolint[2], N. Näf[2], S. Schibler[2], N. Hild[1], W. Stark[1], P. Giovanoli[2], M. Calcagni[2], J. Buschmann[2]

**Suspension of amorphous calcium phosphate nanoparticles impact commitment of human adipose-derived stem cells in vitro**

*ETH Zürich[1], Plastic Surgery and Hand Surgery, USZ[2]*

**Introduction:**
Calcium phosphate (Ca3(PO4)2) is a biomaterial that is often used in orthopedic surgery, either in the form of a cement, ceramic or coating of titanium implants. Nanoparticles of calcium phosphate may originate from mechanical abrasion of implant materials as well as through degradation of larger entities. Nanoscopic calcium phosphate has been reported to represent no health risk to the human body because calcium phosphate nanoparticles are easily resorbed and dissolved by macrophages.

During the last two decades, adipose tissue-derived mesenchymal stem cells (ASCs) have been proven attractive for cellular therapy and bone tissue engineering purposes, because they are easily harvested and available in quite high amounts compared to other sources. For in vitro osteogenic differentiation, a phosphate source should be supplied to the medium in order to enable the alkaline phosphatase (ALP) of ASCs to produce Pi ions which take part in mineralization and the formation of hydroxyapatite. Usually, b-glycerophosphate is used for this purpose, however, critical comments about its high and non-physiological concentration (10 mM) as well as the wide fluctuations during differentiation experiments have been risen. Therefore, other phosphate sources have been suggested, such as sodium hydrogen phosphate buffer or polyphosphate. In our study presented here, we tested if amorphous calcium phosphate (aCaP) nanoparticles suspended in basal culture medium DMEM are also able to evoke an osteogenic commitment.

**Methods:**
The aCaP nanoparticles (Ca/P = 1.5) were synthesized by flame spray pyrolysis. Two hundred thousands of human ASCs of three donors (biological replicates n =3) were exposed to either 5 or 50 µg /mL aCaP nanoparticles suspended in DMEM for 1 or 2 weeks, respectively (control: no nanoparticles). Real-time PCR was performed. Primers for CD73, CD90 and CD105 (MSC minimal criteria), for CD31 and CD34 (markers of endothelial cells), for Runx2 and ALP (early osteogenesis), for collagen I (medium osteogenesis) and osteocalcin (late osteogenesis), for PPAR-γ-2 (key transcription factor for adipogenesis) and Sox9 (key transcription factor chondrogenesis) were used.

Free calcium ion and phosphate ion concentrations were assessed for each condition and ion activity products for a series of phosphate phases were calculated and compared to solubility products.

**Results:**
The addition of aCaP nanoparticles to basal culture medium as a suspension enhanced CD73, CD31 and CD34 gene expression of human ASCs, averaged over three donors. Osteogenic marker genes, such as ALP or Runx2, experienced a downregulation. However, if individual responses were examined, a high inter-donor variability was revealed, with ALP and Runx2 enhancements for distinct conditions. Free calcium and phosphate ion concentrations showed an oversaturated status with respect to several calcium phosphate phases, among them hydroxyapatite. This metastable status, however, did not change much over the period of two weeks and for the concentrations of 5 or 50 µg/mL aCaP, respectively.

**Conclusion:**
The suspension of low concentrations of aCaP nanoparticles in normal culture medium (without any further osteogenic supplementation) may be used to tune stem cells towards an angiogenic/osteogenic commitment, which might be interesting in future bone tissue engineering approaches.

**223**

B. Kovacs[2], U. Graf[3], I. Magyar[3], L. Baehr[3], A. Maspoli[3], F. Duru[1, 2], W. Berger[1, 3, 4], A. Saguner[2]

**Two novel variants in the SLC4A3 gene in two families with Short QT Syndrome: the role of cascade screening**

*Center for Integrative Human Physiology, University of Zurich, Zurich, Switzerland[1], Department of Cardiology, University Hospital Zurich, Switzerland[2], Institute of Medical Molecular Genetics, University of Zurich, Switzerland[3], Neuroscience Center Zurich, University and ETH Zurich, Switzerland[4]*

**Introduction:**
Short QT syndrome (SQTS) is a rare, autosomal dominant disease causing sudden cardiac death (SCD). Genetic testing is recommended according to current guidelines. Variants in *KCNQ1*, *KCNH2*, *KCNJ2* and *SLC4A3* genes have been reported in SQTS. We report implications of genetic testing and cascade screening (CS) in two families with phenotypical presentation of SQTS and novel genetic variants of unknown significance.

**Methods:**
We performed a thorough clinical and electrophysiological work-up of the index patients of both families. In addition, genetic screening was conducted. Subsequently, segregation analysis of potentially pathogenic variants was carried out in available relatives.

**Results:**
Index patient 1 presented with a history of recurrent syncope. His ECG showed a shortened QTc of 340ms. Family history was unremarkable. Structural heart disease was excluded by cardiac MRI and coronary angiography. Genetic testing detected a rare heterozygous missense variant in the *KCNH2* gene (p.(Arg328Cys), frequency 0.053%), predicted to be pathogenic according to various prediction algorithms (Polyphen, SIFT, Align GVGD, mutation taster). CS of relatives did not confirm this variant as the causative mutation. Reanalysis of whole-exome sequencing data revealed a novel heterozygous missense variant, p.(Arg370Cys) in the recently identified *SLC4A3* gene. A variant at the same position has previously been associated with SQTS. CS suggested disease association. The second index patient had a SCD at the age of 17. A previously registered ECG showed a shortened QTc of 340ms. Autopsy revealed no structural heart disease. Post-mortem genetic testing revealed variants in the *LDB3*, *MYH7* and a novel heterozygous missense variant, p.(Ser1039Arg) also in the *SLC4A3* gene. Family history was positive for SCD in three 2° relatives. CS again was highly suggestive for disease association of the variant in the *SLC4A3* gene only.

**Conclusion:**
Genetic testing revealed two novel variants in the *SLC4A3* gene, which was recently implicated in the pathogenesis of the SQTS. Predictive bioinformatic algorithms to assess the pathogenicity of missense variants are of limited relevance, but genetic analysis of additional unaffected and affected family members may be instrumental to identify pathogenic DNA sequence variations.

**224**

S. Barco[1]

**Age-sex specific pulmonary embolism-related mortality in the USA and Canada, 2000-18: an analysis of the WHO Mortality Database and of the CDC Multiple Cause of Death database**

*USZ[1]*

**Introduction:**
Pulmonary embolism (PE)-related mortality is decreasing in Europe. However, time trends in the USA and Canada remain uncertain because the most recent analyses of PE-related mortality were published in the early 2000s.

**Methods:**
For this retrospective epidemiological study, we accessed medically certified vital registration data from the WHO Mortality Database (USA and Canada, 2000-17) and the Multiple Cause of Death database produced by the Division of Vital Statistics of the US Centers for Disease Control and Prevention (CDC; US, 2000-18). We investigated contemporary time trends in PE-related mortality in the USA and Canada and the prevalence of conditions contributing to PE-related mortality reported on the death certificates. We also estimated PE-related mortality by age group and sex. A subgroup analysis by race was performed for the USA.

**Results:**
In the USA, the age-standardised annual mortality rate (PE as the underlying cause) decreased from 6·0 deaths per 100 000 population (95% CI 5·9-6·1) in 2000 to 4·4 deaths per 100 000 population (4·3-4·5) in 2006. Thereafter, it continued to decrease to 4·1 deaths per 100 000 population (4·0-4·2) in women in 2017 and plateaued at 4·5 deaths per 100 000 population (4·4-4·7) in men in 2017. Among adults aged 25-64 years, it increased after 2006. The median age at death from PE decreased from 73 years to 68 years (2000-18). The prevalence of cancer, respiratory diseases, and infections as a contributing cause of PE-related death increased in all age categories from 2000 to 2018. The annual age-standardised PE-related mortality was consistently higher by up to 50% in Black individuals than in White individuals; these rates were approximately 50% higher in White individuals than in those of other races. In Canada, the annual age-standardised mortality rate from PE as the underlying cause of death decreased from 4·7 deaths per 100 000 population (4·4-5·0) in 2000 to 2·6 deaths per 100 000 population (2·4-2·8) in 2017; this decline slowed after 2006 across age groups and sexes.

**Conclusion:**
After 2006, the initially decreasing PE-related mortality rates in North America progressively reached a plateau in Canada, while a rebound increase was observed among young and middle-aged adults in the USA. These findings parallel recent upward trends in mortality from other cardiovascular diseases and might reflect increasing inequalities in the exposure to risk factors and access to health care.

**225**

M. Raeber[1], R. Rosalia[1], D. Schmid[1], U. Karakus[1], O. Boyman[1, 2]

**Interleukin-2 signals converge in a lymphoid–dendritic cell pathway that promotes anticancer immunity**

*Department of Immunology, University Hospital Zurich, Zurich, Switzerland[1], Faculty of Medicine, University of Zurich, Zurich, Switzerland[2]*

**Introduction:**
Dendritic cells (DC) are a subgroup of professional antigen-presenting cells considered indispensable in orchestrating T cell responses to intracellular pathogens and tumors. Tumor-infiltrating DCs correlate with effective anti-cancer immunity and improved responsiveness to anti-PD-1 checkpoint immunotherapy. However, the upstream drivers of DC expansion and intratumoral accumulation are ill-defined. We find that interleukin-2 (IL-2)-mediated, innate and adaptive lymphoid cell-driven DC-poiesis in mice and humans imprints signatures of improved anti-cancer immunity. Thus, IL-2 immunotherapy-mediated stimulation of DCs contributes to anti-cancer immunity by rendering tumors more immunogenic.

**Methods:**
In patients treated within a clinical trial investigating the effects of recombinant human IL-2 (Proleukin) as well in mice treated with IL-2 and improved IL-2 formulations we observed a pronounced expansion of DCs measured by flow-cytometry. To further explore the mechanism of IL-2-driven DC expansion different IL-2-treated mouse models including in vivo antibody-mediated cell depletion models as well as knock-out, transgenic and bone marrow chimeric mouse models were extensively analyzed with flow cytometry, enzyme-linked immunosorbent assay, and RNA sequencing. For further functional studies cell-cycle analysis, in vitro antigen-uptake assays, and in vivo transplantable and transgenic tumor models were used.

**Results:**
We report that IL-2 administration in both human and mouse resulted in pronounced expansion of type-1 and type-2 DCs; these included migratory and cross-presenting DC subsets, although neither their precursors nor mature DCs expressed functional IL-2Rs. In mechanistic studies, IL-2 signals stimulated innate lymphoid cells, natural killer, and T cells to synthesize FMS-like tyrosine kinase 3 ligand (FLT3L), colony-stimulating factor 2 (CSF2), and tumor necrosis factor (TNF); these cytokines redundantly caused DC expansion and activation, which resulted in improved antigen processing and correlated with favorable anti-tumor responses.

**Conclusion:**
The advent of immune checkpoint inhibitors transformed modern oncology by exerting durable responses in selected metastatic cancers. Yet, only patients with highly immune cell-infiltrated, or so-called “hot” tumors, respond to immune checkpoint blockers. The present study shows a complementary difference and unappreciated advantage of interleukin-2 (IL-2) immunotherapy compared to anti-programmed cell death protein 1 (PD-1) immune checkpoint inhibitor treatment. Thus, IL-2 immunotherapy expanded tumor-infiltrating antigen-presenting DCs, and favored the conversion of poorly immunogenic into immunogenic tumors. These insights might help find ways of overcoming primary and secondary tumor-resistance to immune checkpoint inhibitors and provide a strong rationale for combinatorial strategies.

*Reference: Raeber et al., Sci. Transl. Med. 12, eaba5464 (2020)*

**226**

D. Braun[2], M. Zeeb[2], B. Hampel[1], C. Grube[2], S. Burkhard[2], H. Kuster[2], K. Metzner[2], J. Böni[3], R. Kouyos[2], H. Günthard[2]

**Sustained viral suppression with dolutegravir monotherapy during 12'212 patient weeks of follow-up in individuals starting combination antiretroviral therapy during primary HIV infection: a randomized, controlled, multi-site, non-inferiority trial**

*Checkpoint Zurich[1], Division of infectious diseases and hospital epidemiology[2], Institute of Medical Virology[3]*

**Introduction:**
Dolutegravir (DTG) monotherapy has been criticized because of the risk of long-term failure. Our EARLY-SIMPLIFIED trial showed that at week 48 DTG monotherapy was non-inferior to combination antiretroviral therapy (cART) in patients who started cART during primary (HIV-1 infection (PHI) and had a HIV-1 RNA <50 cp/mL plasma for >48 weeks (Braun et al, CID 2019). Here we report on the final results at week 192 .

**Methods:**
EARLY SIMPLIFIED is a randomized, open label, non-inferiority trial. Inclusion criteria were documented PHI, start of cART <180 days after estimated date of infection, and HIV-1 RNA <50 cp/mL plasma for >48 weeks. Exclusion criteria were previous virological failure and resistance associated mutations to INSTIs. We randomly assigned patients (2:1) to DTG monotherapy 50 mg QID or to continuation of standard cART. The trial continued for 4 years in total (ClinicalTrials.gov, NCT02551523).

**Results:**
101 patients were assigned to DTG monotherapy (n=68) or continuation of cART (n=33). After week 48 data had been analyzed, 17 patients from the cART group demanded to switch to DTG monotherapy. There was sustained viral suppression with dolutegravir monotherapy during 12’212 patient weeks of follow-up. In the per-protocol analysis, one virological failure occured at week 192 in the DTG mono-therapy group with emergence of resistance to integrase strand transfer inhibitors. The virological failaure was triggered by imperfect treatment adherence. One patient from the DTG monotherapy group switched back to cART because of extensive weight gain and one patient from the DTG monotherapy group was excluded from the per-protocol analysis because he did not fulfill the criteria of PHI.

**Conclusion:**
We observed only one virological failure during the observational period of 12'212 PWFU after switching to DTG monotherapy in patients who started cART during PHI and were fully suppressed for at least 48 weeks. The virological failure was triggered by imperfect adherence to the study-medication. DTG monotherapy might be a safe and sustainable maintenance therapy in patients who started cART during PHI and show optimal treatment adherence.

**228**

D. Spiess[1, 2], V.F. Abegg[2], A. Chauveau[2], E. Duong[1, 2], O. Potterat[2], M. Hamburger[2], A.P. Simões-Wüst[1]

**Phytomedicines for mental diseases and the placental barrier: an ex vivo study**

*Perinatal Pharmacology and Biochemistry, Department of Obstetrics, University Hospital Zurich, Zurich, Switzerland[1], Pharmaceutical Biology, Department of Pharmaceutical Sciences, University of Basel, Basel, Switzerland[2]*

**Introduction:**
Knowledge of foetal exposure to exogenous compounds is crucial for an informed risk assessment in pregnancy. However, clinical trials in pregnant women for assessment of transplacental transport are facing obvious ethical issues. Animal models are available, but extrapolation of results to humans is difficult because of large interspecies differences. Human *ex vivo* placental perfusion is an alternative and considered as the "gold standard" among translocation models. We established and validated this highly challenging model in order to assess the transplacental transport of pharmacologically active compounds in herbal drugs used in the treatment of nonpsychotic mental disorders in pregnancy, such as sleep disorders, restlessness, anxiety and mild depression. Phytomedicines are used as alternatives to synthetic drugs and are generally well accepted by pregnant women. However, despite a long track record of use, safety data in pregnancy are largely lacking.

**Methods:**
In a first step we established and validated the *ex vivo* placenta perfusion model using placentas obtained after informed consent from caesarean sections. Validation was performed with drugs known to cross in this model from the maternal to the foetal circuit, namely antipyrine as a positive control, and citalopram and diazepam as two medications given in pregnancy as antidepressant and anxiolytic drugs, respectively. In a second step, we used the same model to characterise the transfer of relevant phytochemicals from selected plants, namely humulone (from hops) and protopine (from California poppy). Compounds were quantified by partially validated U(H)PLC-MS/MS bioanalytical methods.

**Results:**
The transfer of citalopram and diazepam was reproducibly observed in our placenta perfusion model, and results were in accord with previously reported data. Protopine was also transferred from the maternal to the foetal circuit. In the case of humulone, a marked decrease in the maternal circuit was seen, but with little transfer to the foetal circuit. Whether the compound is metabolised in the placenta or accumulates in the tissue is currently under investigation.

**Conclusion:**
The placenta perfusion model is now used to measure the transplacental transport of relevant phytochemicals from other medicinal plants, and possible effects on placental functions are under investigation.

**229**

D. Schäfle[1], P. Selchow[1], B. Borer[1], M. Meuli[1], A. Rominski[1], B. Schulthess[1, 2], P. Sander[1, 2]

**Mycobacterium abscessus Arr confers Rifabutin resistance**

*Institute of Medical Microbiology[1], National Center for Mycobacteria[2]*

**Introduction:**
*Mycobacterium abscessus* infections are notoriously difficult to treat since the bacterium harbors a large arsenal of mechanisms to render antibiotics ineffective. The corner stone drug of tuberculosis treatment from the class of rifamycins, rifampicin (RMP), does not affect growth of *M. abscessus* because it is inactivated by the ADP-ribosyltransferase $Arr_{MAB}$. In contrast, rifabutin (RBT) has demonstrated promising activity in pre-clinical models of *M. abscessus* infection implying that it might not be inactivated by $Arr_{MAB}$. We determined the in vitro RBT susceptibility of *M. abscessus* and its isogenic *Δarr* mutant. In other species, Monooxygenases have been identified as resistance determinants against rifamycins and were speculated about in *M. abscessus*. Therefore, we investigated possible resistance determinants beyond Arr i.e., enzymes acting on RMP but not on RBT.

**Methods:**
The susceptibility of the *Δarr* mutant was determined by minimal inhibitory concentration (MIC) testing against RMP, RBT, Rifaximin (RFX) and Tetracycline (TET). Candidate resistance genes encoding homologues of RMP monooxygenases were identified in the chromosome of *M. abscessus* by BlastP and were inactivated by homologous recombination (in a *Δarr* background) as was TetX, a monooxygenase conferring tetracycline resistance.

**Results:**
Deletion of *arr* strongly decreased RBT MIC. The relative resistance ratio (RRR) of wild-type vs. *Δarr* mutant for RBT was even higher than the RRR for RMP indicating additional mechanisms for inactivation of RBT. MICs in any of the monooxygenase deletion mutants were not altered as compared to the parental *Δarr* strain leaving the identity of additional RMP resistance determinants open.

**Conclusion:**
Our results show that the treatment efficacy of RBT for *M. abscessus* infections could be enhanced by rendering RBT resilient to Arr-dependent modification or by blocking the enzymatic activity of *M. abscessus* Arr.

**230**

M. Sutter[1], S. Samodelov[1], GA. Kullak-Ublick[1], M. Visentin[1]

**Cholesterol recognition and interaction in OCT2 – a tough nut to CRAC (and CARC)**

*Department of Clinical Pharmacology and Toxicology[1]*

**Introduction:**
As a transmembrane transporter embedded in the basolateral membrane of the kidneys' proximal tubule cells, the organic cation transporter 2 (OCT2) plays a key role in the reabsorption and secretion of various positively charged substrates. Transmembrane proteins are forced to interact with the surrounding microenvironment within the lipid bilayer by nature, making them susceptible to the variable compositions of these microenvironments. In proximal tubule cells, cholesterol content, one of the main components of eukaryotic plasma membranes, presents as highly dynamic in physiological and pathophysiological conditions such as ageing or acute kidney injury. Our group has previously shown that a reduction of cholesterol content in the plasma membrane impairs the transport activity of OCT2, shifting the transport behavior from allosteric to one binding site kinetics. Since allosterism is crucial for an effective detoxification process, an impaired transport activity and a loss of allosteric behavior may result in unfavorable accumulations of the transporter's substrates and, consequently, abnormal pharmacokinetic and pharmacodynamic profiles. The aim of this study is to elucidate the role of cholesterol recognition motifs - namely the Cholesterol Recognition/interaction Amino acid Consensus (CRAC) sequence and its reverse (CARC) - in the interaction between OCT2 and plasma membrane cholesterol.

**Methods:**
The six fully conserved amino acids within the CRAC and CARC domains have been identified from the annotated protein sequence O15244.2. Missense mutations have been inserted by site directed mutagenesis and confirmed by Sanger sequencing. Wildtype or mutant OCT2-plasmids were transiently transfected in HEK-293 cells using the transfection reagent Lipofectamine2000. Forty-eight hours later, transport activity for model substrate 1-methyl-4-phenylpyridinum (MPP+) was measured at a transport time reflecting the unidirectional influx of the substrate. The assessment of protein stability and localization was performed by surface labelling coupled with western blotting.

**Results:**
The CRAC and CARC domains were found in the putative fifth transmembrane domain of the OCT2 protein sequence. In CRAC, the fully conserved amino acids are: R235, Y241 and V247. In CARC, the fully conserved amino acids are: V251, Y257 and R263. The mutations V247A, V251A and Y257A had neither an effect on protein localization nor MPP+ uptake. Transport activity was dramatically decreased compared to that by OCT2-WT in the presence of the missense mutations R235A, Y241A or R263A. While mutant Y241A showed reduced expression at the plasma membrane, contributing to the impaired transport activity, the two mutated arginine residues (R235A and R263A) on either side of the CRAC and CARC domains maintained a level of protein expression and localization comparable to the wild-type. Unlike the wild-type transporter, the R235A and R263A mutants were relatively insensitive to increased extracellular concentrations of the substrate.

**Conclusion:**
Substitutions in position 247 of the CRAC and in positions 251 and 257 of the CARC domain were tolerated, whereas the mutation in position 241 appears to be critical for the stability of the protein. Arginine 235 and 263, respectively, seem to be the only residues within the cholesterol recognition domains that are pivotal for transport activity. It remains to be understood whether such effect is indeed the result of a disrupted interaction between the protein and cholesterol, or rather an alteration in the protein conformational change independent of cholesterol.

**231**

G. Bortoli[1], D. Canepa[1], H. Pape[1], Y. Neldner[1], S. Märsmann[1], E. Casanova[1], P. Cinelli[1]

**Identification of New Markers Characterizing Adipose-Derived Mesenchymal Stromal Cells with Enhanced Osteogenic Potential**

*Department of Trauma, University Hospital Zurich, Switzerland[1]*

**Introduction:**
Adipose-derived mesenchymal stromal cells (AD-MSCs) represent a promising and viable source for a broad spectrum of cell-based therapies. However, their heterogeneity and different ability to differentiate toward defined cell types represent a strong limitation for an effective use for clinical applications. We have recently investigated the subcellular composition of 17 AD-MSCs at single cell level (Canepa et al, Stem Cell Research & Therapy (2021) 12:7), revealing the presence of a specific subpopulation (ALP+/CD73low) with enhanced osteogenic potential. To better characterize these cells and compare their cellular identity we have performed RNA sequencing with the goal to identify genes regulating this specific cell subpopulation and eventually mediating osteogenic differentiation.

**Methods:**
RNA sequencing (RNA-Seq) was performed to analyze the transcriptome of four different AD-MSCs subpopulations with either enhanced or low osteogenic differentiation potential (ALP+/CD73+, ALP+/CD73-, ALP-/CD73+, ALP-/CD73-). RNA-Seq results were validated through FACS sorting followed by RT-qPCR analysis. The expression of the genes of interest was assessed during 21 days of osteogenic differentiation and quantified by RT-qPCR. To verify the presence, at the protein level, of ALDH1A1 within the subpopulation with enhanced osteogenic potential, a FACS analysis was performed. AD-MSCs osteogenic differentiation was further evaluated after selective inhibition of ALDH1A1 expression using the theophylline-based inhibitor NCT-501. Osteogenesis was assessed by quantification of calcium deposition using Alizarin Red staining.

**Results:**
RNA-seq results were confirmed and validated through FACS sorting and RT-qPCR, revealing 18 potential genes of interest. Four genes, namely ALDH1A1, SFRP4, CXCL6 and HHIP were found to have an increased mRNA expression level in the “good” compared to the “bad” differentiating cell lines, therefore being employed for further analyses. ALDH1A1 mRNA expression levels increased in the first four days of osteogenic differentiation. Analysis of the ALDH1A1 expression after targeted inhibition with NCT-501 during the first 4 days of osteogenic differentiation is currently in progress.

**Conclusion:**
Our data revealed ALDH1A1 as a potential marker characterizing AD-MSCs subpopulation with enhanced osteogenic potential. The exact role of this enzyme has to be further analyzed. Of particular interest is its potential dual role in maintaining the stem cell identity of ALP+/CD73low cells and in regulating osteogenic lineage commitment of these cells. Modulation of ALDH1A1 activity can be further employed for long-term culture and expansion of MSCs, improving their maintenance in a stem cell state.

**232**

S. Ambrosini[1], F. Montecucco[2], D. Pedicino[3], A. Akhmedov[1], S. Mohammed[1], G. Liuzzo[3], A. Beltrami[4], F. Crea[3], T. Lüscher[1], S. Costantino[1], F. Paneni[1]

**The methyltransferase SETD7 drives myocardial ischemic injury by modulating the Hippo pathway: a study in mice and humans**

*Center for Molecular Cardiology, University of Zürich[1], First Clinic of Internal Medicine, University of Genoa[2], Polyclinic Agostino Gemelli, Catholic University of the Sacred Heart[3], University of Udine[4]*

**Introduction:**
Ischemic heart disease is a leading cause of death worldwide. Although revascularization strategies significantly reduce mortality after acute myocardial infarction (MI), a significant number of MI patients develop heart failure. Protein methylation is emerging as a key biological signal implicated in the pathophysiology of cardiovascular (CV) disease. In this regard, the methyltransferase SETD7 was recently shown to methylate proteins relevant to CV homeostasis. The present study aims to investigate the role of SETD7 in myocardial ischemia-reperfusion (I/R) injury.

**Methods:**
Experiments were performed in neonatal rat ventricular myocytes (NRVM), SETD7 knockout mice (SETD7-/-) undergoing myocardial I/R injury, myocardial samples from patients with and without ischemic heart failure as well as peripheral blood mononuclear cells from patients with ST elevation MI (STEMI, n=25) and age-matched healthy controls (n=20).

**Results:**
Glucose deprivation (GD) in NRVM led to upregulation of SETD7 and direct mono-methylation of the Hippo signaling effector YAP. SETD7-dependent methylation of YAP led to its cytosolic retention thus impeding YAP binding to the promoter of pro-survival genes. Selective pharmacological inhibition of SETD7 by (R)-PFI-2 blunted YAP mono-methylation thereby restoring its nuclear retention. We show that YAP binds the promoter of antioxidant genes catalase and superoxide dismutase, thus preventing GD-induced mitochondrial oxidative stress, organelle swelling and apoptosis. Consistently, infarct size, myocardial oxidative stress and left ventricular dysfunction were reduced in SETD7-/- mice undergoing I/R as compared to wild-type littermates. Of clinical relevance, we found that SETD7/YAP signaling was deregulated in myocardial samples from patients with ischemic heart failure as well as in peripheral blood mononuclear cells from STEMI patients.

**Conclusion:**
We demonstrate that SETD7-dependent methylation of YAP is an important mechanism underpinning myocardial oxidative stress, mitochondrial damage and apoptosis during ischemia. Pharmacological modulation of SETD7 by (R)-PFI-2 may represent a potential therapeutic approach to prevent myocardial ischemic damage through modulation of the Hippo pathway.

**234**

O. Verhoek[2, 3], O. Lauk[1, 3], I. Opitz[1, 3], T. Frauenfelder[2, 3], K. Martini[2, 3]

**Sarcopenia, tumor volume and mediastinal fat as outcome predictors in surgically treated malignant pleural mesothelioma.**

*Department of Thoracic Surgery, University Hospital Zurich, Switzerland[1], Diagnostic and Interventional Radiology, University Hospital Zurich[2], University of Zurich[3]*

**Introduction:**
Sarcopenia, high tumor-volume and low mediastinal-fat is associated with poor outcome in cancer-patients. We evaluated the prognostic value of different morphometric measurements such as sarcopenia, tumor volume and mediastinal fat in long-term-outcome of surgically-treated malignant pleural mesothelioma (MPM).

**Methods:**
From September 2005 to June 2020 consecutive surgically-treated MPM patients having a pre-operative computed tomography (CT) scan were retrospectively included. Sarcopenia was assessed by CT-based parameters measured at the level of the fifth thoracic vertebra by excluding fatty-infiltration based on CT-attenuation: cross-sectional Total Paraspinal Area (TPA), Total Rotator-cuff Area (TRA), and Total Pectoral Area (TPeA). Total Muscle Area (TMA) was defined as the sum of the former three measurements. Findings were stratified for gender, and a threshold of 33rd percentile was set to define sarcopenia. Additionally, tumor volume as well as mediastinal fat was measured. Findings were correlated with progression-free survival and long-term mortality.

**Results:**
One-hundred-forty-six patients with surgically-treated MPM were analysed. Logistic regression showed the independent negative predictive value of gender ($p=0.001$), pathologic stage ($p=0.028$), tumor volume ($p<0.001$) and sarcopenia ($p=0.003$). For mortality, logistic regression showed the independent negative predictive value of patient age ($p=0.005$) and tumor volume ($p<0.001$).

Kaplan-Meier statistics showed tendencies, that sarcopenic patients (Sarcopenia defined as TMA) have higher long-term mortality after surgically treated MPM (25.5±2.6 months vs. 38.8±4.6 months; $p=0.073$). Mediastinal fat was not associated with tumor progression or mortality.

**Conclusion:**
Sarcopenia defined as the sex-related 33rd percentile of TMA at the level of the fifth thoracic vertebra as well as tumor volume are associated with progression-free survival and mortality in surgically-treated MPM.

**235**

N. Karavasiloglou[1, 2], E. Michalopoulou[1, 2], M. Limam[1, 2], D. Korol[1], M. Wanner[1, 2], S. Rohrmann[1, 2]

**Net survival of women diagnosed with breast cancers: a population-based study in Switzerland**

*Cancer Registry Zurich, Zug, Schaffhausen, and Schwyz, University Hospital Zurich, Zurich, Switzerland[1], Division of Chronic Disease Epidemiology, Institute for Epidemiology, Biostatistics and Prevention, University of Zurich, Zurich, Switzerland[2]*

**Introduction:**
Breast carcinoma in situ (BCIS) is a heterogeneous group of intraepithelial lesions with malignant potential. The majority of BCIS are detected through mammography and generally, the survival of BCIS patients is good. One of the main difficulties of reporting cancer-specific survival outcomes is that the cause of death needs to be identified and correctly classified as cancer- or non-cancer specific. Due to the considerable uncertainty in distinguishing between these two, we estimated and compared the net survival of breast cancer (BCIS, invasive cancer, or BCIS and then invasive cancer) patients using a relative survival framework.

**Methods:**
Data were obtained from the Cancer Registry of the Cantons of Zurich, Zug, Schaffhausen, and Schwyz. All women were diagnosed with breast cancers between 2003 and 2016 and were living in the canton of Zurich at the time of diagnosis. We distinguished between (a) women whose first-ever cancer diagnosis was primary BCIS and were not diagnosed with another cancer before or at BCIS diagnosis (D05.0–D05.9; n=1,136); (b) women with primary BCIS, later diagnosed with primary invasive breast cancer (n=93); and (c) women whose first-ever cancer diagnosis was invasive breast cancer (C50; n=12,279). We performed net survival analyses using the nonparametric Pohar Perme estimator and population life tables for the canton of Zurich. Women were followed from the date of tumor diagnosis (first primary tumor diagnosis for women diagnosed with BCIS or invasive breast cancer; second primary tumor diagnosis for women diagnosed with BCIS and invasive breast cancer) until the date of emigration, date of death, or end of follow-up (5 years after cancer diagnosis), whichever came first.

**Results:**
Invasive tumors diagnosed in women with previous BCIS were more frequently detected via mammographic screening compared to those diagnosed in women without previous BCIS (41% vs. 12%). Additionally, they were detected at an earlier stage and had less missing information in tumor-specific variables compared to invasive tumors diagnosed in women without previous BCIS. BCIS patients had a net survival of 1.02 (95% confidence interval [CI]: 1.01-1.03), whereas invasive breast cancer patients without previous BCIS had a net survival of 0.89 (95% CI: 0.88-0.90). Patients diagnosed with BCIS followed by invasive breast cancer showed a 5-year net survival of 0.92 (95% CI: 0.85-1.01). Small differences in net survival were seen when stratifying the results by age at diagnosis or stage of the invasive breast tumor.

**Conclusion:**
Invasive breast tumors that were preceded by a recorded BCIS diagnosis were detected more frequently by screening and at an earlier stage, compared to those who were not. The 5-year net survival of BCIS patients and of patients diagnosed with invasive breast tumors, irrespective of whether a BCIS was previously recorded, was high. Larger studies should aim to further investigate the survival of BCIS patients who later develop invasive breast cancer, focusing on factors associated with better breast cancer-specific survival outcomes.

**236**

N. Alijaj[1], B. Pavlovic[1], P. Oechslin[1], K. Saba[2], C. Poyet[1], T. Hermanns[1],P. Martel[3], L. Derré[3], M. Valerio[3], N. Rupp[4], D. Eberli[1], I. Banzola[1]

**Novel Urine Biomarkers for the Early Detection of Prostate Cancer**

*Department of Urology, University Hospital of Zürich, Zurich, Switzerland[1], Department of Urology, Kantonsspital Graubünden, Chur, Switzerland[2], Department of Urology, Urology Research Unit, University Hospital of Lausanne, Lausanne, Switzerland[3], Department of Pathology, University Hospital of Zürich, Zurich, Switzerland[4]*

**Introduction:**
Worldwide, prostate cancer (PCa) is the most common male malignancy, accounting for 15% of all cancers. The current screening of PCa is based on the measurements of the prostate specific antigen (PSA) in blood to select men with a higher risk of harboring a tumor and thus eligible for the prostate biopsy. However, PSA testing has a high rate of false positives, leading to unnecessary biopsies in 50 - 75% of cases, and consequently exposes a relevant number of patients to potentially severe side-effects. In a previous study, we have demonstrated that Indoleamine 2,3 Dioxygenase (IDO), measured in urines, can predict the presence of a PCa prior to biopsy with 17% to 50% specificity (protein and mRNA, respectively) and a sensitivity of 100%. We therefore aim to develop a urine test based on multiple specific biomarkers that can represent a game-changer in the screening and diagnosis of PCa. The test will be indicated for men who have elevated levels of PSA, to select, with higher specificity and 100% sensitivity, those men who should perform a biopsy to diagnose PCa.

**Methods:**
Urine samples from men with elevated levels of PSA were collected before prostate biopsy. A mass-spectrometry (MS) screening was performed on a cohort of 45 samples to identify biomarkers, which showed a significantly different distribution in tumors ($p < 0.05$). The validation of the candidate biomarkers by commercial ELISAs has been completed on 159 urine samples. Currently specific antibodies are generated via phage display selection and mouse immunization for the development of an ultrasensitive multi-plex immunoassay.

**Results:**
We have identified through a mass spectrometry screening, six novel biomarkers and five control molecules that can complement our first biomarker IDO by increasing the specificity of the test while maintaining an extremely high sensitivity. We have validated the biomarkers and controls with commercial ELISAs to confirm the mass-spectrometry results. The preliminary analysis show that different combinations of the candidate biomarkers and controls achieve 80% specificity at 100% sensitivity, which means that not a single patient with PCa will be missed and that 80% of men without tumor will be spared from performing an unnecessary biopsy. Specific antibodies targeting biomarkers and control molecules are under generation for the development of a reliable urine test, that allows multiplexing, thus quantifying several molecules at the same time. So far, antibodies targeting three biomarkers have been successfully generated and we have selected immunoassay sandwich antibody-pairs for one of the biomarkers.

**Conclusion:**
Our data show that urine biomarkers can be quantified for the screening and detection of PCa. We were able to identify 12 target molecules that can be measured with immunoassays and complement PSA to increase test specificity, while ensuring a 100% sensitivity. We are now optimizing assay conditions for the proprietary antibodies and are performing further phage display selections for other biomarkers. The clinical implementation of a non-invasive and risk-free test will enable the early detection of prostate tumors and, by sparing a relevant number of healthy men from unnecessary biopsies, it will improve the quality of life of patients resulting in a marked reduction of the healthcare costs related to the diagnosis and treatment of prostate cancer.

**237**

J. Prinz[1, 2], I. Waldmann[2], T. Schmid[3], B. Mühleisen[1], R. Zbinden[3], I. Laurence[1], Y. Achermann[2]

**Photodynamic therapy improves skin antisepsis as a prevention strategy in arthroplasty procedures: A pilot study**

*Department of Dermatology, University Hospital Zurich, University of Zurich, Zurich, Switzerland[1], Division of Infectious Diseases and Hospital Epidemiology, University Hospital Zurich, University of Zurich, Zurich, Switzerland[2], Institute of Medical Microbiology, University of Zurich, Zurich, Switzerland[3]*

**Introduction:**
Current standard skin antisepsis to prevent surgical site infections are ineffective to eradicate all skin-colonizing bacteria. Photodynamic therapy (PDT) has shown bactericidal effects in vitro, but no clinical study with improvements in skin antisepsis has been documented.

**Methods:**
We investigated the effect of methyl aminolevulinate (MAL)-PDT versus no PDT for skin antisepsis treatment (povidone-iodine/alcohol) in the groin of 10 healthy participants. Skin swabs were taken at baseline, immediately after PDT, and after skin antisepsis treatment to cultivate bacteria. At day 7 and 21, bacterial cultures were repeated before and after antisepsis treatment without PDT. Skin biopsies were performed to examine the grade of inflammation.

**Results:**
Skin-colonizing bacteria were found in all 20 participants at baseline sampling. Immediately after MAL-PDT, skin was sterile in 7 (70%) participants before and in all 10 (100%) participants after skin antisepsis treatment. In contrast, we found skin-colonizing bacteria in 5 (50%) participants of the control group receiving only skin antisepsis. After 7 and 21 days, skin sterility was similar to the baseline. We observed slight perivascular inflammation with lymphocytes and eosinophils without changes in the histomorphology of eccrine or sebaceous glands in skin biopsies. PDT was generally well tolerated except for localized redness.

**Conclusion:**
MAL-PDT with skin antisepsis treatment sterilized skin immediately after its use but did not maintain sterility 7–21 days post-treatment. Due to local side effects, further clinical studies with less intensive PDT conditions or other photosensitizers are needed before PDT is integrated into clinical practice.

**238**

S. Saeedi Saravi[1, 2], N. Bonetti[1, 2], A. Vukolic[1], L. Liberale[1, 3], T. Lüscher[1, 4], G. Camici[1, 5, 6], J. Beer[1, 2]

**Dietary omega-3 fatty acid reverses age-linked heart failure with preserved ejection fraction**

*Center for Molecular Cardiology, University of Zurich, 8952 Schlieren, Switzerland[1], Department of Internal Medicine, Cantonal Hospital Baden, 5404 Baden, Switzerland[2], First Clinic of Internal Medicine, Department of Internal Medicine, University of Genoa, Genoa, Italy[3], Royal Brompton and Harefield Hospitals and Imperial College, London, United Kingdom[4], University Heart Center, Department of Cardiology, University Hospital Zurich, Zurich, Switzerland[5], Department of Research and Education, University Hospital Zurich, Zurich, Switzerland[6]*

**Introduction:**
Heart failure with preserved ejection fraction (HFpEF) is the most common type of HF in aged adults, yet no optimal pharmacological therapy has emerged for improved outcomel in HFpEF. Therefore, there is an urgent need for novel effective interventions in the age-related HFpEF. The plant-derived omega-3-fatty-acid α-linolenic-acid (ALA) has emerged to confer potential protective effects in cardiovascular disease. Our recent findings reveal that lifelong dietary ALA dampens thrombotic and cerebrovascular events in aged mice. The purpose of this study was to elucidate the reversal of age-related HFpEF phenotype by long-term nutritional ALA supplementation.

**Methods:**
6-month-old (young) wild-type C57BL/6J mice were fed a low, as control, or high ALA diet for more than 12 months. Here, we show that aged (>18 months) mice on low ALA diet recapitulate major hallmarks of HFpEF, including diastolic dysfunction with preserved left ventricular ejection fraction, cardiac interstitial fibrosis, impaired acetylcholine-induced relaxation of aortic segments, and arterial stiffness.

**Results:**
Intriguingly, we revealed that long-term ALA-rich diet reverses diastolic dysfunction, vascular relaxation capacity, reduced pulse wave velocity, interstitial cardiac fibrosis, and coincident hemodynamic abnormalities in aged mice. These findings are accompanied by blunting of inflammatory responses and a remarkable reduction in the expression of matrix-metalloproteinase-2 (MMP-2) by high ALA diet.

**Conclusion:**
Our results demonstrate previously unrecognized protective effects of dietary ALA against impaired cardiovascular functional outcomes and cardiac structural changes typical of HFpEF in aged mice. Taken together, these data support the ALA-based nutritional intervention as a safe, plant derived and easily accessible therapeutic strategy for age-related HFpEF.

**239**

R. Werner[1], M. Kirschner[1], I. Opitz[1]

**Establishment and validation of primary non-small cell lung cancer organoids as in vitro lung cancer models**

*Department of Thoracic Surgery, University Hospital Zurich[1]*

**Introduction:**
Lung cancer is the most common cause of cancer-related death worldwide. Among lung cancers, the most common subtype is the non-small cell lung cancer (NSCLC), making up for approximately 85% of all lung cancer cases. For both the identification of tumor-specific biomarkers, as well as for the development and early assessment of personalized candidate cancer treatments, representative in vitro systems that reflect tumor heterogeneity are needed. While common cancer cell lines do not generally maintain their original heterogeneity and three-dimensional structure, they are fundamentally limited in representing the complexity of NSCLC. We therefore aimed to create new model systems that may operate as patient avatars for precision medicine and offer a reliable platform for further investigations.

**Methods:**
Small pieces from surgically resected NSCLC tissue were collected between January and October 2020. Tissue pieces were mechanically processed and passed through 70µm cell strainers. The cell suspension was mixed with a gelatinous extracellular matrix for three-dimensional cell culture. Organoid growth medium was adapted from existing protocols based on DMEM-F12 and was complemented with human epidermal growth factor (hEGF), basic fibroblast growth factor (bFGF) and a rho kinase inhibitor among other supplements. The organoids were cultured at 37°C and passaged after 5-20 days. For histological validation, the growing NSCLC organoids were transferred into plasma-thrombin cell blocks, formalin-fixed and paraffin embedded.

**Results:**
From 35 resected NSCLC samples, 10 organoid cultures were successfully established and expanded during early passages in vitro. The growing organoids were histologically and immunohistochemically validated (Hematoxylin-Eosin and Elastica van Gieson staining, immunohistochemistry of Thyroid Transcription Factor-1, p40 and Pan-Cytokeratin) and showed identical characteristics of the resected primary tumor. Validated histological subtypes included adenocarcinoma, squamous-cell carcinoma, adeno-squamous / mucoepidermoid carcinoma and lung carcinoid.

**Conclusion:**
The establishment of primary NSCLC organoids from surgically resected tissue is feasible. The expanded organoids maintain the histological and immunohistochemical characteristics of its parental tumor. However, low establishment rates and slow organoid growth currently restrict the application of NSCLC organoids in the clinical context.

**240**

T. Thavayogarajah[1], G. Nair[1], D. Müller[2], U. Schanz[1]

**Fludarabine pharmacokinetics: a new tool for reduction of conditioning regimen toxicity?**

*Department of Medical Oncology and Hematology, University Hospital and University of Zurich, Switzerland[1], Institute of Clinical Chemistry, University Hospital Zurich, Switzerland[2]*

**Introduction:**
In allogeneic hematopoietic cell transplantation (HCT), fludarabine is a frequently used agent mainly in reduced conditioning regimes. It is often combined with busulfan for which pharmacokinetics with area under the curve (AUC) determination and corresponding dose adaptions is used for many years. It is highly likely that this results in less toxicity. For the fludarabine dose calculation in adults, only the body surface area is used, which might result in interindividually variable fludarabine exposure. This might result in higher exposition (AUC) and higher or even excessive toxicity resulting in an increase in transplant related toxicity (TRM) or with lower exposition to an increase in the relapse incidence (RI). To optimize TRM and RI we established pharmacokinetics for fludarabine in addition to the established pharmacokinetics for busulfan. Only one publication (Langenhorst et al.) on fludarabine AUC and HCT outcome so far does exist.

**Methods:**
Fludarabine was measured with a validated LC-MS/MS method. The exposure as AUC was calculated for each patient using a three-compartmental model (adapted from Langenhorst et al.) in n=8 consecutive patients receiving a conditioning regime with fludarabine. Fludarabine was given on days -7 to -2 with a dose calculation based on 30mg/m2 with an infusion rate of 30 minutes. The time points of analysis were 30 minutes, 4h, 6h, and 7h after the end of infusion. In addition patients received peroral busulfan 4mg/kg bw on days -3 and -2 and ATG 10mg/kg bw (Grafalon®) on days -4 to -1.

**Results:**
In contrast to the published data of Langenhorst et al., we saw significant differences in our patients concerning the dose calculation and its pharmacokinetics e.g., fludarabine AUC were higher within our patients. We did not observe any acute toxicity. In the analysis of Langenhorst et al. the optimal AUC was postulated to be 20 mg*h/l. In our (n=44) patients the median range of the AUC was 34.94 (+/- 8.11) mg*h/l, clearly over the recommend level for an optimal toxicity profile. In our analyzed population, there was no major toxicity seen at day 100, even though the AUC was higher than the suggested optimal levels.

**Conclusion:**
In a regimen with more doses (6 vs 4), lower single dosage (30mg/m2 vs 40mg/m2) but faster infusion rate (30min vs 60min) resulting unexpectedly in higher AUC (30mg*h/l vs 20 mg*h/l) we did not observe more transplant-related toxicity. This is in contrast to the published data. Therefore, we suggest a new modell which allows dose-adapted fludarabine calculation based on the AUC of the patients to reduce the toxicity of the conditioning regimen.

**241**

C. Diaz-Canestro[1], Y. Puspitasari[1], L. Liberale[1, 4], T. Guzik[5, 7], A. Flammer[2], N. Bonetti[1], P. Wüst[1], S. Constantino[1], F. Paneni[1, 2, 6], A. Akhmedov[1], J. Beer[1, 3], F. Ruschitzka[2], M. Hermann[2], T. Lüscher[1, 8], I. Sudano[2], G. Camici[1, 2, 6]

**Therapeutic MMP-2 knockdown blunts age-dependent carotid stiffness by decreasing elastin degradation and augmenting eNOS activation**

*Center for Molecular Cardiology, University of Zurich, Schlieren, Switzerland[1], Department of Cardiology, University Heart Center, University Hospital Zurich, Zurich, Switzerland[2], Department of Internal Medicine, Cantonal Hospital Baden, Baden, Switzerland[3], Department of Internal Medicine, University of Genoa, Genoa, Italy[4], Department of Medicine, Jagiellonian University Collegium Medicum, Cracow, Poland[5], Department of Research and Education, University Hospital Zurich, Zurich, Switzerland[6], Institute of Cardiovascular and Medical Science, BHF Glasgow Cardiovascular Research Centre, University of Glasgow, Glasgow, United Kingdom[7], Royal Brompton & Harefield Hospitals and Imperial College London, United Kingdom[8]*

**Introduction:**
Arterial stiffness is a well-characterized hallmark of vascular aging that precedes and strongly predicts the development of cardiovascular diseases. Age-dependent stiffening of large elastic arteries is primarily attributed to increased levels of matrix metalloproteinase-2 (MMP-2). However, the mechanistic link between age-dependent arterial stiffness and MMP-2 remains unclear. The purpose of this study was to investigate the efficacy of therapeutic MMP-2 knockdown using small interfering RNA (siRNA) on age-dependent arterial stiffness.

**Methods:**
Pulse wave velocity (PWV) was assessed in right carotid artery of wild type (WT) mice from different age groups. MMP-2 levels in the carotid artery and plasma of young (3 months) and old (20-25 months) WT mice were determined. Old WT mice (18-21-month-old) were treated for 4 weeks with either MMP-2 or scrambled (Scr) siRNA via tail vein injection. Carotid PWV was assessed at baseline, 2 and 4 weeks after start of the treatment. Desmosine (DES), an elastin breakdown product, was measured in plasma of treated mice and in a human cohort (n=47, 23-85 years old), in whom carotid-femoral PWV was also assessed.

**Results:**
Carotid PWV as well as vascular and circulating MMP-2 were elevated with increasing age in mice. MMP-2 knockdown reduced vascular MMP-2 levels and attenuated age-dependent carotid stiffness. siMMP-2 treated mice showed increased elastin to collagen ratio, lower plasma DES and enhanced phosphorylation of endothelial nitric oxide synthase (eNOS). A direct protein-protein interaction between MMP-2 and eNOS, which was higher with increasing age, was also observed. Lastly, plasma DES directly correlated with age and arterial stiffness in the human cohort.

**Conclusion:**
Therapeutic MMP-2 knockdown attenuates age-dependent carotid stiffness by blunting elastin degradation and augmenting eNOS activation. Given the increasing clinical use of siRNA technology, MMP2 knockdown should be investigated further as a therapeutic strategy in the attempt to mitigate age-dependent arterial stiffness and eventually CV diseases.

**242**

L. Roth[2], L. Russo[2], C. Pauli[1], E. Breuer[2], PA. Clavien[2], A. Gupta[2], K. Lehmann[2]

**The impact of locoregional treatment on the anticancer immune response against peritoneal metastasis from colon cancer**

*Department of Pathology, University Hospital Zurich[1], Surgical Oncology Research Laboratory, Department of Surgery and Transplantation, University Hospital Zurich[2]*

**Introduction:**
Locoregional treatment, including the complete resection of macroscopic tumor and application of heated chemotherapy in the peritoneal cavity (HIPEC), of peritoneal metastasis (PM) from colon cancer has improved survival of selected patients. Nevertheless, peritoneal recurrence, presumably due to remnant cancer cells, is common and requires further optimization of this short-term chemotherapy application. Therefore, it is important to understand mechanisms operating behind HIPEC. We hypothesize that the combination of chemotherapy and hyperthermia might not only be cytotoxic, but may also induce strong immunogenic changes on the tumor and its microenvironment. We therefore assessed effects of Mitomycin C/Doxorubicin (M/D) and Oxaliplatin (Oxa), widely used in clinical settings, on the immunogenicity of colorectal cancer cell-lines and patient derived organoids in-vitro and assessed immunogenic changes in a PM-mouse model.

**Methods:**
Colorectal cancer cell-lines and organoids derived from patients with colorectal cancer were treated with M/D or Oxa for 30 minutes with and without hyperthermia (430C). MHC-I expression on cancer cells was analyzed 48 h after treatment using FACS and cancer testis antigen (CTA) expression 72 hours after treatment, using RT-PCR and western blot. To assess Mo-DC maturation, we set up a co-culture between differentially treated colorectal cancer cells and Mo-DC`s from a healthy human donor. We analyzed surface markers such as HLA-DR and CD 83 to assess Mo-DC maturation using FACS. Further, Mo-DC`s that were pre-incubated with treated and untreated colorectal cancer cells were added to purified CD8+ T-cells to measure their activation via intracellular IFN-y staining. To examine these findings in-vivo, C57BL/6 mice were injected with MC-38-Ova murine colon cancer cells and treated 7 days post tumor cell injection with a single dose chemotherapy intraperitoneally. The tumor load intraperitoneal was assessed with the mouse peritoneal cancer index (PCI). Furthermore, peritoneal tumors of treated and sham mice were analyzed regarding their CD8+ T-cell infiltration and their activation status with the markers CD 39 and PD-1 via FACS analysis.

**Results:**
HIPEC treatment induced the expression of MHC-I molecules and six CTAs out of a panel of nine different CTAs. Similar findings could be confirmed on different patients derived organoids generated from PM lesions. Furthermore, one CTA Cyclin A1 was highly increased compared to control treatment ($p=0.004$) on protein level. On Mo-DC`s, after co-culturing with HIPEC treated colorectal cancer cells, we noticed a significant expression of CD83 and HLA-DR, both DC maturation markers. Furthermore, Mo-DCs after activation by co-culture with HIPEC-treated cancer cells, were able to prime CD 8+ T-cells, leading to enhanced IFN-y production by CD8+ T cells. In-vivo, the single dose intraperitoneal application of M/D resulted in a lower tumor load (PCI sham:11.5, PCI M/D:6). The M/D treated beard a higher frequency of CD8+ T-cells in the peritoneal tumor compared to the sham group (18.25% vs 6.57%). Furthermore, these T-cells were tumor – specific and less exhausted.

**Conclusion:**
HIPEC treatment induces immunogenic changes in colorectal cancer cells and organoids via upregulation of MHC-I molecules and CTAs. Furthermore, the locoregional treatment leads to an attraction of active, tumor-specific T-cells in-vivo. These novel insights may explain observed long-term effects in selected patients, and represent a novel aspect of HIPEC, beyond cytotoxicity allowing fine tuning of this treatment approach.

**243**

L. Volta[1], R. Myburgh[1], C. Catalano[2], C. Pellegrino[1], J. Müller[1], C. Wilk[1], D. Neri[2], M.Manz[1]

**Universal on-off switchable anti-FITC CAR T-Cells for Tumor Therapy**

*Department of Medical Oncology and Hematology, University Hospital Zurich[1], Institute of Pharmaceutical Sciences, Department of Chemistry and Applied Biosciences, ETH Zurich[2]*

**Introduction:**
Acute Myeloid Leukemia (AML) originates from immature hematopoietic stem and progenitor cells (HSPC). While some AML are curable, disease relapse occurs in most of patients upon application of current standard chemotherapy approaches. Recently, eradication of lymphocytic leukemia or lymphoma cells by immunological targeting of lineage specific surface antigens (e.g. CD19, CD20, BCMA) has been achieved. To date, however, the search for AML-specific surface antigens not expressed on healthy HSPC has remained largely elusive. In addition, targetable surface antigen heterogeneity is a main challenge to overcome. The use of CAR-T cells against AML poses therefore relevant clinical risks, as successful engraftment of those engineered T cells would lead to permanent ablation of hematopoiesis. All of these challenges might be overcome by using a versatile universal CAR T-cell technology approach, in which CAR T-cells via small molecules can be a) turned on and off and b) can be directed against multiple antigens. Here we describe a novel universal CAR-T strategy for the conditional killing of AML blasts, using the most promising target antigens emerging from a comparative immunological profiling of patient-derived material.

**Methods:**
We generated a lentiviral vector which incorporates the anti-fluorescein FluA CAR. Human CD117 was lentivirally expressed on human CD117 negative MOLM-13, MOLM-14 and HL-60 AML cells. Additionally, cell lines with endogenous expression of CD117, CD33 and CD371 were used as target cells. Antibody-derivatives in IgG1 or Diabody format directed against CD33, CD117 or CD371 were cloned, expressed and site-specifically or stochastically conjugated with fluorescein. Fluorescein-labelled antibodies were then tested as bridges between FluA CAR-Ts and various leukemia cells at an effector-to target ratio (E:T) of 1:1.

**Results:**
The expression of several AML antigens was assessed by flow cytometry on healthy and AML patient-derived samples. As shown before, CD33, CD117 and CD371 were expressed on healthy HSPCs as well as on leukemic blasts in the majority of AML patients. In vitro, CAR T-cells eliminated more than 90% of CD33+, CD117+ or CD371+ leukemia cell lines within 24 hours. Site-specifically fluoresceinated diabody bridges yielded the best cytotoxicity results over a broad range of antibody concentrations. With primary cells, autologous FluA CAR T-cells effectively depleted >60% of patient derived CD33+, CD117+ and CD371+ leukemic blasts within 24 hours. Aiming to minimize on-target off-tumor toxicity, different antibodies can be simultaneously administered at low concentrations to allow for a combinatorial and preferential accumulation at the tumor site. Simultaneous addition of two bridges – each one at its EC50 concentration – resulted in improved killing (>80% tumor cell lysis).

**Conclusion:**
We provide proof-of-concept for the generation of highly potent universal targeting FluA CAR T-cells from healthy donors and AML patients. By choosing suitable CAR-adaptors with respect to their conjugation chemistry and size, it is possible to tightly regulate CAR-T cell activity against CD33, CD117 and CD371 expressing AML cells and likely any tumor cell expressed antigen.

**244**

N. Miglino[2], R. Dummer[1], V. Heinzelmann[3], A. Theocharides[2], M. Manz[2], A. Wicki[2]

**Tumor Profiler (TuPro): a multi-omics tumor profiling platform to enable molecularly matched therapy prediction beyond genomics**

*Dept. of Dermatology USZ[1], Dept. of Medical Oncology and Hematology USZ[2], University Hospital Basel[3]*

**Introduction:**
Molecular tumor boards are institutional rounds to discuss treatment strategies for patients with newly diagnosed or advanced malignancies where approved treatments do not exist or options have been exhausted. In addition to routine imaging and standard immunohistochemistry, targeted Next-Generation Sequencing data are routinely generated to further investigate the molecular tumor profile to identify potential druggable molecular targets. However, NGS-based approaches analyze only genomic alterations from bulk tissue. The fast-paced advent of new high-throughput molecular and cellular omics platforms, capable of analysing several hundred to thousand parameters simultaneously on single-cell resolution, allows to comprehensively elucidate clinically-relevant questions beyond genomics, such as tumor micro-environment, heterogeneity and drug response. In this study, the Tumor-Profiler (TuPro) consortium explores to which extent a comprehensive in-depth profiling of tumors can enhance our understanding of the tumor biology and whether this information can be translated into clinical routine/decision making to predict the optimal molecularly matched therapy.

**Methods:**
The TuPro study includes patients with three different indications: melanoma (stage III/IV cutaneous and rare melanomas), ovarian carcinoma (high-grade primary or recurrent adenocarcinoma of ovarian, tubal, or peritoneal origin), and relapsed/refractory acute myeloid leukemia (AML) (n=240 patients in total). Tumor samples are analyzed by (i) Emerging Standard Diagnostics (Digital Pathology and Targeted Next-Generation Sequencing) and (ii) TuPro Exploratory Technologies (Single-cell Genomics and Transcriptomics, Bulk Transcriptomics, Proteotype Analysis, Mass Cytometry, Imaging Mass Cytometry, Pharmacoscopy, 4i Drug Response Profiling, NGS of cfDNA). Data integration and visualization is then executed for specifically designed molecular Tumor Boards.

**Results:**
To date tumor samples from >200 eligible patients are being analyzed by TuPro Exploratory Technologies in a fast diagnostic loop (2 weeks turn-around time from sample collection to analyses). The data are then integrated with the results from the Emerging Standard Diagnostics (targeted NGS panel sequencing and digital pathology), and clinical data to generate a Molecular Research Report (MRR) for the patient. The MRR is discussed in a pre-tumor board (pre-TB), where a multidisciplinary group of physicians generates treatment recommendations based on three levels of evidence: (I) standard clinical guidelines (ESMO) and routine diagnositcs; (II) level (I) plus Emerging Standard Diagnostics ; and (III) all previous evidence levels plus data from TuPro Exploratory Technologies. Recommendations based on level (III) are compiled into a synopsis to produce a Molecular Summary Report (MSR) for the Tumor Board.

**Conclusion:**
A quantitative assessment of the clinical utility will only be completed at the end of the study. However, we already observe a significant impact of the MRR and MSR on clinical decision making and (hypothetical) treatment recommendations in both pre-Tumor Boards and Tumor Boards. Furthermore, we show the feasibility of a comprehensive “omics-guided” treatment allocation for patients beyond standard of care with respect to (i) sample availability, (ii) data reproducibility/robustness and (iii) turn-around time within a clinically relevant time frame across all three entities. Therefore, we envisage establishing our multi-omics tumor profiling approach as a routine platform for patients with neoplasia and expected poor outcomes on current standard-therapy with the aim to enable future precision-medicine mediated curative approaches.

**245**

Z. Kotkowska[1, 2], P. Schineis[1], I. Kolm[2], Y. Waeckerle-Men[2], C. Halin[1], P. Johansen[2]

**Photochemical internalization (PCI): a novel vaccination method for induction of cytotoxic CD8 T-cell responses**

*ETH Zurich, Department of Chemistry and Applied Biosciences[1], University Hospital Zurich, Department of Dermatology[2]*

**Introduction:**
**Background:** Cancer is a public health matter and one of the leading causes of death worldwide. Cancer vaccines aim to stimulate anti-tumor immune response, especially cytotoxic T lymphocytes (CTLs). CTLs recognize tumor antigens presented on antigen presenting cells (APCs) in complex with major histocompatibility complex (MHC) class I molecules. One major problem of cancer vaccines is the inefficacious delivery of antigens to the MHC class I pathway of antigen presentation. Here, photochemical internalization (PCI) may bypass this problem based on the co-delivery of antigens and photosensitizer. Upon uptake into APCs, the photosensitizer localizes in the endosomal membranes. Subsequent light treatment causes activation of the photosensitizer and disruption of the membrane with release of the endosomal content into the cytosol for association to MHC class I.

**Objectives:** The primary objective is to develop PCI-based vaccination as a method for the stimulation of CTLs. As a secondary objective, the current project studies treatment-associated innate immune reactions in the skin.

**Methods:**
Mice received intradermal injections of photosensitizer or photosensitizer and antigen. Eighteen hours later, light was administered, and at various time points thereafter, skin and organs were harvested for analysis of immune responses. Antigen-specific CD8 T-cell responses were measured in the spleen by flow cytometry and ELISA, while the treated skin was characterized for innate immune responses by histology and fluorescence microscopy.

**Results:**
PCI improved proliferation of antigen-specific CD8 T cells and cytokine production as compared with PCI-free vaccination. Histological and microscopic analysis of the skin revealed light- and photosensitizer-dose-dependent innate inflammatory responses in the skin. The symptoms of inflammation observed in the treated skin included acanthosis, edema and infiltration of immune cells.

**Conclusion:**
The results demonstrate the PCI can facilitate proliferation and activation of antigen-specific CTLs. The results further suggest that early innate immune responses may be an important part of the mechanism of action of PCI-based vaccines, and further studies will focus on how these innate immune responses translate into effective anti-tumor CTL responses.

**246**

A. Kraft[1, 2], M. Meerang[2], M. Kirschner[2], V. Boeva[1, 3, 4], I. Opitz[2]

## Screening for extracellular vesicle-derived biomarkers for early detection of malignant pleural mesothelioma

*Computational Genetics and Epigenetics of Cancer Group, Department of Computer Science, Institute for Machine Learning, ETH Zurich, Zurich[1], Department of Thoracic Surgery, University Hospital Zurich, Zurich[2], INSERM, U1016, Cochin Institute, CNRS UMR8104, Paris Descartes University, Paris, France[3], Swiss Institute of Bioinformatics (SIB), Zurich, Switzerland[4]*

**Introduction:**
Malignant pleural mesothelioma (MPM) is an aggressive cancer of the mesothelial layer of pleura. Environmental and occupational exposure to asbestos is considered the main cause of MPM so far, but recent studies suggest exposure to carbon nanotubes, erionite fibers and therapeutic ionizing radiation may also be risk factors. The number of MPM cases worldwide is rising and is expected to peak between 2020-2025. Most cases are detected at a late stage and have very poor survival (6-12 months). Late diagnosis is a consequence of a long latency period (average 44 years) and non-specific symptoms. Imaging scans are insufficient for diagnosis and invasive tissue biopsies are not suitable for all patients. The standard treatment based on pemetrexed and cisplatin is relatively ineffective at increasing patients' survival. Early detection of the disease would likely increase treatment options and improve clinical outcomes. MiRNAs and RNAs encapsulated in extracellular vesicles have been shown to be relatively stable in the circulation, therefore can serve as potential blood-based diagnostic biomarkers. Our project is aimed at the identification of extracellular vesicle-derived biomarkers that could be used in blood-based diagnostic tests for early detection of MPM.

**Methods:**
We established primary cell cultures from pleural effusion of 4 MPM and 3 non-MPM patients. Extracellular vesicles from cell culture supernatants were extracted using Qiagen Exoeasy Maxi kit. RNA was extracted using the mirVana PARIS kit followed by transcriptome and small RNA sequencing. Small RNA and transcriptomic data was processed using exceRpt and Trimmomatic, respectively. Reads were mapped on the GRCh38 reference genome and gene counts were calculated using exceRpt and Kallisto. Transcriptomic counts were normalized using TMM normalization from edgeR and small RNA counts were normalized using rlog transformation from DESeq2. Differential gene expression analysis was performed on both datasets using edgeR and DESeq2. Genes with FDR <0.05 and log2 fold change >1 were selected as candidate MPM-biomarkers, which were then compared with TCGA MPM and ExoRBase data.

**Results:**
We identified 32 genes upregulated in MPM compared to non-MPM samples, including 16 protein coding genes, 10 lncRNAs and 3 miRNAs. All of the candidate biomarkers have been previously detected in exosomes from normal samples and breast, colorectal and pancreatic cancers. LncRNAs SCARNA10, SNHG17 and SNHG20 were already linked with higher exosomal expression in these cancers. SNHG15 was previously linked with worse overall survival in mesothelioma, while SNHG17 was associated with cell cycle progression and proliferation in a pan cancer study. SCARNA10, SNHG15, MAGEA3, MAGEA1, TAF1D, EIF4A2 and SNGH20 were upregulated in some of the MPM samples in the TCGA cohort. Our miRNA-biomarker candidate, hsa-miR-3648, was previously shown to be overexpressed in MPM. Moreover, we identified hsa-miR-30a-5p to be upregulated in MPM. Previous studies have reported miR-30 family to be one of the most enriched miRNA families in mesothelioma, with miR-30e-5p significantly associated with poorest survival.

**Conclusion:**
We identified extracellular vesicle-derived candidate biomarkers for MPM using primary cell cultures. More primary cells will be subjected to screening in the next months. We will further evaluate the level of candidate biomarkers using qPCR applied to matched plasma and tissue samples of already profiled samples. In further steps, we will validate our findings using additional patients' plasma samples.

**247**

L. Hänsch[4], M. Peipp[3], R. Myburgh[1], T. Weiss[4], F. Vasella[2], M. Manz[1], M. Weller[4], P. Roth[4]

**Characterizing CD317 as a novel target for chimeric antigen receptor (CAR) T cell therapy in glioblastoma**

*Department of Medical Oncology and Hematology, University Hospital Zurich and University of Zurich, Zurich, Switzerland[1], Department of Neurosurgery, University Hospital Zurich and University of Zurich, Zurich, Switzerland[2], Division of Stem Cell Transplantation and Immunotherapy, Department of Medicine, Christian-Albrechts-University, Kiel, Germany[3], Laboratory of Molecular Neuro-Oncology, Department of Neurology, University Hospital Zurich and University of Zurich, Zurich, Switzerland[4]*

**Introduction:**
Because of the limited success of current therapies for gliomas, novel therapeutic strategies are urgently needed. Chimeric antigen receptor (CAR) T cell-based therapies have resulted in clinical benefit in patients with hematological malignancies. However, targeting solid tumors such as glioblastoma with adoptively transferred T cells is more challenging. Here, we aimed at generating a CAR construct directed against CD317 (BST-2, HM1.24), a transmembrane protein, which is overexpressed by several types of tumors including gliomas. It may therefore serve as a novel target for CAR T cell therapy against glioblastoma.

**Methods:**
CD317-targeting CAR T cells were generated by genetic engineering of human T cells using lentiviral vectors. The anti-tumor activity of CD317-CAR T cells against various glioma cell lines with different antigen expression levels was verified in cell lysis assays. Finally, the anti-tumor activity of CD317-CAR T cells was determined in clinically relevant orthotopic xenograft glioma mouse models.

**Results:**
We successfully designed and generated a second-generation CAR construct targeting CD317. CD317-specific CAR T cells lysed significantly more target cells and expressed higher IFN-y levels than non-transduced T cells upon co-culture with antigen-expressing glioma cells. A CRISPR/Cas9-mediated CD317 knockout in glioma cells abrogated the sensitivity to CD317-specific CAR T cells. Since CD317 is also expressed by human T cells, we integrated a shRNA targeting CD317 into the CAR vector in order to down-regulate CD317 in T cells. Silencing of CD317 in CAR T cells restored their viability and expansion rate and increased their cytotoxic function by reducing fratricide and by decreasing T cell exhaustion. Local in vivo treatment with CD317-specific CAR T cells prolonged the survival and cured a significant fraction of glioma-bearing nude mice.

**Conclusion:**
We observed strong lytic activity of CD317-specific CAR T cells against various glioma cell lines in vitro and provide preclinical proof-of-concept of CD317-CAR T cell therapy in xenograft glioma models in vivo. Further investigation of additional tumor models, combination with other treatment modalities and a thorough evaluation of potential on-target off-tumor toxicities in syngeneic glioma models are required in order to translate this immunotherapeutic strategy into clinical neuro-oncology.

**248**

K. Slankamenac[1], F. Mathis[1], DI. Keller[1]

**Gender-specific differences in hypertensive crisis and the need for hospitalization**

*Institut für Notfallmedizin[1]*

**Introduction:**
Uncontrolled hypertension and its symptoms are common reasons for medical urgencies and emergencies. To date, little is known about gender-specific differences in hypertensive crisis. Therefore, the aim was to investigate gender-specific differences in the prevalence of hypertensive crisis, its management, and outcome in patients presenting to a tertiary care emergency department (ED).

**Methods:**
In a retrospective study, we enrolled consecutively all ED patients with uncontrolled hypertension from January to December 2018 if blood pressure values of ≥180 mmHg systolic and/or ≥110 mmHg diastolic were measured at home, by emergency medical service or at arrival at the ED.
The primary endpoint investigated gender-specific differences in the prevalence of hypertensive crisis. Furthermore, the management and outcome of hypertensive crisis as well as risk factors for hospitalization and recurrence were evaluated. Descriptive, univariate and multivariable logistic regression models were used.

**Results:**
In total, 44'661 patients visited the ED in 2018. Two hundred sixty patients (0.6%) presented with hypertensive crisis. The majority of these patients (96.9%) presented in the ED due to symptoms of hypertensive urgency while eight patients (3.1%) sustained a hypertensive emergency.
There were no gender-specific differences in the prevalence, management or outcome of hypertensive crisis. However, female patients presented significantly more often with headache (adjusted OR 1.9, 95% CI 1.1 – 3.3, p=0.022).
Calcium-channel blockers (43.1%) alone or in combination with transdermal nitrates (34.3%) were most commonly administered to treat hypertensive crisis during the ED stay whereas alpha-blockers (13.1%) or diuretics (7.3%) were used less frequently.
Some risk factors were associated with an increased risk of hospitalization: increased age over 72 yrs. (adjusted OR 3.5, 95% CI 1.7 – 7.1, p=0.002), persistently elevated systolic blood pressure (≥ 150 mmHg) despite drug treatment in the ED (adjusted OR 3.3, 95% CI 1.6 – 6.6, p=0.001), increased Charlson co-morbidity index (≥4) (adjusted OR 3.6, 95% CI 1.8 – 7.3, p<0.001), pre-existing chronic kidney (adjusted OR 2.6, 95% CI 1.1 – 5.7, p=0.023) or pre-existing coronary heart disease (adjusted OR 3.5, 95% CI 1.4 – 8.8, p=0.007).
Thirty-one patients (11.9%) re-presented to the ED after a median of six days (IQR 2 – 58) due to recurrence of uncontrolled hypertension, caused by non-compliance in only five patients (1.9%). Protective or risk factors for recurrence, e.g. errors in prescription and instruction of antihypertensive therapy at time of discharge after initial presentation, could not be identified. A trend towards follow-up examinations by the general practitioner as a protective factor for recurrences (p=0.087) can be supposed.

**Conclusion:**
Gender-specific differences in the prevalence, management or outcome of hypertensive crisis were not found, indicating an equivalent treatment of both genders in an acute situation. Vulnerable patients mainly showed the need for hospitalization due to hypertensive crisis when they were older and multimorbid. Recurrence of uncontrolled hypertension occurs in one in ten ED patients and is not primarily caused by non-compliance.

**249**

A. Fischer[1], S. Hiltbrunner[1], L. Bankel[1], C. Britschgi[1], M. Rechsteiner[2], J. Rüschoff[2], E. Rushing[2], A. Laure[1], S. Kasser[1], A. Curioni-Fontecedro[1]

**Targeted treatments should be offered to patients with advanced non-small cell lung cancer harboring MET aberrations, despite abundance of co-mutations.**

*Department of Medical Oncology and Hematology, University Hospital Zurich[1], Institute of Pathology and Molecular Pathology, University Hospital Zurich[2]*

**Introduction:**
*MET* exon 14 skipping mutations occur in 3-4% and *MET* gene amplification in 3-5% of non-small cell lung cancer (NSCLC) patients. Several tyrosine kinase inhibitors (TKIs) of MET have recently developed and showed promising results in patients with oncogenic *MET* alterations. MET overexpression detected by immunohistochemistry can occur in absence of genetic *MET* aberrations, therefore better screening tools are necessary to identify this patients' population and to ultimately guide treatment decisions.

**Methods:**
We retrospectively identified 188 advanced stage NSCLC patients treated at the University Hospital Zurich with available MET immunohistochemistry (IHC) results and identified those harboring genetic MET aberrations. Available next-generation sequencing (NGS) data were evaluated. We identified the cases harboring genetic *MET* aberrations and analyzed these in association with co-occurring mutations, PD-L1 expression and response to treatment.

**Results:**
From 188 patient's samples, 94 were positive for MET IHC (50%); PD-L1 expression was available from 131 patients, here, 69 samples typed positive for PD-L1 with a cutoff of 1% on tumor cells (53%). From 109 tumors, NGS was available. *MET* exon 14 skipping alterations were identified in 16 (15%), *MET* amplifications in 11 (10%) and another oncogenic *MET* mutation in 1 (1%) sample. 93% of tumors with genetic *MET* aberrations overexpressed MET. *MET* exon 14 skipping alterations, in absence of MET overexpression, occurred in one squamous cell carcinoma and one pleomorphic carcinoma. 80% (12/15) of tumors harboring *MET* exon 14 alterations and 63% (7/11) of *MET* amplified tumors expressed PD-L1 compared to the ones with no aberrations, namely 50% (29/58) of MET IHC positive and 43% (20/46) of MET IHC negative tumors. Tumors harboring *MET* exon 14 skipping alterations were significantly more likely to express PD-L1 than MET wildtype IHC positive (p=0.045) and MET IHC negative tumors (p=0.016). 75% of tumors with *MET* aberrations harbored oncogenic co-mutations or copy number variations. *TP53* (36%) was the most frequent co-mutation followed by *EGFR* (18%), *KRAS* (14%), *BRAF* (14%) and *CDK4* (14%). The most frequent oncogenic mutations in wildtype MET IHC positive tumors were *KRAS* (48%) followed by *TP53* (18%) and *CKDN2A* (13%).
Out of 28 patients with *MET* aberrations, 15 received treatment with at least one MET TKI. Median progression free survival on MET TKI therapy was 9 weeks (4 - 23 weeks) and 21 weeks (18 - 43 weeks) for patients with *MET* exon 14 skipping alterations and *MET* amplification, respectively. In two patients with *MET* exon 14 alterations and two patients with *MET* amplification prolonged response to immunotherapy (pembrolizumab or nivolumab) was observed.

**Conclusion:**
We demonstrate that neither *MET* exon 14 skipping alterations nor *MET* amplification are mutually exclusive events to other oncogenic alterations. As *MET* alterations are not routinely tested in NSCLC patients, our study suggests to include MET IHC as screening tool and then, to perform NGS to guide treatment decision. Our results further indicate that despite the abundance of co-mutations, patients with *MET* aberrations should be offered target treatments.

**250**

L. Bankel[2, 5], R. Wegmann[5], K. Dedes[1], D. Franzen[4], K. Bode[3], H. Moch[3], M. Manz[2], C. Britschgi[2], B. Snijder[5]

## Early results of a single-cell ex vivo drug response testing platform on fluid samples from patients with solid tumors

*Department of Gynecology, Comprehensive Cancer Center Zurich, University Hospital Zurich[1], Department of Medical Oncology and Hematology, Comprehensive Cancer Center Zurich, University Hospital Zurich[2], Department of Pathology and Molecular Pathology, Comprehensive Cancer Center Zurich, University Hospital Zurich[3], Department of Pulmonology, Comprehensive Cancer Center Zurich, University Hospital Zurich[4], Institute of Molecular Systems Biology, ETH Zurich[5]*

**Introduction:**
In patients with metastatic malignancies there is an urgent need for predictive biomarkers. Fluids containing tumor cells, like pleural effusion or ascites, are easily accessible and could potentially provide information on drug sensitivities *ex vivo*.

**Methods:**
Image-based single-cell drug response testing (pharmacoscopy) on fluid samples containing malignant cells is used to investigate drug response variability on an intra- and interpersonal level. A population of malignant and healthy cells is incubated with a drug panel for 24 hours. After staining with fluorescent antibodies, cells are imaged using automated microscopy. A convolutional neural network (CNN) infers cell types directly from single-cell images. Eventually, data will be correlated with clinical response.

**Results:**
So far, the clinical cohort includes 130 samples from 86 patients. 71% of included samples had a sufficient viability and cancer cell content to be analyzed. Our CNN, which was trained on curated single-cell images from all biopsies, accurately discriminated cancer cells from healthy immune cells. In multiple patients, pharmacoscopy was repeated on specimens taken within a short period of time, for which we observed a high intra-individual reproducibility of the drug response profiles. Taken together, these results highlight the technical feasibility and robustness of pharmacoscopy on fluid biopsies.
At this early stage of this study, we want to highlight one case of a patient with BRAF p.V600E mutated lung adenocarcinoma. Combined tyrosine kinase inhibition with dabrafenib (BRAF inhibitor) and trametinib (MEK inhibitor) was started and resulted in a partial response. In parallel, pharmacoscopy predicted an *ex vivo* response to dabrafenib, ranking highest as the most effective drug.

**Conclusion:**
Pharmacoscopy on fluid samples is a feasible diagnostic tool to test drug responses. Integration of drug response profiles and morphological profiles with molecular analyses comprising genomic profiling and transcriptomics will provide further insights into the molecular mechanisms underlying drug response variability.

**251**

C. Magnani[3], R. Myburgh[3], N. Russkamp[3], S. Pascolo[2], A. Müller[3], D. Neri[1], M. Manz[3]

**anti-CD117 CAR T cells demonstrate potent anti-leukemic activity against acute myeloid leukemia and ablate human normal hemopoiesis in vivo**

*Department of Chemistry and Applied Biosciences, Institute of Pharmaceutical Sciences, ETH Zurich, Comprehensive Cancer Center Zurich (CCCZ), Zurich[1], Department of Dermatology, University Hospital Zurich and University of Zurich, Zurich[2], Department of Medical Oncology and Hematology, University Hospital Zurich and University of Zurich, Comprehensive Cancer Center Zurich (CCCZ)[3]*

**Introduction:**
AML arises from the accumulation of mutations within the hematopoietic stem and progenitor cells (HSPC), leading to the emergence of a heterogeneous population of malignant leukemia-initiating cells (LIC). AML-LIC maintain high phenotypic similarity with their cells-of-origin and play a key role in post-treatment relapse. Immunotherapy with chimeric antigen receptor (CAR) T cells is an innovative approach to tackle relapsed forms of cancer. We recently proposed the use of CAR T cells specific for the CD117 antigen to deplete LIC and replace HSPC by allogeneic hematopoietic stem cell transplantation (HSCT). Here, we exploit the non-viral technology for the generation of anti-CD117 CAR T cells incorporating a safety switch.

**Methods:**
We designed a Sleeping Beauty (SB) transposon vector that includes the inducible Caspase 9 (iC9) switch and the anti-CD117CAR, separated by 2A peptide. The system uses the pT4 SB vector that has optimized the donor vector architecture and allows for the stoichiometric expression of the two transgenes, with iC9 upfront to the CAR. iC9 allows for rapid termination of CAR T cells by activation of the apoptotic pathway in case of treatment with a small molecule that acts as a chemical inducer of dimerization (CID). Transgene integration has been achieved using the hyperactive SB100X transposase, which provides improved transposition efficiency, supplied as mRNA. As an alternative, mRNA encoding anti-CD117 CAR was electroporated in human T cells.

**Results:**
CAR T cells generated with SB had a high level of viability, were mostly CD8+, with a naïve-like phenotype, retaining a high proportion of T stem cell memory population and with low levels of the exhaustion markers PD1, LAG3, and TIM3. Anti-CD117 CAR T cells exhibited potent cytotoxic activity against the AML cell line MOLM-14, transduced, and sorted to express human CD117, luciferase, and GFP. The addition of 200nM of the CID AP20187 to cultures of anti-CD117 CAR T cells induced apoptosis of transduced CAR T cells within 24h but had no effect on the viability of non-transduced cells. Anti-CD117 CAR T cells mediated depletion of CD117+ MOLM-14 cells in vivo, leading to a significant survival advantage compared to control CAR T cell-treated mice. SB-transduced CAR T cells were as efficient as CAR T cells transduced with lentiviral vectors. In mice reconstituted with human CD34+ cord blood, anti-CD117 CAR T cells were able to achieve complete CD117+ HSPC depletion after two weeks of treatment. Treatment with a combination of CID and ATG completely eliminated anti-CD117 CAR T cells and T cells of the previous transplant donor. Finally, transient expression of anti-CD117 CAR by mRNA conferred T cells the ability to kill CD117+ HL-60 target cells throughout 72 hours post mRNA electroporation. The cytotoxic activity decreased overtime as mRNA-electroporated CAR T cells proliferate and correlated with CAR expression. Treatment of humanized NSG mice with two subsequent doses of anti-CD117 CAR mRNA T cells resulted in HSPC depletion.

**Conclusion:**
Anti-CD117 CAR T cells engineered with the SB vector showed anti-leukemic activity and completely depleted healthy HSPC in vivo. iC9 transgenes induced CAR-T cell apoptosis and allowed rapid depletion of CAR T cells that alternatively also could be achieved with mRNA electroporation of anti-CD117 CAR. The ability to control CAR T cell pharmacokinetic properties is attractive to enable subsequent HSCT and in case of unexpected toxicities. Anti-CD117 CAR T cells could be used prior to HSCT in refractory AML.

**252**

S. Dudli[1, 3], I. Heggli[1, 3], L. Guidici[5], R. Schüpbach[6], N. Farshad-Amacker[4], N. Herger[1, 3], A. Juengel[1, 3], M. Betz[2], J. Spirig[2], F. Wanivenhaus[2], N. Ulrich[2], F. Brunner[3], M. Farshad[2], O. Distler[1, 3]

**Type III collagen is a hallmark of the fibrotic pathomechanism in Modic type 1 changes and is linked to myofibroblast differentiation**

*Center of Experimental Rheumatology, Department of Rheumatology, University Hospital, University of Zurich, Switzerland[1], Department of Orthopeadic Surgery, Balgrist University Hospital, ZuriUniversity of Zürich, Switzerland[2], Department of Physical Medicine and Rheumatology, Balgrist University Hospital, University of Zurich, Switzerland[3], Department of Radiology, Balgrist University Hospital, University of Zurich, Switzerland[4], Institute of Pathology and Molecular Pathology, University Hospital Zurich, Switzerland[5], Unit of Clinical and Applied Research, Balgrist University Hospital, University of Zurich, Switzerland[6]*

**Introduction:**
Modic changes (MC) are specific for chronic low back pain. Despite the high prevalence of MC, the histopathology of MC remains poorly understood. There are only two historical studies that describe MC histology based on the analysis of three hematoxylin/eosin stained biopsies. They described Modic type 1 changes (MC1) as vascularized fibrous tissue and Modic type 2 changes (MC2) as fibrotic adipose marrow replacement. While fibrosis seems to be important in MC1 and MC2, no molecular data is available that would help to understand the MC pathomechanism. The aim was to characterize MC histopathology with histology and immunohistochemistry (IHC) to better understand MC pathomechanism.

**Methods:**
From patients undergoing lumbar spondylodesis, vertebral bone marrow biopsies (n=4 MC1, n=4 MC2, n=6 control) were taken through pedicle screw trajectory before screw insertion. Intraoperative X-ray confirmed correct placement of biopsy needle. MC and degeneration of the adjacent disc were rated by an experienced radiologist based on T1- and T2-weighted MR images. Fixed biopsies were analyzed with histology and IHC. Histology/IHC: sections were stained histologically with eosin/hematoxylin to assess cellularity and edema (seen as interstitial water), and with Masson trichrome to assess connective tissue. IHC staining for type I and type III collagen, and cellular fibronectin was done to assess fibrosis. Bone marrow stromal cells (BMSC) were quantified with CD90 staining and myofibroblasts were quantified with alpha smooth muscle actin (aSMA) staining. Tissue sections were scored (0-3) by an experienced pathologist. Scores were compared between different groups (MC1, MC2, Ctrl) using Kruskal-Wallis test with Holm's p-value adjustment.

**Results:**
There was no difference between groups in mean age 65±14 years (p=0.63) and sex (11/14 male, p=0.99) of the patients. Discs were all strongly degenerated (Pfirmann grad 4-5) in all groups (p=0.90). MC1 had more type III collagen (MC1=1.75, Ctrl=0.75, p=0.03), that was located interstitially (IS) and in basement membranes of vascular sinusoids (VS) (Fig. a-b). MC1 also had more CD90-positive stromal cells (MC1=1.25, Ctrl=0, p=0.01) (Fig. a,c) and more aSMA-positive myofibroblasts (MC1=0.5, Ctrl=0, p=0.06) (Fig. a,d). No elongated CD90 or aSMA positive cells were found in Ctrl biospies. Type I collagen also tended to be more abundant in MC (MC1=1.0, MC2=1.2, Ctrl=0.5, p=0.12). No significant differences were found with the other stains and for all stains in MC2.

**Conclusion:**
We found that collagen type III is an important mediator of MC1 bone marrow fibrosis. This may be linked more BMSC and the occurrence of myofibroblasts in MC1. Type III collagen turnover has recently been suggested as biomarker for MC. Here, we provide face validity for such serum biomarker. More BMSC and myofibroblast in MC1 indicate BMSC proliferation and their differentiation into pro-fibrotic myofibroblasts. In conclusion, fibrosis is an important pathomechanism in MC1 that should be targeted in biomarker studies and anti-fibrotic treatment approaches targeting BMSC should be considered.

**253**

M. Meerang[1], J. Kreienbühl[1], V. Orlowski[1], S. Müller[1], M. Kirschner[1], I. Opitz[1]

**Importance of Cullin4 Ubiquitin Ligase in Malignant Pleural Mesothelioma**

*Department of Thoracic Surgery, University Hospital Zürich, Zürich, Switzerland[1]*

**Introduction:**
Malignant pleural mesothelioma (MPM) is primarily driven by loss of tumor suppressor genes. In this study, we explored importance of cullin4 (CUL4; 2 paralogs, CUL4A and CUL4B), a member of the cullin protein family that have been shown to be dysregulated in MPM as a consequence of tumor suppressor gene NF2 loss. We also evaluated the efficacy of the cullin inhibition by pevonedistat, a small molecule inhibiting cullin neddylation.

**Methods:**
We assessed the expression of CUL4A and CUL4B in tissues using immunohistochemistry (IHC) and quantitative real time PCR. We tested the efficacy of pevonedistat in 13 MPM cell lines in 2D and 3D culture compared to non-malignant mesothelial cells. Four groups of severe combined immunodeficiency SCID mice (n=8/group) bearing intraperitoneal (ip.) pevonedistat sensitive (MSTO211H) or resistant (ACC-Meso1) cell lines were treated with pevonedistat (50 mg/kg; ip.) on a 5day on/5day off schedule for 3 cycles. Treatment efficacy was assessed by means of overall survival. To evaluate the mechanism of treatment, additional groups of mice (n=5/group) were treated for one cycle followed by tissue collection and analysis.

**Results:**
Gene expression of CUL4A and CUL4B were upregulated in MPM tumor specimens compared to non-malignant pleural tissues. Data from the TCGA MPM cohort revealed that high CUL4B gene expression was associated with short disease free survival. Accordingly, using IHC on tissue microarray, we demonstrated that high CUL4B protein expression was associated with short progression free survival of MPM patients. Five MPM cell lines (38%) were highly sensitive to cullins inhibition by pevonedistat (IC50<0.5 µM). This remained true in 3D spheroid culture. The treatment induced S/G2 cell cycle arrest and accumulation of cells undergoing DNA rereplication (containing >4N DNA content) more predominantly in the sensitive cell lines. DNA rereplication is known to be mediated by CDT1 accumulation and indeed the accumulation of CDT1 was detected after the treatment. Nevertheless, there was no difference in the extent of CDT1 accumulation comparing between sensitive and resistant cell lines. In vivo, pevonedistat treatment significantly prolonged survival of mice bearing both sensitive (MSTO211H) and resistant (ACC-Meso-1) MPM tumors. Pevonedistat treatment reduced growth in pevonedistat sensitive tumor but increased apoptosis in pevonedistat resistant tumor. Thus, we analyzed cells associated with tumor microenvironment including mouse macrophage (F4/80+) and vessel formation (CD31+) that may explain the efficacy of pevonedistat in the resistant model. The treatment significantly reduced numbers of tumor associated macrophage in resistant tumors, while it showed no effect in sensitive tumors. The treatment did not alter polarization of macrophage as shown by no change in the expression of Arginase1, a marker of immunosuppressive M2 macrophage, after treatment. There was no effect on blood vessel formation in both tumor models at this time point.

**Conclusion:**
High CUL4B expression may play a role in MPM progression. Inhibition of cullins by pevonedistat induced growth arrest and DNA re-replication in a subset of MPM. Pevonedistat showed favorable effect for MPM treatment in vivo, even for a resistant tumor model. This effect may be mediated by reduced tumor-associated macrophage infiltration.

**254**

S. Fazio[2], S. Isringhausen[2], M. Chambovey[2], B. Ludewig[1], C. Nombela-Arrieta[2]

**Unraveling the role of a novel subtype of bone marrow mesenchymal stromal cell in healthy and pathological hematopoiesis**

*Institute of Immunobiology, Kantonal Hospital St. Gallen[1], University Hospital and University of Zürich[2]*

**Introduction:**
The orchestration of hematopoiesis is highly dependent on local cues derived from the bone marrow (BM) stromal microenvironment. Among BM stromal components, mesenchymal cells, termed CXCL12-abundant reticular cells (CARc), have been best characterized for their role in hematopoietic stem cell (HSC) maintenance and progenitor differentiation. Once regarded as a homogenous pool of cells, recent single-cell sequencing data suggest that CARc include a number of distinct subsets with potentially distinct functional properties. However, the identity, spatial distribution, and roles in the control of hematopoietic development of different subpopulations of these cytokine-producing cells remain poorly understood.

**Methods:**
In this project, we aim to study a specific fraction of CARc, which is stably labeled in the CXCL13-Cre/ROSA26YFP mouse model (designated hereon as CXCL13-YFP$^+$). We will assess this novel subtype in detail, determining its frequencies, localization, and interactions with other cell types using 3D quantitative microscopy and describe their transcriptomic landscape via scRNA-seq. To evaluate their functional relevance for the hematopoietic compartment, we will use genetic models to specifically delete the expression of key supportive cytokines in CXCL13-YFP$^+$ cells and assess the potential effects on HSC fitness and hematopoietic regulation during homeostasis and inflammation-induced hematopoiesis.

**Results:**
Preliminary results demonstrate that CXCL13-YFP$^+$ CARc are found distributed throughout the entire BM parenchyma, displaying a subtle tendency to accumulate in periendosteal and metaphyseal BM regions, and do not increase in numbers during the ageing process, as visualized via 3D microscopy.

**Conclusion:**
Altogether, these studies will provide new nuanced insights on the faceted regulatory activities of BM mesenchymal stroma in healthy and pathological BM function.

**255**

O. Eichhoff[2], P. Cheng[2], N. Yumi[1], P. Turko[2], S. Freiberger[2], C. Stoffel[2], J. Käsler[2], R. Dummer[2], M. Levesque[2]

**Establishment of primary melanoma cell cultures with c-Kit mutations enables the development of novel pharmacological treatment options for patients with ALM**

*Kyoto University Hospital[1], University Hospital Zurich[2]*

**Introduction:**
In recent years, new targeted therapies have drastically improved the prognosis of malignant melanoma patients with MAPK mutations. However, those without MAPK mutations still have few treatment options in their advanced stages. Mutations in the receptor tyrosine kinase (c-kit) has been reported in melanoma patients, especially in the acral lentiginous melanoma (ALM) subtype, which is known as the most clinically malignant. It has been demonstrated that cancer cells harboring a Kit mutation are sensitive to the tyrosine inhibitors such as Imatinib, leading to several clinical trials but without significant clinical outcome. In contrast to cutaneous melanoma, in which successful treatment strategies for patients with metastatic disease have been established, late stage ALM patients have a poor survival prognosis whether treated or not.
This lack of treatment options for late stage ALM patients is also due to the lack of viable cell culturing techniques, which are the basis of drug-screenings and mouse models. Only few publications have employed established ALM cell cultures, but frequently without c-Kit mutations. Maintaining melanoma cells harboring c-Kit mutations in culture remains challenging.
Here we have successfully established five primary cell cultures derived from metastatic sites of ALM patients with confirmed c-Kit mutation. These in vitro tools are urgently needed in order to develop new protocols for the treatment of metastatic ALM patients.

**Methods:**
We have established five melanoma cell cultures with confirmed c-Kit mutations derived from surplus surgery material of consenting patients, using a special growth medium containing the c-Kit receptor ligand SCF (stem cell factor). We have gnomically and transcriptionally analyzed these primary cell cultures, in addition to tumor material, elucidating distinct cellular phenotypes. We further established in vitro assays (e.g. viability assays, migration assays) using these patient-derived primary ALM cell cultures. Furthermore, we conducted a high-throughput viability drug screening with 466 clinical compounds in order to find new potential therapeutic targets for the treatment of ALM patients with confirmed c-kit mutations.

**Results:**
All of our established ALM cell cultures with confirmed c-Kit mutations showed a dependency on the addition of SCF into the growth medium, where c-Kit receptor activation could be confirmed by protein analysis. Moreover, SCF is not only required for the maintenance of growth kinetics, but also for cell motility. Single-cell RNA sequencing of tumor material also confirmed that in vivo the SCF is not produced by the cancer cells themselves, suggesting a paracrine signaling. Next generation sequencing of hot-spot mutations using a melanoma-specific primer panel (Mel-Array) also revealed other oncogenic mutations alongside c-kit (e.g. loss of NF-1, CDKN2A deletions or c-Kit gene amplifications) in the ALM cell cultures as well as in the corresponding tumor material. High-throughput screening of the clinical compound library highlighted PI3K/mTOR inhibitors, HSP90 inhibitors or CDK inhibitors as potential candidates for the treatment of ALM patients.

**Conclusion:**
Up to date ALM remains a difficult to treat melanoma subtype and in vitro tools are urgently needed to change this situation for the patient. With the development of a viable ALM in vitro cell culture system, and the evaluation of potential new drug targets (which can be tested in human Xenograft models in the future), our work will enable a route towards novel therapeutic strategies for patients with c-kit mutated melanomas.

**256**

J. Jang[4], M. Haberecker[4], A. Curioni-Fontecedro[4], A. Soltermann[4], I. Gil-Bazo[1], F. Janker[4], I. Hwang[2], K. Kwon[2], W. Weder[4], W. Jungraithmayr[3]

**CD26/DPP4 - a novel prognostic marker for lung adenocarcinoma**

*Clinica Universidad de Navarra[1], Keimyung University Dongsan Medical Center[2], University Hospital Freiburg[3], University Hospital Zürich[4]*

**Introduction:**
CD26/dipeptidyl peptidase 4 (CD26/DPP4) is an exopeptidase expressed on a variety of malignancies and is associated with epithelial-mesenchymal transition (EMT). We found previously that the activity of CD26/DPP4 in human lung cancer is four times higher than in normal lung tissue and the inhibition of CD26/DPP4 decreased the growth of lung tumors in experimental models. These data prompted us to analyze large number of clinical samples for the expression of CD26/DPP4 and EMT markers in non-small cell lung cancer to unravel the function of CD26/DPP4 as a prognostic marker and potential therapeutic target for lung cancer.

**Methods:**
We employed tissue micro array (TMA) of non-small cell lung cancer patients from two institutions, University Hospital Zurich and Dongsan Medical Center. To identify CD26/DPP4 and EMT markers (Ecadherin, Vimentin, beta-Catenin, Elastin, Periostin, and Versican), immunohistochemistry (IHC) on TMA was performed. Three pathologists scored the intensity IHC from zero to six in a blinded manner. The cohort consisted of 1126 patients (adenocarcinoma: 593; squamous carcinoma: 443; others (large cell carcinoma, adeno-squamous carcinoma): 90). The overall survival rate of patients was considered as a measure of prognosis. To identify a correlation between CD26/DPP4 and EMT related protein expression in lung cancer the Pearson correlation coefficient test was applied.

**Results:**
CD26/DPP4 IHC score data revealed that adenocarcinoma expresses significantly higher amount of the protein compared to normal lung or squamous carcinoma or others ($p=0.035$, $p<0.0001$, $p<0.0001$ respectively). In adenocarcinoma, patients with high CD26/DPP4 score (4-6) showed the worst overall survival compared to patients scoring low (1-3) or zero. The correlation analysis of CD26/DPP4 with EMT markers in adenocarcinoma showed that the epithelial marker Ecadherin was negatively correlated ($p=0.001$), while mesenchymal proteins Vimentin, beta-Catenin, Elastin were positively correlated with CD26/DPP4 ($p=0.03$, 0.01, and 0.001 respectively). Periostin and Versican showed no correlation with CD26/DPP4 expression.

**Conclusion:**
The expression of CD26/DPP4 was significantly higher in adenocarcinoma among non-small cell lung cancers and associated with worse survival of adenocarcinoma patients. Furthermore, the expression of CD26/DPP4 was significantly correlated with the EMT status. We therefore deem CD26/DPP4 to be a novel prognostic marker for lung adenocarcinoma. The inverse association of CD26/DPP4 expression and patient survival suffering from lung cancer suggests that the inhibition of CD26/DPP4 can potentially restrict lung cancer and improve patients' survival.

**258**

Y. Zhang[1, 2], F. Schläpfer[2], V. Orlowski[2], I. Opitz[2], M. Kirschner[2]

**Evaluating the role of microRNAs in chemotherapy response of malignant pleural mesothelioma**

*Department of Thoracic Surgery, the 2nd Hospital of Jilin University, China[1], Department of Thoracic Surgery, University Hospital Zurich, Switzerland[2]*

**Introduction:**
Predicting the response of malignant pleural mesothelioma (MPM) patients to platinum-based chemotherapy, the current gold-standard for MPM, remains a challenge as no reliable predictive marker has been identified thus far. Applying microRNA profiling to tumour tissue of responders and non-responders to induction chemotherapy before extrapleural pneumonectomy, we identified candidate predictive microRNAs. Candidates from this profiling are now investigated in vitro for their potential to alter the response of MPM cell lines to cisplatin and/or pemetrexed.

**Methods:**
Commercially available MPM cell lines MSTO-211H, H28, Meso1, and Mero82 were reverse transfected with mimics of microRNAs that showed differential expression in responders and non-responders to cisplatin-pemetrexed chemotherapy. 24h post transfection, cells are treated with increasing concentrations of cisplatin or pemetrexed for 72h or 120h, at which point the effect on cell growth is being assessed.

**Results:**
Initial analyses of five candidates revealed that five days post transfection, overexpression of miR-380-5p resulted in at least 40% decreased cell growth in all investigated MPM cell lines. Similarly, miR-221-3p overexpression resulted in reduced cell growth (minimum 30%) in all investigated cell lines. Further, the effect of overexpression of miR-380-5p and miR-221-3p on response to cisplatin and pemetrexed was investigated. For cisplatin, we observed that overexpression of a microRNA can indeed result, in a subset of cell lines, in increased sensitivity. This effect was most pronounced for miR-221-3p, for which we saw significantly lower IC50 values in MSTO-211H (IC50 17.59 vs 2.65, $p<0.001$) and Meso1 (IC50 21.59 vs 5.54, $p<0.001$). Furthermore, in Meso1 cells, overexpression of miR-380-5p, also resulted in a significant increase in sensitivity to cisplatin (IC50 21.59 vs 10.36, $p=0.045$), while in Mero82 cells, overexpression of miR-30e-5p increased the cisplatin sensitivity (IC50 4.35 vs 1.76, $p<0.001$). Interestingly, when we overexpressed miR-221-3p, the microRNA with the strongest sensitising effect towards cisplatin, in the same cell lines, we could observe a trend towards increased resistance against pemetrexed.

**Conclusion:**
First in vitro investigations of the effect of altered expression of microRNAs previously linked to response to cisplatin-pemetrexed chemotherapy, suggest that overexpression of these microRNAs has the potential to increase the sensitivity to cisplatin. Interestingly, preliminary data for pemetrexed suggest that some microRNA might render cells more resistant to this drug. Further evaluations of the response to the combined treatment as well as the effect of overexpression of additional microRNAs is currently underway.

**259**

L. Liberale[1], A. Akhmedov[1], Y. Puspitasari[1], A. Vukolic[1], F. Montecucco[2], J. Beer[1], T. Luscher[1], J. Jin[3], G. Camici[1]

**JCAD enhances arterial thrombosis by regulating endothelial plasminogen activator inhibitor-1 and tissue factor expression**

*Center for Molecular Cardiology, University of Zurich, Zurich, Switzerland[1], Department of Internal Medicine, University of Genoa, Genoa, Italy[2], Department of Medicine, University of Rochester School of Medicine and Dentistry, Rochester, NY, USA[3]*

**Introduction:**
Arterial thrombosis is the crucial event in most acute CV events including myocardial infarction (MI) and acute ischemic stroke. Variants in the *Junctional cadherin 5 associated* (*JCAD*, also known as *KIAA1462*) locus enhancing the expression of this protein were consistently shown to associate with increased risk of coronary artery disease and MI by multiple genome-wide association studies. JCAD is a protein highly expressed in endothelial cells where it was found to colocalize with VE-Cadherin being a component of cell junctions. Recently, JCAD was also shown to promote endothelial dysfunction, inflammation and atherosclerosis by acting on the Hippo pathway. Here we further investigated the effect of JCAD CV disease by exploring its putative role in arterial thrombosis.

**Methods:**
*Jcad* knock-out (*Jcad*-/-) mice were exposed to photochemically-induced carotid artery endothelial injury to trigger arterial thrombosis. To increase the translational value of our findings, primary human aortic endothelial cells (HAECs) treated with *JCAD* silencing RNA (si-*JCAD*) or control siRNA (si-SCR) and stimulated with tumour necrosis factor (TNF)-α were also investigated.

**Results:**
Compared to WT animals, *Jcad*$^{-/-}$ mice displayed reduced arterial thrombus formation following endothelial-specific damage. Pointing towards a blunted activation of the extrinsic coagulation cascade, Jcad$^{-/-}$ animals showed reduced tissue factor (TF) activity in carotid artery lysates as well as reduced level of arterial TF expression. Furthermore, augmented number of thrombus embolization episodes and increased circulating D-dimer levels suggested an increased activation of the fibrinolytic system in *Jcad*$^{-/-}$ mice. Indeed, *Jcad*$^{-/-}$ mice showed reduced vascular expression of the fibrinolysis inhibitor plasminogen activator inhibitor (PAI)-1. In HAECs, *JCAD*-silencing inhibited TF and PAI-1 gene and protein expression both at basal level and in response to TNF-α. Furthermore, endothelial cells lacking JCAD displayed increased levels of LATS2 Kinase, which blunts the Hippo pathway by increasing YAP phosphorylation. Accordingly, p-YAP levels were higher in *Jcad*$^{-/-}$ animals as compared to WT littermates.

**Conclusion:**
JCAD promotes arterial thrombosis by modulating coagulation cascade activation and fibrinolysis through endothelial TF and PAI-1. Whether JCAD also plays a role in platelet aggregation, the third pathway of arterial thrombosis, remains to be explored. Our findings support the importance of JCAD as a therapeutic target for CV prevention by showing for the first time its involvement in regulation of atherothrombosis.

**260**

S.L. Samodelov[1], K. Becker[2], K. Haldimann[2], Z. Gai[1], S.N. Hobbie[2], M. Visentin[1], G.A. Kullak-Ublick[1]

**Reduction of colistin-induced kidney injury by the vitamin-like compound L-carnitine in mice**

*Clinical Pharmacology and Toxicology, University Hospital of Zürich[1], Medical Microbiology, University Hospital of Zürich[2]*

**Introduction:**
Colistin is a polymixin antibiotic experiencing renewed clinical interest due to its efficacy in the treatment of multidrug resistant (MDR) bacterial infections. The frequent onset of acute dose-dependent drug-induced kidney injury (DIKI), with the potential of long-term renal damage, has limited its use and hampered adequate dosing regimens, risking serum values below bacterial Minimal Inhibitory Concentrations (MIC) during treatment. The mechanism of colistin-induced renal toxicity is largely unknown but postulated to stem from its specific accumulation in renal tissue, coupled with mitochondrial toxicity and reactive oxygen species (ROS) formation in proximal tubule cells (PTC). The vitamin-like compound L-carnitine is abundant in dietary meats and has protective properties against intracellular ROS as well as being able to positively affect membrane stability and cellular energy metabolism. In this study, the protective effects of L-carnitine on colistin-DIKI are studied on the subcellular, cellular, and whole organism level, using mice as a model.

**Methods:**
MIC assays for colistin in the presence and absence of L-carnitine were performed with MDR *E. coli* and *P. aeringinosa* strains. PTC from wildtype female C57/BJ mice were harvested and cultured for in vitro studies on ROS production, ER and mitochondrial stress, utilizing staining and imaging. Mitochondria were extracted from mouse kidneys and, using a rhodamine 123 dye, studies on mitochondrial membrane potential in the presence of one or both substrates were conducted. *In vivo* studies were completed by treating mice with either 20 mg/kg colistin sulfate, 30 mg/kg L-carnitine, both, or PBS as a control, for 7 days via *i.p.* injection. Histological examination of kidney sections was performed, as well as urine and serum analyses for several biomarkers of kidney injury. Accumulated colistin in kidney tissue was quantified in treated mice. A pharmacokinetic study was completed with colistin only or colistin and L-carnitine treatment over a time span of 4 h.

**Results:**
The antimicrobial activity of colisitin against MDR bacterial strains was not altered in the presence of L-carnitine, as MICs remained unchanged under all concentrations of L-carnitine tested. *In vitro* studies with colistin and L-carnitine in PTC showed induction of ER (GRP-78 staining) and mitochondrial stress (TOM20 and Rho123 stainings) under colistin treatment, with reduction upon cotreatment with L-carntine. Mitochondrial membrane potential studies showed a depolarization of mitochondria treated with colistin, which could be averted by cotreatment with L-carnitine. *In vivo* studies in mice treated with colistin showed marked signs of kidney injury upon immunuhistochemical analysis of kidney injury biomarkers Kim-1 and Ngal. Urinary elevations in Kim-1 and glucose were also noted, although serum creatinine was not increased, indicating early or subclinical kidney injury. Proximal tubule dilation, brush border disruption, and protein cast formation were observed in HE-stained kidney sections. Co-treatment with L-carnitine reduced but did not alleviate all markers and assessments of kidney function and damage analyzed. Colistin quantification in kidney tissue of treated mice revealed no differences in tissue accumulation between groups. Likewise, pharmacokinetics of colistin were not altered under co-treatment with L-carnitine.

**Conclusion:**
L-carnitine is able to protect mitochondria against colistin-induced depolarization, reducing both mitochondrial and ER stress on a cellular level. *In vivo*, cotreatment with L-carntine, under the conditions tested here, was able to decrease, but not completely protect, against colistin-DIKI. L-carnitine is a commonly used dietary supplement and found naturally in dietary protein. As no impact on colistin antimicrobial activity or pharmacokinetics could be observed under L-carnitine co-treatment, this supplement may aid in reducing kidney injury incurred during colistin treatment of severe MDR bacterial infections.

**261**

F. Lehner[1], S. Salemi[1], C. Millan[1], C. Kündig[2], T. Sulser[1], D. Eberli[1]

## Anti-tumor effect of a recombinant protease inhibitor targeting human kallikrein-related peptidase 2 in prostate cancer

*Department of Urology, University Hospital Zurich, Zurich, Switzerland[1], Med Discovery SA, Epalinges, Switzerland[2]*

**Introduction:**
Therapy options for castration-resistant prostate cancer (CRPC) are limited and mainly affecting the androgen axis. Kallikrein 3 (or prostate specific antigen, PSA), a chymotrypsin-like serine protease, is the current and in the blood detectable tumor marker for screening and monitoring prostate cancer (PCa) in clinics. As PSA, human kallikrein 2 (hK2) is a serine protease produced and secreted by prostate epithelial cells. The hK2 is a promising target for therapy of CRPC because of its high prostate tissue specificity and its expression rate correlates to the rising grade and stage of the PCa. Therefore, we hypothesize that the inhibition of hK2 can lead to suppression of tumor growth.

**Methods:**
Human PCa cell lines (PNT1A, LNCaP, C4-2, CWR1, PC3, DU145 and hK2 transfected DU145) were cultured in 2D and 3D to test hK2 expression. Immunoblotting (WES) of cell lysates and conditioned media was performed. Cells were then treated daily with MDPK67b (0.1, 0.5 and 1mg/mL), which is a recombinant protease inhibitor targeting hK2, or vehicle. Cell proliferation was measured by CellTiter-Glo assay.

**Results:**
Immunoblotting revealed protein expression of hK2 in LNCaP, C4-2 cell lines as well as in the transfected DU145 in both 2D and 3D models. However, increased expression of hK2 was observed in cells cultured in 3D compared to 2D after 3 days. The non-transfected DU145, which served as a negative cell line, did not express any hK2. Treatment with MDPK67b in the hK2 expressing cells led to a dose- and time-dependent cell death. The inhibitory effect on cell proliferation was observed from day 1, reaching its maximal effect at day 3 in all the cell lines. LNCaP showed a reduction of 50% cell proliferation with 1mg/mL of MDPK67b, whereas C4-2 and transfected DU145 cells were reduced by 30%. No relevant differences in cell proliferation of DU145 were observed after 3 days.

**Conclusion:**
Our study demonstrates that blockage of hK2 has a potent inhibitory effect in a dose- and time-dependent manner on cell proliferation in all tested PCa cell lines, which mimic the different types of PCa. Therefore, selective inhibition of hK2 might provide a valuable and new therapeutic approach independently of the androgen axis in CRPC and an attractive add-on to second-line therapies as of today.

**262**

A. Hariharan[1], M. Sculco[2], M. Ronner[1], E. Felley-Bosco[1]

**Oncogenic effect of RNA editing enzyme Adar2 in mesothelioma**

*Laboratory of Molecular Oncology, Department of Thoracic Surgery, University Hospital Zürich, Zürich, Switzerland[1], Unit of Health Sciences, University of Eastern Piedmont, Novara, Italy[2]*

**Introduction:**
Mesothelioma is a rare, aggressive cancer caused by asbestos exposure. In a mouse model of mesothelioma development, exposure to asbestos increased A-to-I RNA editing paralleled by an increase in RNA editing enzymes, adenosine deaminases acting on RNA (Adar1, Adar2). The destabilisation of double-stranded RNA (dsRNA) by Adar activity suppresses other mechanisms of dsRNA sensing such as Pkr-induced autophagy and interferon-stimulated inflammatory response. High *Adar2* and low interferon stimulated gene (ISG - *Ddx58*, *Ifitm1*, *Ifit2*) expression are associated with worst overall survival in mesothelioma patients.

**Methods:**
Adar2 knockout cell lines were developed from mouse RN5 mesothelioma cell line using CRISPR/Cas9 system. Single clones were characterised for Adars using sequencing, qPCR, and western blotting. The region flanking the RNA editing site of *Copa* (Adar2-specific editing target) was amplified using PCR and sequenced. A-to-I editing in the sequence was quantified using ImageJ software. Expression of ISGs were analysed by qPCR. Pkr signalling was analysed by western blotting. In-vitro assays - colony forming and spheroid building assay - were performed to follow cell growth. Spheroids were treated with pemetrexed (standard therapy for mesothelioma patients) and tested for cell viability using Cell Titer Glo.

**Results:**
*Adar2* functions as an essential gene. Hence, clones heterozygous for *Adar2* were isolated. qPCR and western blotting confirmed reduced Adar2 expression in two clones, which were selected for further characterisation. The clones showed a significant decrease in *Copa* editing compared to RN5 cells. The clones had increased Adar1 expression as well as ISG expression including interferon β. Western blotting showed increased Pkr phosphorylation followed by downstream activation of eIf2a. Colony forming and spheroid building assays showed that the clones grow slower compared to RN5 cells. In addition, increased sensitivity to pemetrexed treatment was observed in the clones compared to RN5 cells. A mechanism of resistance to pemetrexed is upregulation of dihydrofolate reductase (Dhfr), due to increased RNA editing by Adars, and the clones had reduced *Dhfr* expression compared to the RN5 cells.

**Conclusion:**
Adar2 contributes to increased cell growth in mesothelioma. Adar2 knockout upregulates type I interferon as well as Pkr signalling in mesothelioma. Adar2 may also play a role in the development of resistance towards pemetrexed in mesothelioma via the editing of *Dhfr*. Hence, Adar2 seems to have an oncogenic function in mesothelioma.

**263**

M. Wipplinger[1], A. Abukar[1], A. Hariharan[1], M. Ronner[1], E. Felley-Bosco[1]

**RNA binding motif protein 8a, a novel RNA editing target in mesothelioma**

*Laboratory of Molecular Oncology, Thoracic Surgery, University Hospital Zürich, Zürich,[1]*

**Introduction:**
Malignant Pleural Mesothelioma (MPM) is a rare, aggressive cancer caused by asbestos exposure. In a mouse model of mesothelioma development, exposure to asbestos increased A-to-I RNA editing paralleled by an increase in RNA editing enzymes, adenosine deaminases acting on RNA (ADAR1, ADAR2) and high ADAR2 levels are associated with worst overall survival in MPM patients. RNA binding motif protein 8a (RBM8a), a member of the Exon Junction Complex, functions as an essential gene in a BRCA-associated protein 1 proficient mesothelioma. A-to-I RNA editing in RBM8a increases upon asbestos exposure and high RBM8a levels are associated with the worst overall survival in MPM patients.

**Methods:**
We performed PCR using primers that specifically target the regions inside the RBM8A 3'UTR, which contains the editing sites. Sanger sequencing (Mycrosynth) was performed and A-to-I editing was determined using ImageJ software. Small interfering RNA (siRNA) was used to silence ADAR1 or ADAR2 in mesothelioma cell lines and editing levels were measured. mADAR2 was cloned into a pCi puro vector and normal mesothelial cells were transfected followed by measurement of RNA editing levels. RBM8A expression levels upon silencing ADAR 1/2 and ADAR2 overexpression were determined by qPCR and Western Blot.

**Results:**
RBM8As known A-I editing sites are located within ALU elements in the 3'UTR. In two of these ALU elements, we found significantly increased editing rate in MPM cells compared to normal mesothelial cells. By using siRNA mediated knockdown of either ADAR1 or ADAR2 we could significantly reduce the editing at certain sites, while ADAR2 overexpression in normal mesothelial cells increased editing and protein levels. We further observed that silencing ADAR1/2 had no effect on RBM8a mRNA expression but significantly increased protein levels in mesothelioma but not in normal mesothelial cells.

**Conclusion:**
We conclude that RNA editing seems to regulate RBM8A protein expression by possibly mediating the binding of RNA binding proteins (RBP) to the 3'UTR.

**264**

L. Russo[1], L. Roth[1], A. Gupta[1], K. Lehmann[1]

**Improving loco-regional treatment of peritoneal metastasis**

*Viszeral- und Transplantationschirurgie[1]*

**Introduction:**
Selected patients with peritoneal metastasis arising from colorectal cancer show survival benefits when treated with the combination of cytoreductive surgery (CRS) and hyperthermic intraperitoneal chemotherapy (HIPEC). Unfortunately, the limitation of this treatment is the recurrence of the disease, which is associated with poor prognosis and most likely the result of inefficient HIPEC treatment. Therefore, it is urgently needed to understand mechanisms behind loco-regional treatment in order to increase therapy efficacy. Previously, our lab could show that next to the cytotoxic effect of the treatment, HIPEC can induce immunogenic changes of cancer cells in vitro. To confirm these findings in-vivo, we have established a peritoneal metastasis (PM) mouse model. First, we will explore the effect of Oxaliplatin, standard HIPEC drugs in clinics, on the peritoneal tumor growth and the tumor microenvironment. Furthermore, we aim to find novel drug combinations, for example with immunotherapies or DNA damage signalling inhibitors to increase therapy efficacy and provide long-term control of PM-lesions, which will be selected from in-vitro studies.

**Methods:**
Female C57BL/6 mice were intraperitoneal injected with different numbers of cancer cell line MC-38 and the luciferase expressing cell-line LLC-Luc .To define tumor incidence and development, mice were sacrificed at different timepoints. In order to find the most reliable tool to quantify PM lesions, we compared different measuring methods like IVIS imaging, peritoneal cancer index (PCI) and l measuring the lesion size using a calliper.
In parallel, novel drug combinations were tested in vitro on human colorectal cancer cell lines. In order to find a more potent treatment, cells were treated with standard HIPEC drugs in combination with different DNA damage signalling inhibitors. Cell viability was measured with a Cell Titer Glo Assay.
The combination with immunotherapies was only tested in-vivo. Thereby, C57BL/6 mice were first injected s.c. with MC-38 cancer cells. As soon as a subcutaneous tumor could be measured (approx.10 days after tumor injection), mice were 3 times treated with a locoregional application of Oxa in combination with Anti-PD-1 Antibody. Tumor size was assessed every third day using a calliper. 21 days after tumor cell injection, mice were sacrificed and s.c. tumors harvested to determine the immune cell composition using flow cytometry.

**Results:**
Tumor development in the peritoneal cavity after i.p. injection occurs predominantly on the peri splenic fat tissue, on the meso of the small intestine and on the surface of the liver lobes. Typically, no macroscopic tumor lesion were found for the first 4 days after tumor cell injection. Only later time points revealed visible tumor lesions. Furthermore, limitations of quantifying tumor lesions were found in all tested measuring methods. However, the PCI is the most reliable method to determine peritoneal tumor load.
Of all novel drug combinations tested in vitro so far, Oxa in combination with the inhibition of the DNA damage transducer ATR, resulted in a synergistic therapeutic efficacy.
Oxa treated s.c. tumors showed only minimal effects on tumor growth, whereas its combination with Anti PD-1 Antibody caused strong tumor remission. The synergic effect was found to be associated with more activated (CD39 marker) and less exhausted CD8 T cell (PD-1 marker) infiltration in the tumor microenvironment.

**Conclusion:**
We developed a PM mouse model that is promising to investigate the effect of locoregional treatment, the subsequent immune response and to test novel treatment combinations in future. Moreover, our first set of experiments indicated that Oxa treatment can trigger T-cell recruitment into tumors and sequential PD-1 blockade could prevent T-cell from becoming exhausted in the tumor microenvironment. These findings highlight the importance of involving the tumor immune infiltrate for combined therapy strategies.

**265**

S. Sun[3], F. Frontini[3], W. Qi[2], A. Hariharan[3], M. Ronner[3], M. Wipplinger[3], C. Blanquart[1], H. Rehrauer[2], J. Fonteneau[1], E. Felley-Bosco1[3]

**Endogenous Retrovirus expression activates type-I interferon signaling in an experimental mouse model of mesothelioma development**

*CRCINA, INSERM UMR 1232, Nantes[1], Functional Genomics Center Zurich, ETH Zurich, University of Zurich[2], Laboratory of Molecular Oncology Lungen- und Thoraxonkologie Zentrum Zurich University Hospital[3]*

**Introduction:**
Early events in an experimental model of mesothelioma development include increased levels of RNA editing by adenosine deaminase acting on double-stranded RNA (dsRNA). We made the hypothesis that expression of endogenous retroviruses (ERV) contributes to dsRNA formation and type 1 interferon signaling.

**Methods:**
ERV and ISGs expression was determined in RNA-seq data from tissues in three groups of mice: sham and asbestos exposed mice with or without tumors. ERV and ISGs expression was confirmed by qPCR. Methylation of genomic DNA was assessed after treatment with sodium bisulfite followed by quantitative methylation specific PCR. DNA demethylation was induced in mouse embryonic fibroblasts (MEF) and mesothelioma cells by 5-Aza-2'-deoxycytidine (5-Aza-CdR) treatment. Double strand RNA was quantified by flow-cytometry. To block the type-I IFN signaling, cells were treated with Ruxolitinib.

**Results:**
ERV and ISGs expression were significantly higher in tumor compared to non-tumor samples. 12 tumor specific ERV were identified and verified by qPCR in mouse tissues. "MesoERV1-12" expression was lower in mouse embryonic fibroblasts (MEF) compared to mesothelioma cells. "MesoERV1-12" levels were significantly increased by demethylating agent 5-Aza-2'-deoxycytidine treatment and were accompanied by increased levels of dsRNA and ISGs. Basal ISGs expression was higher in mesothelioma cells compared to MEF and was significantly decreased by JAK inhinibitor Ruxolitinib. "MesoERV7" promoter was demethylated in tissue from asbestos exposed compared to sham mice and in mesothelioma cells and MEF upon 5-Aza-CdR treatment.

**Conclusion:**
These observations undercover novel aspects of asbestos-induced mesothelioma whereby ERV expression increases due to promoter demethylation and is paralleled by increased levels of dsRNA and activation of type-I IFN signaling. These features are important for early diagnosis and therapy.

**266**

B. Schmid[1], A. Künstner[2], A. Fähnrich[2], E. Bersuch[1], P. Schmid-Grendelmeier[1], H. Busch[2], M. Glatz[1], P. Bosshard[1]

**Characterization of the skin microbiome in patients with atopic dermatitis versus healthy controls**

*Department of Dermatology, University Hospital Zurich (USZ), University of Zurich (UZH), Raemistrasse 100, CH-8091 Zurich, Switzerland[1], Institute of Experimental Dermatology, University of Luebeck, Ratzeburger Allee 160, 23538 Luebeck, Germany[2]*

**Introduction:**
Atopic dermatitis (AD) is a multifactorial, chronic relapsing inflammatory skin disease. Characteristics are an impaired skin barrier and an altered skin immune system, which often come along with predominant colonization by Staphylococcus aureus. The role of fungi, i.e. the mycobiome, remains poorly investigated although AD patients are frequently sensitized to Malassezia, the most abundant fungus on skin. We aim to improve the understanding of the skin mycobiome in AD and compare it to the bacteriome.

**Methods:**
Skin swabs of 17 AD patients and 16 healthy controls (HC) were taken from 4 skin sites (antecubital crease, glabella, vertex, and dorsal neck). To assess temporal shifts in the mycobiome, AD patients were sampled at 3 time points (0, 2 and 4 weeks), whereas HC were sampled at 2 time points (0, 4 weeks). Amplicon-based next-generation sequencing (NGS) of the ITS1 (fungal analysis) and 16S (bacterial analysis) regions were applied for the analysis of relative abundance, α-, and ß-diversities.

**Results:**
The most abundant fungi were Malasseziomycetes (figure 1a). For all skin sites except the antecubital crease, non-Malassezia fungi were more abundant in patients with severe AD. Those findings were confirmed by the analysis of α-diversity (Shannon diversity index) which was significantly higher in patients with severe AD. Furthermore, ß-diversities depicted as distances in ordination plots reveal significantly different clusters for HC, mild to moderate AD, and severe AD. In most HCs and patients with mild to moderate AD, the mycobiome was comparable between individuals and stable over time. In contrast, in severe AD the mycobiome was different between individuals and changed over time. Analysis of the bacteria has shown an increase of relative abundance of Bacilli (mostly Staphylococci) in severe AD patients, whereas the relative abundance of Actinobacteria including Cutibacterium was lower in those patients (figure 1b). Particularly, Staphylococcus aureus was highly increased in severe AD patients.

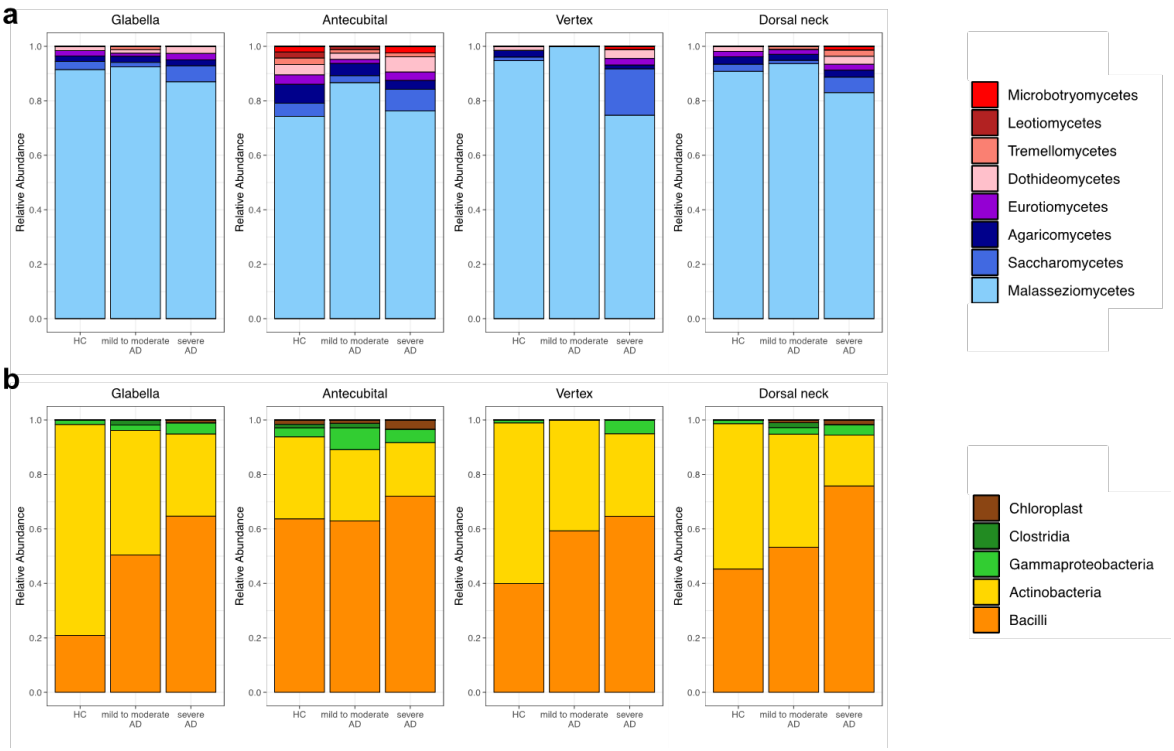


Figure 1: Relative abundance of fungal (a) and bacterial (b) classes at the glabella, the antecubital crease, the vertex, and the dorsal neck for merged sample sets (healthy controls (HC), mild to moderate atopic dermatitis (AD), and severe AD.

**Conclusion:**
Patients with severe AD were more often colonized with non-Malassezia fungi and had a high intra- and interpersonal species diversity. Unlike the increased fungal diversity, the diversity of bacteria was decreased in severe AD patients with a dominance of S. aureus. We speculate that the impaired skin barrier in severe AD allows colonization with more different fungi than healthy skin. Vice versa, the altered mycobiome may cause activation of the skin immune system leading to inflammation and eczema.

**269**

P. Frey[2, 3, 4], J. Baer[3], J. Bergada-Pijuan[3], C. Lawless[9], P. Bühler[7], R. Kouyos[3], K. Lemon[1, 4, 6, 8], A. Zinkernagel[3], S. Brugger[3, 4, 5]

**Quantifying variation in bacterial reproductive fitness: a high-throughput method**

*Alkek Center for Metagenomics & Microbiome Research, Department of Molecular Virology & Microbiology, Baylor College of Medicine, Houston, Texas, USA[1], Department of General Internal Medicine, Bern University Hospital, University of Bern, Switzerland[2], Department of Infectious Diseases and Hospital Epidemiology, University Hospital Zurich, University of Zurich, Switzerland[3], Department of Microbiology, The Forsyth Institute, Cambridge, MA, United States[4], Department of Oral Medicine, Infection and Immunity, Harvard School of Dental Medicine, Boston, MA, United States[5], Division of Infectious Diseases, Boston Children's Hospital, Harvard Medical School, Boston, MA, United States[6], Institute for Intensive Care Medicine, University Hospital Zurich, University of Zurich, Switzerland[7], Section of Infectious Diseases, Department of Pediatrics, Texas Children's Hospital and Baylor College of Medicine, Houston, Texas, USA[8], Translational and Clinical Research Institute, Medical School, Newcastle University, Newcastle upon Tyne, UK[9]*

**Introduction:**
To evaluate changes in reproductive fitness of bacteria, e.g., after acquisition of antimicrobial resistance, a low-cost high-throughput method to analyse bacterial growth on agar is desirable for broad usability. This method would provide information about fitness of infective strains isolated from patients, helping to estimate clinical outcomes.

**Methods:**
In our bacterial quantitative fitness analysis (BaQFA), arrayed cultures are spotted on agar and photographed sequentially while growing. These time-lapse images are analysed using a purpose-built open-source software to derive normalised image intensity (NI) values for each culture spot. Subsequently, a Gompertz growth model is fitted to NI values and fitness is calculated from model parameters, in particular the maximum growth rate and the time to achieve the maximum growth rate. To represent a range of clinically important pathogenic bacteria, we used different strains of Enterococcus faecium, Escherichia coli and Staphylococcus aureus, with and without antimicrobial resistance. Relative competitive fitness (RCF) was defined as the mean fitness ratio of two strains growing competitively on one plate.

**Results:**
BaQFA permitted the accurate construction of growth curves from bacteria grown on semisolid agar plates and fitting of Gompertz models. Normalised image intensity values showed a strong association with the total CFU/ml count per spotted culture ($p<0.001$) for all strains of the three clinically significant species. BaQFA showed relevant reproductive fitness differences between individual strains, suggesting substantial higher fitness of methicillin-resistant S. aureus JE2 than Cowan (RCF 1.58, $p<0.001$). Similarly, the vancomycin-resistant E. faecium ST172b showed higher competitive fitness than susceptible E. faecium ST172 (RCF 1.59, $p<0.001$).

**Conclusion:**
Our BaQFA method allows detection of fitness differences between bacterial strains, and may help to estimate epidemiological antimicrobial persistence, or contribute to the prediction of clinical outcomes in severe infections.

**270**

I. Martinez Lopez[2], M. Kirschner[2], F. Schläpfer[2], V. Orlowski[2], S. Ulrich[1], I. Opitz[2]

## Establishment of in vitro models for the study of chronic thromboembolic pulmonary hypertension

*Department of Pulmonology, University Hospital Zurich[1], Department of Thoracic Surgery, University Hospital Zurich[2]*

**Introduction:**
For any disease, well-characterized in vitro cell culture models represent an invaluable resource for a first and relatively simple evaluation of potential novel treatment approaches regarding their effect on diseased but also healthy cells. While endothelial cells and smooth muscle cells from pulmonary arteries (PA) are commercially available, to the best of our knowledge there is a lack in cell lines derived from patients with chronic thromboembolic pulmonary hypertension (CTEPH).

Therefore, we here embark on the establishment of a primary cell bank for CTEPH to be used for in vitro studies to further understand the pathomechanism and potential targets for CTEPH patients.

**Methods:**
Peripheral fibrotic obstructive material and intima removed during pulmonary endarterectomies were routinely collected. Tissue samples were digested mechanically and enzymatically, then plated in gelatin-coated tissue culture flasks, and cultured at 37°C, in 5% CO2, and 95% humidity. Successfully growing cell lines will be characterized and identified by a series of immunohistochemical stainings.

**Results:**
So far, we have successfully established well growing cell lines from 10 fibrotic peripheral tissues as well 1 intima and 1 media sample. As exemplified by the photographs for intima samples collected from the left and right side of the same patient (Fig. 1 A vs B), a great diversity in cell morphology, growth rate and distributions patterns can be observed. Cell blocks for all cell lines are currently prepared in order to examine them by immunohistochemical stainings.

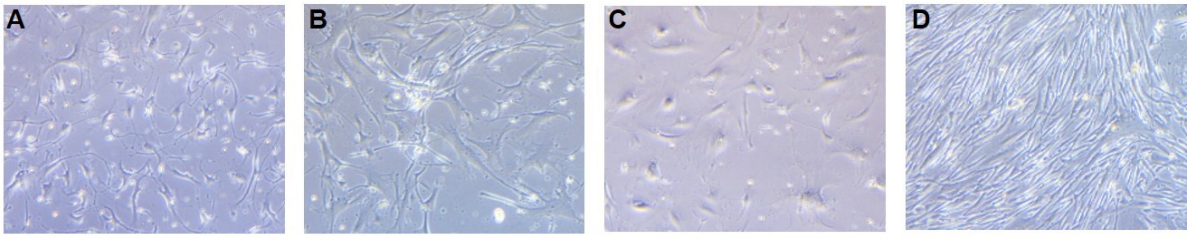


**Fig. 1. Images of cell lines derived from tissue of one CTEPH patient.**
Cells were derived from left side **(A)** and right side **(B)** intima as well as peripheral tissue from the left side **(C)** and right-sided media **(D)**.

**Conclusion:**
So far, we have shown that the establishment of primary cell cultures from the obstructive tissue as well as intima and media of CTEPH patients is feasible, and can result in well-growing cell cultures. The obtained cell lines are currently being characterized by immunohistochemical stainings.

**271**

K. Burelo[1, 2], M. Sharifshazileh[1, 2], J. Sarnthein[1, 3], G. Indiveri[2, 3]

**Detecting High-frequency Oscillations in scalp EEG recordings using a Spiking Neural Network**

*Department of Neurosurgery, University Hospital Zurich, University of Zurich, 8091 Zurich, Switzerland[1], Institute of Neuroinformatics, University of Zurich and ETH Zürich, 8057 Zurich, Switzerland[2], Neuroscience Center Zurich, ETH Zurich, 8092 Zurich, Switzerland[3]*

**Introduction:**
There is recent evidence that the HFOs, biomarkers for epileptogenic zone detected in invasive EEG recordings, are also detected in non-invasive scalp EEG recordings in young patients. The automatic detection of this biomarker is promising for long-term monitoring of the disease as well as pre-surgical studies. This kind of application can therefore benefit from an embedded system able to detect HFOs in real-time, without the need to process large amounts of data off-line, with external computers or cloud servers.

**Methods:**
In this study, we use an artificial Spiking Neural Network (SNN) for detecting clinically relevant HFOs found in pre-and postsurgical scalp EEG recordings, measured from eleven children with drug-resistant focal epilepsy that underwent epilepsy surgery. The proposed SNN consists of a core HFO detection part, already validated with intraoperative ECoG data, extended with a new artifact rejection part used to eliminate false positive HFOs caused by sharp transients.

**Results:**
Here we show that the HFO rates found by this novel SNN architecture compare favorably to those detected in the same dataset by a clinically validated automatic HFO detector (mean 2.13 HFO/min vs 2.82 HFO/min in 16 pre-resection recordings).

**Conclusion:**
The SNN proposed was designed using elements and parameters fully compatible with mixed-signal neuromorphic circuits. This therefore represents an important step towards the construction of a low-power embedded neuromorphic signal processing system for continuous-time on-line detection of HFOs and long-term non-invasive assessment of disease severity in patients with epilepsy.

**272**

S. Salemi[1], B. Kranzbühler[1], L. Prause[1], V. Baumgartner[1], D. Eberli[1]

**Apalutamide and autophagy inhibition in xenograft mouse model of human prostate cancer**

*Department of Urology, University Hospital Zürich, Wagistrasse 21, Schlieren[1]*

**Introduction:**
Apalutamide (APA) is a unique androgen receptor antagonist for the treatment of castration resistant prostate cancer. Previously we have shown that upregulation of autophagy is one of the mechanisms by which PCa cells survive APA anti-tumor treatment in vitro. Therefore, we investigated the characteristics of autophagic response to APA treatment alone and in combination with autophagy inhibitors in in vivo model.

**Methods:**
Nude mice (32) underwent an initial castration procedure before tumor injection. Four groups of mice bearing LNCaP xenografts were treated with daily intraperitoneal (i.p.) injections of vehicle (control), APA (10 mg/kg), and APA (10 mg/kg) + Chloroquine (10 mg/kg) and Chloroquine (10 mg/kg). The animals were kept for the duration of 2 and 3 weeks. At the end of the experiments, animals were sacrificed and all samples were assessed for tumor weight, size, histological analysis, immunoblotting (WES) and immunofluorescence.

**Results:**
Tumor weight was significantly reduced in mice treated with the APA plus Chloroquine (203.2 ± 5.0, SEM, P= 0.0066) compared to vehicle control (380.4 ± 37.0). Importantly, the combined treatment showed higher impact on tumor weight than APA (320.4 ± 45.5) or Chloroquine (337.9 ± 35) alone. The mice treated with a combination of APA and Chloroquine, exhibited a reduced expression of ATG5, Beclin 1 and LC3 punctuations and increase in P62 visualized by immunofluorescent and WES. In addition, ki67 nuclear staining was detected in all the samples however staining was reduced in APA + Chloroquine (58%) compared to vehicle control (100%). Reduction in Ki67 protein was associated with an increase in caspase 3 and CD31 (endothelial) protein expression.

**Conclusion:**
This data demonstrates that treatment with APA leads to increased autophagy levels in LNCaP cells. Furthermore, APA in combination with autophagy inhibitor Chloroquine, significantly increases its antitumor effect providing a new therapeutic approach potentially translatable to patients.

**273**

T. Schweizer[2], F. Andreoni[2], C. Acevedo[2], E. Marques Maggio[3], I. Heggli[4, 5], N. Eberhard[2], S. Dudli[1, 4, 5], A. Zinkernagel[1, 2]

**Intervertebral disc cells undergo chondroptosis and elicit strong immune response upon Staphylococcus aureus challenge**

*Center for applied Biotechnology and Molecular Medicine (CABMM), University of Zurich, Zurich, Switzerland[1], Department of Infectious Diseases and Hospital Epidemiology, University Hospital Zurich, University of Zurich, Zurich, Switzerland[2], Department of Pathology and Molecular Pathology, University Hospital Zurich, University of Zurich, Zurich, Switzerland[3], Department of Physical Medicine and Rheumatology, Balgrist University Hospital, University of Zurich, Switzerland[4], Department of Rheumatology, Balgrist University Hospital, University of Zurich, Zurich, Switzerland[5]*

**Introduction:**
The incidence of vertebral bone and disc infection, termed spondylodiscitis, has doubled over the last two decades, in particular in the elderly. *Staphylococcus aureus* is the most frequent pathogen isolated in spondylodiscitis. In order to ameliorate disease, patients receive long-term antibiotics as well as surgical debridement, when indicated. Interestingly, the disc is an immune-privileged site and hence the initial immune reaction has to be orchestrated by intervertebral disc (IVD) cells. However, it remains largely unknown how IVD cells initiate an immune response upon *S. aureus* challenge. Here, we combined clinical insights and laboratory assays to understand the key biological aspects of the initial phase of the immune response.

**Methods:**
Clinical cases of *S. aureus* spondylodiscitis were assessed by histology. Furthermore, we established a novel porcine *ex vivo* spine model of spondylodiscitis, allowing to determine bacterial growth within the spinal environment as well as understanding the response of annulus fibrosus cells towards *S. aureus* by standard microbiological enumeration, transmission electron microscopy and flow cytometry. Additionally, IVD cells isolated from patients undergoing lumbar spinal fusion surgery, due to various non-infectious spinal pathologies, were challenged with *S. aureus* and assessed by flow cytometry, confocal laser scanning microscopy and multiplex-based readouts.

**Results:**
Histology revealed infiltration of mostly neutrophils into the infected disc tissue. Evidence for IVD cells cell death was found as indicated by empty lacunae and necrotic disc tissue. In our newly established *ex vivo* porcine spondylodiscitis model, bacteria were able to grow in the disc environment and furthermore caused accelerated annulus fibrosus cell death. Of note, cell death presented with hallmarks of chondroptosis, such as membrane blebbing and the presence of autophagic vacuoles. *In vitro* challenged human IVD cells revealed the same cell death-prone phenotype, mediated mostly via caspases, highlighting chondroptosis as a regulated cell death mechanism upon *S. aureus* challenge. Interestingly, IVD cells elicited a strong cytokine-driven immune response, with secreted factors such as IL-8, G-CSF, CXCL1 and CXCL2, proposing a neutrophil recruitment and activation potential.

**Conclusion:**
We show that IVD cells play an important role in the orchestration of the immune response upon presence of *S. aureus*. *S. aureus* induced rapid IVD cells cell death, both within their native tissue site as well as in isolated cells in culture, accompanied by a strong neutrophil-activation secretion profile. Importantly, we showed that IVD cells commit caspase-mediated regulated cell death. Since antibiotic penetration into the disc is impaired and therefore delaying treatment efficacy, targeting caspases in order to slow down IVD cells cell death and the elicited strong tissue-destructive immune response might offer a potential future therapeutic application.

**274**

T. Schweizer[2], S. Mairpady Shambat[2], V. Dengler Haunreiter[2], C. Mestres[1], A. Weber[3], A. Zinkernagel[2], B. Hasse[2]

**Polyester Vascular Graft Material and Risk for Intracavitary Thoracic Vascular Graft Infection**

*Department of Cardiovascular Surgery, University Hospital Zurich, University of Zurich, Zurich, Switzerland[1], Department of Infectious Diseases and Hospital Epidemiology, University Hospital Zurich, University of Zurich, Zurich, Switzerland[2], Heart Surgery, HerzZentrum Hirslanden Zurich, Zurich, Switzerland[3]*

**Introduction:**
Prosthetic vascular graft infections (PVGIs) of the thoracic aorta occur rather rarely, however they are linked to lethality rates exceeding 20%. Infections most often occur during the perioperative period as a consequence of inoculation with bacteria, mostly originating from the patient's own skin flora. PVGIs are biofilm-associated infections in which the matrix around the bacteria impairs the chances of treatment success. Therefore, the primary aim is to prevent perioperative infections by identifying underlying risk factors. One such, extremely understudied, risk factor is the type and material of the prosthesis. Prosthetic vascular grafts are usually coated with proteinaceous solutions, allowing for quick integration into host tissue. However, these differences might also pose a serious risk factor. Therefore, we compared the susceptibility of two different graft materials to biofilm formation in vitro and assessed the rate of infections associated to graft material in patients.

**Methods:**
We compared two prosthetic vascular woven polyester grafts with different coatings – collagen (collagen graft, InterGard Hemabridge) and gelatin (gelatin graft, Terumo Aortic Gelweave) to biofilm formation in a controlled in vitro set-up. The grafts were challenged with various bacterial strains (laboratory strains and clinical PVGI isolates) and the resulting biofilmmass was assessed by optical bacterial density measurement and confocal laser scanning microscopy. Furthermore, we analyzed 412 prospective participants of the VASGRA cohort study with either of the two grafts implanted to assess the in vivo infection rate.

**Results:**
The experiments revealed a striking difference in susceptibility to biofilm formation between the two different grafts. Bacteria formed significant more biofilmmass on the collagen graft as compared to the gelatin graft. These findings were linked to better adherence towards collagen as compared to gelatin for selected bacteria. Furthermore, the calculated percentage of intracavitary thoracic PVGI (n = 28) in VASGRA patients who underwent cardiac surgery and succumbed from PVGI was significantly higher in the collagen graft (10.8%) as compared to the gelatin graft group (3.52%; $p < 0.005$).

**Conclusion:**
We discovered significant differences in the susceptibility of graft material towards bacterial biofilm formation, which was linked to the coating of the graft. The clinical findings supported the experimental results and propose that the graft material is a crucial risk factor. So far, design and manufacture of prosthetic vascular grafts perceived mostly parameters such as vascularization potential, secure pseudointima growth, and reduced thrombogenicity important for functionality. However, based on our findings, further parameters, such as the here described risk of infection, should be considered in the future design and development of vascular prostheses to reduce the emerging trend of PVGI.

**275**

J. Bär[1], M. Boumasmoud[1], S. Mairpady Shambat[1], C. Vulin[1], M. Huemer[1], T. Schweizer[1], A. Gómez-Meja[1], N. Eberhard[1], Y. Achermann[1], S. Brugger[1], R. Schüpbach[2], R. Kouyos[1, 3], B. Hasse[1], A. Zinkernagel[1]

**Clinical factors affecting within-patient persister levels during Staphylococcus aureus infections**

*Department of Infectious Diseases and Hospital Epidemiology, University Hospital Zurich, University of Zurich, Zurich[1], Institute for Intensive Care Medicine, University Hospital Zurich, CH-8091 Zurich[2], University of Zurich, Institute of Medical Virology , Zurich, Switzerland[3]*

**Introduction:**
Persisters are a dormant subpopulation of bacteria which tolerate high concentrations of antibiotics. Both the proportion and the dormancy depth of persisters are variable and modulated by the environmental conditions. The current knowledge regarding persister formation is mainly based on *in vitro* and animal experiments and little is known about the actual extent of this phenomenon within patients suffering from bacterial infections. Because of their ability to survive optimal antibiotic therapy, persisters have been hypothesized to be at the origin of difficult-to-treat infections. The pathobiont *Staphylococcus aureus* commonly causes such severe infections that often require prolonged therapy. Here we aimed to quantify dormancy depth of individual cells in *S. aureus* populations recovered from patients' material, by plating directly upon sampling and measuring the delays until growth resumption of colonies on nutrient agar.

**Methods:**
Samples of infected tissues from infective endocarditis, vascular graft, skin and soft tissue as well as prosthetic joint infections were collected during surgical procedures at the University Hospital Zurich and Balgrist University Hospital between 2017 and 2020 (n = 132). The bacterial populations were isolated, washed, and directly plated on nutrient agar. The colony growth was monitored with time-lapse imaging. A combination of univariable and multivariable linear regression models was used to identify clinical variables influencing population-wide shifts of growth delays of the bacterial colonies.
Aiming to model the *ex vivo* findings, *in vitro* experiments were subsequently performed. A subset of clinical isolates was grown to static biofilms, which were exposed to various antibiotics. The biofilm eradication capacity of these antibiotics, as well as the collaterally induced resistant or dormant subpopulations were quantified. Finally, the persistence of the surviving populations to the beta-lactam antibiotic flucloxacillin was assessed.

**Results:**
In this study, we focused on 36 samples of monomicrobial *S. aureus* infections. The other 96 samples were either from infections caused by other species, polymicrobial infections, or culture-negative. Growth delays within monomicrobial *S. aureus* populations isolated from patients were very heterogeneous compared to populations derived from exponentially growing cultures. Between populations, the mean and variance of growth delays were positively correlated. Increased growth delays were associated with certain antibiotic treatments that patients received. Notably, the bacterial populations derived from patients treated with rifampicin (n = 4) had the longest growth delays. This phenotypic observation of increased growth delay upon antibiotic exposure was reproducible in static biofilm assays, although with a smaller magnitude. Additionally, rifampicin exhibited the best biofilm eradication capacity of all tested antibiotics. Rifampicin resistance evolution was reduced by combining rifampicin with either levofloxacin or clindamycin, but these antibiotic combinations did not further improve the killing capacity. Moreover, exposure to rifampicin alone or in combination resulted in increased persistence towards flucloxacillin.

**Conclusion:**
We found that the proportion and the dormancy-depth of *S. aureus* persisters within-patients varied strongly. Antibiotic treatment was the most important factor contributing towards growth delays, reflecting dormant cells. This is of great clinical relevance since persisters have been associated with difficult-to-treat infections.

**276**

G. Treichler[2], D. Akhoundova[2], S. Höller[1], M. Rechsteiner[1], S. Freiberger[1], M. Zoche[1], H. Moch[1], F. Lisy[2], C. Britschgi[2], A. Curioni-Fontecedro[2]

**An efficient algorithm for molecular testing of advanced lung cancer**

*Institut für Pathologie und Molekularpathologie, Universitätsspital Zürich[1], Klinik für Medizinische Onkologie und Hämatologie, Universitätsspital Zürich[2]*

**Introduction:**
Molecular testing has become an essential part of the diagnostic work-up and guides daily decision making for therapeutic management of lung cancer patients. International guidelines integrate up-front molecular testing to subclassify non-small cell lung cancer (NSCLC), and therapeutic algorithms are based on this categorization. When possible, a broad genomic analysis of tumor tissue using next-generation sequencing (NGS) is recommended. However, algorithms guiding optimal selection and sequence of testing assays in the clinic are still lacking, and molecular testing is performed in a heterogeneous way across distinct centers. The aim of this project was to establish a new diagnostic algorithm for NSCLC and to evaluate the efficacy of this approach.

**Methods:**
A retrospective analysis of 76 patients with advanced stage NSLCL was performed including molecular, histopathological and clinical characteristics. At diagnosis, the tumor samples from these patients underwent immunohistochemical analysis for PD-L1; if the histological subtype was adenocarcinoma, at the same time further immunohystochemical analysis for ROS1, ALK was performed and the sample was sequenced for BRAF, EGFR, KRAS with a fast testing namely Idylla. After obtaining the patient's signature of approval, further comprehensive genomic profiling of the tumor by the FoundationOne CDx (FO) was carried out. If there was not enough DNA material available for FO, the OncomineTM Focus Assay (OFA) was performed instead.

**Results:**
All samples derived from the 76 patients underwent the above mentioned algorithm for analysis. The median time until availability of results was 2.5 days for the Idylla test and 3 days for the IHC. The FoundationOne CDx testing took a median time of 42 days from the day of order until the final results were available. This time includes the transportation of the samples to the designated laboratory and their preparation for the molecular testing. The actual running time of the Foundation One CDx, meaning the time from when the test was started until the completion of it including publication of results amounted to a median of 14 days. The median duration for the testing by OFA counted up to 27 days. We detected 34 potentially targetable genomic alterations with the diagnostics performed. IHC and Idylla testing, respectively, identified both the ALK rearrangements as well as the seven EGFR mutations. Out of the eight identified KRAS G12C mutations, six were uncovered by Idylla, and two additional by FO. Collectively, 16 potentially targetable mutations were discovered only by the use of NGS. A total of nine patients received targeted treatment for the molecular alterations detected.

**Conclusion:**
Through the use of this newly developed lung algorithm time for treatment decision was importantly reduced, leading to correct treatment allocation for patients with advanced NSCLC. This allowed a homogenous evaluation of all cases and the finding of targetable alterations, which were otherwise not detectable through routine analysis.

**277**

M. Hirt[2], A. Barukcic[2], V. Haunerdinger[2], T. Albert[2], A. Bosch[1, 2], M. Hauri-Hohl[2]

**Novel Phenotypic and Functional Characterization of CD34-Positive Cells in Steady-State Peripheral Blood**

*The Hospital for Sick Children, Toronto, Canada[1], University Children's Hospital, Zurich, Switzerland[2]*

**Introduction:**
Under steady-state conditions a minute fraction (< 0.05%) of human peripheral blood (PB) cells express CD34, a marker for hematopoietic stem and progenitor cells (HSPC). Yet, their detailed phenotype and functional capacity in comparison to HSPC in the bone marrow is poorly defined. It remains unclear, whether they are restricted to particular lineages or retain true stemness. A detailed characterization will contribute to a better understanding of the complex processes of hematopoiesis.

**Methods:**
We applied multiparametric flow cytometry to characterize CD34-positive cells from unstimulated PB from healthy donors. In addition, their expansion and differentiation potential as well as lineage-restriction was assessed in ex vivo assays.

**Results:**
We find that CD34-positive cells in unstimulated PB demonstrate a preponderance for both the erythroid and megakaryocytic lineage. This contrasts with CD34+ cells isolated from G-CSF-mobilised peripheral blood stem HSPC, which preferentially differentiate into myeloid progenitors with a significantly lower tendency for the erythroid and megakaryocytic lineages.
However, we also find a small fraction of phenotypically ‘true’ hematopoietic stem cells (HSC) (defined as CD34+ CD38- CD133+ CD90+ CD45RA-). Interestingly, we see a clear upregulation of these stem cell markers within the first seven days of culture. Functionally, these HSC are capable of self-renewal and give rise to downstream progenitor cells ex vivo, with a strong tendency for the megakaryocytic lineage.

**Conclusion:**
Our findings indicate that the majority of CD34-positive cells under steady-state conditions in PB preferentially differentiate into either the erythroid or megakaryocytic lineage. In further experiments we will assess whether these cells are lineage-restricted or can still be driven towards other lineages. Transplantation of sort-purified cells with a stem cell phenotype into NSG mice will provide evidence whether they retain long-term repopulation capacity of all hematopoietic lineages in vivo.

**278**

N. Jarzebska[1], S. Pascolo[1], M. Tusup[1]

**Optimization of RNA-based formulations for targeted cancer therapy**

*Department of Dermatology USZ[1]*

**Introduction:**
Chemotherapy remains one of the most common methods of cancer treatments. However, traditional drugs are nonspecific and affect cancerous as well as normal dividing cells, which frequently causes systemic side effects. Recently, nanoparticles (NPs) applied in drug delivery systems have attracted increasing attention. Used as drug carriers, NPs could provide site-specific delivery of anticancer agents. The external surface of NPs is modified with various ligands (peptides, nucleic acids, antibodies, and small molecules) to enhance targeting and tumoral uptake.
In our research group, we use polyplex formulations based on protamine, a natural cationic peptide that is used as a drug to inhibit heparin. Due to its cationic nature, protamine spontaneously associates with RNA, generating nanoparticles that can protect and deliver the nucleic acid.
As a therapeutic agent, we invented “immuno-chemotherapeutic RNA”. In this innovative compound, the nucleobase U residues are replaced with 5-fluoro-uracil (5FU), which is a chemotherapeutic agent. The modified 5FURNA is as chemotherapeutic as free 5FU. In addition, this substitution does not interfere with the capacity of the RNA to trigger Toll Like Receptor-7 and induce production of type I interferons. Thereby the 5FURNA is immuno-chemotherapeutic.
Hyaluronic acid (HA) is a commonly used cancer-targeting agent due to its receptor (CD44) being overexpressed in many types of tumor cells. We investigated whether decoration of protamine-RNA nanoparticles with HA could improve in vivo efficacy of immuno-chemotherapeutic RNA.

**Methods:**
Two types of hyaluronic acid were tested: short, 70 kDa and long, 120-350 kDa, to create particles called SHARP and HARP, respectively. Formulations of various content of HA and positive: negative charge ratio were tested in their ability to form nanoparticles of the desired size. Accumulation of selected NPs with fluorescently-labelled RNA in tumors was tested in CT26 tumor-bearing BALB/c mice. For in vivo treatment, tumor-bearing BALB/c mice were injected three to five times with appropriate protamine formulation containing 20 micrograms of immuno-chemotherapeutic 5FURNA. The tumor volumes were measured every other day.

**Results:**
Among 18 formulations, three with the smallest particle diameters were chosen for biodistribution assays, as smaller particles supposedly accumulate better at tumor sites. One formulation with short HA (called here SHARP 1355) showed the best and the most reproducible tumor homing. We decided to use it as an immuno-chemotherapeutic RNA carrier in tumor-bearing mice. After a series of injections, mice treated with SHARP-5FURNA had notably smaller tumors in comparison with mice treated with protamine-5FURNA alone.

**Conclusion:**
We discovered that coating with hyaluronic acid of 70 kDa size improved tumor homing of protamine-RNA nanoparticles. Meanwhile we invented immuno-chemotherapeutic RNA that are oligonucleotides with dual activity: chemotherapeutic and immunostimulatory. Tumor growth was delayed in mice treated with SHARP-5FURNA. Anticancer treatment utilizing SHARP-5FURNA nanoparticles has great potential to have a wide-ranging impact on cancer therapies. Additional experiments are ongoing to further optimize the method and test with combination treatments (e.g. anti-PD1 therapy) to reach superlative anti-cancer efficacy with fewer side-effects.

**279**

F. Caiado[1], L. Kovtonyuk[1], M. Manz[1]

**Contribution of IL-1 Mediated Inflamm-ageing to Clonal Hematopoiesis Progression in Murine Models**

*UniversitätsSpital Zürich[1]*

**Introduction:**
Clonal Hematopoiesis of indeterminate Potential (CHiP) is defined as the presence of an expanded somatic blood cell clone carrying a mutation in genes that are drivers of hematologic malignancy including DNMT3A, TET2 (and others) at a variant allele frequency of at least 2% in the absence of other hematological abnormalities. CHiP has a prevalence of about 10% in the 70-80 year old population, further increases with ageing and associates with an increased risk of hematological malignancies, cardiovascular disease and all-cause mortality. Recent studies indicate that decades may elapse between acquisition of a mutation (DNMT3A, TET2) and CHiP development, suggesting that environmental factors contribute to clonal expansion. Thus, it is key to decipher CHiP pathobiology and drivers for progression. Here we hypothesize that hematological ageing and inflammation (inflamm-ageing) are drivers of CHiP and that therapeutic targeting of these processes can prevent progression to malignancy.

**Methods:**
Mouse models of CHiP (hematopoietic-specific chimeric animals generated by bone marrow (BM) transplantation or inducible genetic models) carrying a minor fraction of hematopoietic Tet2+/- cells (10% to 90% wild-type, WT) were aged up to 1 year. We assessed clonal expansion rates at young and old ages by measuring relative frequency of WT and Tet2+/- clones in the peripheral blood (PB) of chimeric animals. In order to identify the inflammatory cues acting in aged BM, we quantified expression levels of key cytokines (RNA and protein) in 1 year old WT and Tet2+/- total BM cells. Identified cytokine and its respective neutralizing compound were chronically injected in chimeric animals and its effect on WT and Tet2+/- clonal expansion was assessed in PB and BM. To gain insight into cellular mechanism by which identified cytokine impacts Tet2+/- clonal expansion we measured its effects on hematopoietic stem and progenitor cell (HSPCs) numbers, proliferation and survival. Furthermore, in vivo competition assay were preformed to determine the effect of identified cytokine exposure on WT and Tet2+/- HSPC fitness.

**Results:**
We observed higher Tet2+/- clonal expansion rates in aged ChIP mouse models compared to their young counterparts. Expression levels of IL-1a/b (as well as TNFa) were increased in aged Tet2+/- BM cells compared to WT and in vivo administration of IL-1 to chimeric mice resulted in a significant expansion of Tet2+/- clones in both mature and HSPC populations. Conversely, reduction of IL-1 availability by administration of recombinant human IL-1Ra (Anakinra) on chimeric mice prevented age-induced Tet2+/- clonal expansion. We further observed that IL-1 in vivo treatment leads to a selective expansion of Tet2+/- HSPCs, via enhanced proliferation while not affecting their survival. By performing in vivo competition assays, we observed that while chronic IL-1 treatment significantly impairs HSPCs fitness of both phenotypes, Tet2+/- HSPCs are significantly more resistant to this deleterious effect than WT.

**Conclusion:**
We show that age-induced IL-1 is a major pro-inflammatory cytokine regulating the expansion of Tet2+/- hematopoietic clones, further implicating inflamm-ageing as a key driver of CHiP progression and potential neoplastic transformation. Further dissection of the cellular and molecular networks underlying this effect will further clarify the impact of inflamm-ageing derived factor IL-1 on Tet2-derived CHiP opening potential avenues for preventive therapeutic interventions.

**280**

I. Heggli[1, 4], R. Schüpbach[6], N. Herger[1, 4], T. Schweizer[2], N. Farshad-Amacker[5], M. Betz[3], J. Spirig[3], F. Wanivenhaus[3], N. Ulrich[3], F. Brunner[4], M. Farshad[3], O. Distler[1, 4], S. Dudli[1, 4]

**Infectious and autoinflammatory Modic type 1 changes have different pathomechanisms**

*Center of Experimental Rheumatology, Department of Rheumatology, University Hospital, University of Zurich, Switzerland[1], Department of Infectious Diseases and Hospital Epidemiology, University Hospital Zurich, University of Zurich, Zurich, Switzerland[2], Department of Orthopeadic Surgery, Balgrist University Hospital, University of Zurich, Zurich, Switzerland[3], Department of Physical Medicine and Rheumatology, Balgrist University Hospital, University of Zurich, Switzerland[4], Department of Radiology, Balgrist University Hospital, University of Zurich, Zurich, Switzerland[5], Unit of Clinical and Applied Research, Balgrist University Hospital, University of Zurich, Zurich, University of Zurich, Switzerland[6]*

**Introduction:**
Modic type 1 changes (MC1) are vertebral bone marrow (BM) edema that associate with non-specific low back pain (LBP). Two etiologies have been described. In the infectious etiology the anaerobic aerotolerant Cutibacterium acnes (C. acnes) invades damaged intervertebral discs (IVDs) resulting in disc infection and endplate damage, which leads to the evocation of an immune response. In the autoinflammatory etiology disc and endplate damage lead to the exposure of immune privileged disc cells and matrix to leukocytes, thereby evoking an immune response in the BM. Different etiologies require different treatment strategies. However, it is unknown if etiology-specific pathological mechanisms exist.The aim of this study was to identify etiology-specific dysregulated pathways of MC1 and to perform in-depth analysis of immune cell populations of the autoinflammatory etiology.

**Methods:**
BM aspirates and biopsies were obtained from LBP patients with MC1 undergoing spinal fusion. Aspirates/biopsies were taken prior screw insertion through the pedicle screw trajectory. From each patient, a MC1 and an intra-patient control aspiration/biopsy from the adjacent vertebral level was taken. If C. acnes in IVDs adjacent to MC1 were detected by anaerobic bacterial culture and 16S qPCR, patients were assigned to the infectious, otherwise to the autoinflammatory etiology. Total RNA was isolated from aspirates and sequenced (Novaseq) (inf. n=3+3, autoinfl. n=5+5). Differentially expressed genes (DEG) were considered if p-value was <0.01 and log2fc> ±0.5. Gene ontology (GO) enrichment was performed in R (GOseq), gene set enrichment analysis (GSEA) with GSEA software. Changes in cell populations of the autoinflammatory etiology were analyzed with single cell RNA sequencing (scRNAseq): Control and MC1 biopsies (n=1+1) were digested, $CD45^{+}CD66b^{-}$ mononuclear cells isolated with fluorescence activated cell sorting (FACS), and 10000 cells were sequenced (10x). Seurat R toolkit was used for analysis. Transcriptomic changes (n=5+5) of $CD45^{+}CD66b^{+}$ neutrophils isolated with FACS from aspirates were analyzed as with total bulk RNAseq. Neutrophil activation (n=3+3) was measured as $CD66b^{+}$ expression with flow cytometry. $CD66b^{high}$ and $CD66bl^{ow}$ fractions in MC1 and control neutrophils were compared with paired t-test.

**Results:**
Comparing MC1 to control in total bulk RNAseq, 204 DEG in the autoinflammatory and 444 DEG in the infectious etiology were identified with only 67 shared genes (Fig. 1a). GO enrichment revealed “T-cell activation” (p = 2.50E-03) in the autoinflammatory and “complement activation, classical pathway” (p=1.1E-25) in the infectious etiology as top enriched upregulated biological processes (BP) (Fig 1b). ScRNAseq of autoinflammatory MC1 showed an overrepresentation of T-cells (p= 1.00E-34, OR=1.54) and myelocytes (neutrophil progenitor cells) (p=4.00E-05, OR=2.27) indicating an increased demand of these cells (Fig. 1c). Bulk RNAseq analysis of neutrophils from the autoinflammatory etiology revealed an activated, pro-inflammatory phenotype (Fig 1d), which was confirmed with more $CD66b^{high}$ neutrophils in MC1 (+11.13 ± 2.71%, p=0.02) (Fig. 1e).

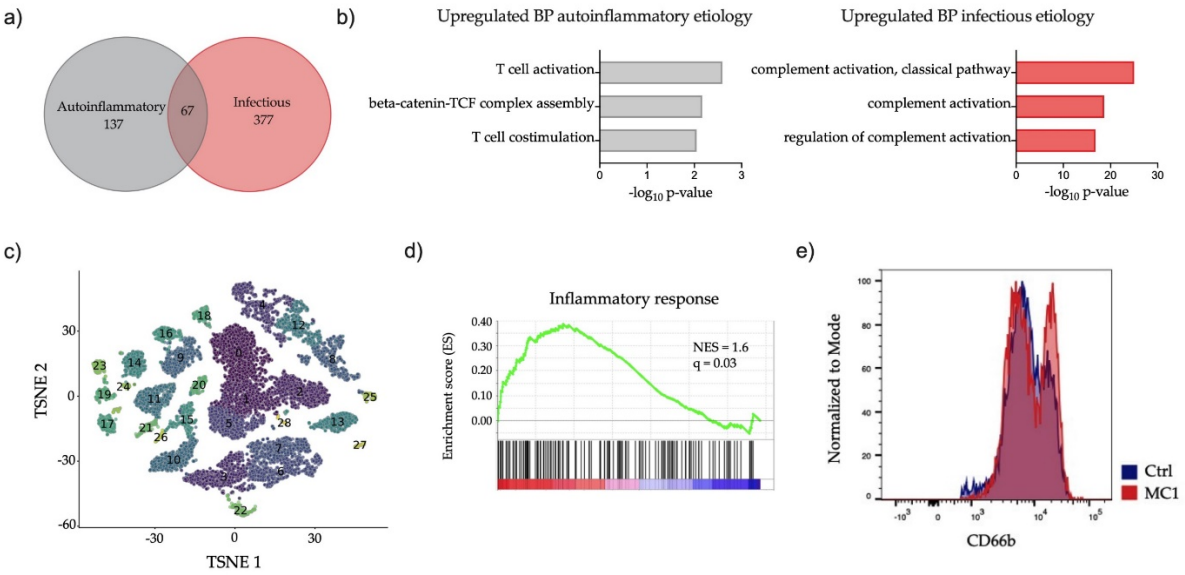


**Figure 1:** (a) Overlapping DEG from total bulk RNAseq (b) Top enriched upregulated BP of autoinflammatory (left) and infectious (right) etiology (c) Cell clustering of autoinflammatory MC1 BM (d) Enrichment of “inflammatory response” gene set in autoinflammatory MC1 neutrophils (e) Representative histogram of CD66b+ expression in MC1 and control neutrophils.

**Conclusion:**
Autoinflammatory and infectious etiologies of MC1 have different pathological mechanisms. T-cell and neutrophil activation seem to be important in the autoinflammatory etiology. This has clinical implication as it could be explored for diagnostic approaches to distinguish the two MC1 etiologies and supports developing targeted treatments for both etiologies.

**281**

F. Meier-Abt[1, 5], J. Lu[2], L. Kunz[4], B. Collins[7], P. Xue[1], M. Gwerder[5], M. Roiss[5], J. Hüllein[6], S. Scheinost[6], S. Dietrich[8], W. Huber[2, 6, 8], R. Aebersold[1, 3], T. Zenz[5]

**The Proteome Landscape of Chronic Lymphocytic Leukemia (CLL)**

*Department of Biology, Institute of Molecular Systems Biology (IMSB), ETH Zurich, Zurich, Switzerland,[1], European Molecular Biology Laboratory (EMBL), Heidelberg, Germany,[2], Faculty of Science, University of Zurich, Zurich, Switzerland[3], Functional Genomics Center Zurich, ETH/University of Zurich, Zurich, Switzerland[4], Medical Oncology and Hematology, University Hospital and University of Zurich, Zurich, Switzerland,[5], National Center for Tumor Diseases (NCT), Heidelberg, Germany,[6], School of Biological Sciences, Queen's University, Belfast, United Kingdom[7], University Hospital Heidelberg, Heidelberg, Germany,[8]*

**Introduction:**
Many functional consequences of mutations on tumor phenotypes in chronic lymphocytic leukemia (CLL) are only incompletely known. This is partly due to a scarcity of information on the proteome of CLL.

**Methods:**
To address this need, we analyzed 49 CLL patient samples with data-independent acquisition mass spectrometry (DIA-MS) using two different measurement platforms (LUMOS and timsTOF). We integrated these data with DNA-sequencing, RNA-sequencing, *ex-vivo* drug screen and clinical outcome data for the same patients, focusing particularly on the effect of copy number variation on protein levels, on protein complex formation and on individual protein markers explaining drug responses in CLL.

**Results:**
We found trisomy 12 and IGHV to be major determinants of proteome variation in CLL with 1073 and 512 differential proteins compared to CLL without these genetic drivers. For these disease drivers, differential RNA and protein expression was linked with publicly available experimental data on protein complex formation. This identified functional units involving BCR/PI3K/AKT signaling in trisomy 12 CLL and STAT1/STAT2 transcription factors in IGHV unmutated CLL. We studied the concept of protein buffering in CLL in detail and detected overall limited protein buffering in trisomy 12 CLL, which is in contrast to other biological systems. Key differentially regulated candidates (STAT2, PTPN11) and pathways (PI3K-AKT-MTOR and IL6-JAK-STAT3) in trisomy 12 CLL were amongst least buffered proteins or enriched in non-buffered proteins, indicating their relevance for mediating the fitness advantage of cells with trisomy 12 during the tumorigenesis. We tested the functional relevance of protein expression for associations with response to anticancer drugs, and STAT2 protein expression emerged as a biomarker for the prediction of response to kinase inhibitors including BTK and MEK inhibitors.

**Conclusion:**
This study identified limited buffering for chromosome 12 proteins in trisomy 12 CLL, suggesting a competitive advantage of chromosome 12 protein expression in CLL. It detected STAT2 as a critical performer in CLL biology. The study underscores the emerging importance of protein abundance profiling in CLL biology and presents a publicly available proteomic resource for CLL.

**282**

S. Mohammed[2], M. Alberio[4], K. Gergely[3], S. Ambrosini[5], T. Lüscher[1], S. Costantino[5], F. Gian Paolo[4], F. Paneni[3]

**The BET protein inhibitor Apabetalone (RVX-208) restores angiogenic response in type 1 and type 2 diabetes by transcriptional regulation of Thrombospondin-1**

*Royal Brompton and Harefield Hospital Trust, London, UK[1], ETH Zürich[2], Universitäts Spital Zürich[3], University of Padova, Italy[4], University of Zürich[5]*

**Introduction:**
Peripheral artery disease (PAD) is highly prevalent in people with diabetes, and associates with limb ischemia and poor prognosis. Understanding the mechanisms of impaired blood vessel growth in diabetic patients is of paramount importance to develop new angiogenic therapies in this setting. Dysregulation of epigenetic mechanisms of gene transcription in vascular cells contributes to cardiovascular disease development but is currently not targeted by therapies. Apabetalone (RVX-208) is an FDA-approved small molecule inhibitor of bromodomain and extra-terminal (BET) proteins-histone acetylation readers which has recently shown to modulate transcriptional programs implicated in vascular inflammation, calcification and atherosclerotic disease. Whether RVX-208 modulates angiogenic response and post-ischemic vascularization in experimental in the setting of diabetes remains elusive.

**Methods:**
Primary human aortic endothelial cells (HAECs) were exposed to normal glucose (NG, 5 mM) or high glucose (HG, 20 mM) for 48 hours in presence of RVX-208 (20μM) or vehicle (DMSO). Scratch and tube formation assays were performed to investigate the impact of RVX-208 on the angiogenic properties of HAECs. Gene expression profiling by real-time PCR array was employed to unveil transcriptional signatures regulated by RVX-208 in HAECs exposed to NG and HG. Thrombospondin1 (THBS1), VEGF as well as acetylation of histone 3 and 4 were investigated by Western blot. Chromatin immunoprecipitation (ChIP) assays were performed to check the binding of BET proteins to the promoter region of top-ranking genes. Knockdown of THBS1 and BET-proteins was performed by small interfering RNA(siRNA), while a scrambled-siRNA was used as a negative control. In vivo and ex vivo experiments were performed in experimental mouse models of T1D (streptozotocin-induced diabetes) and T2D (Lepdb/db), treated with apabetalone or vehicle orally. Hindlimb ischemia was induced in T1D mice and blood flow recovery analyzed at 30 min, 7 and 14 days by laser Doppler imaging. Sprouting and matrigel plug assays were performed in Lepdb/db mice.

**Results:**
: HG significantly impaired HAECs migration and tube formation as compared to NG, whereas treatment with RVX-208 was able to rescue HG-induced impairment of angiogenic properties. Real time PCR arrays in HG-treated HAECs showed that RVX-208 treatment prevents the dysregulation of genes implicated in endothelial migration, sprouting and inflammation, namely THBS1, VEGF-A, IL-1β, IL-6, VCAM-1, and CXCL1. Of interest, both gene silencing of BET protein (BRD4) or its pharmacological inhibition by RVX-208 reduced the expression of the anti-angiogenic molecule THBS1 while restoring VEGF levels in HG-treated HAECs. ChIP assays showed the enrichment of both BRD4 and the active regulatory mark H3K36 acetylation in the proximity of THBS1 promoter. Of interest, treatment of T1D mice with RVX-208 improved blood flow reperfusion and vascular density at 14 days as compared to vehicle-treated animals. Moreover, RVX-208 improved endothelial sprouting in Lepdb/db mice, thus suggesting a consistent effect of RVX-208 in modulating the angiogenic response in both T1D and T2D.

**Conclusion:**
Our study shows for the first time that in vivo targeting BET-proteins by RVX-208 represents a novel epigenetic therapy to promote post-ischemic neovascularization in diabetes.

**283**

J. Prange[1, 2], D. Mohr-Haralampieva[1, 2], N. Steinke[1, 2], N. Hensky[1, 2], F. Schmid[1], D. Eberli[1]

**Challenging milestones for a phase I clinical trial for incontinence treatment between GMP and GCP**

*Department of Urology, USZ[1], University of Zurich[2]*

**Introduction:**
Stress Urinary Incontinence is affecting over 200 million people worldwide. Patients suffer from reduced quality of life. The treatment of the disease is associated with high healthcare costs and only limited success. A constantly aging population demonstrates the urgent clinical need for novel treatment modalities. Recent advances in cell-based therapies have provided a variety of opportunities to seek alternative solutions to restore damaged sphincter function in patients with urinary incontinence. Various pre-clinical studies have shown promising results towards successful skeletal muscle regeneration using autologous injection of patients muscle progenitor cells (MPCs). During the production of MPCs a tightly regulated network ensures highest product quality (good manufacturing practice, GMP) to rule out any chance of contamination. Especially in the interface, where GMP regulations meet the clinics, challenges may arise while implementing the MPC therapy and turn into bottlenecks for the clinical application.

**Methods:**
For the first time, we will combine autologous cell injection of MPCs with early neuro-muscular electromagnetic stimulation in patients suffering from stress urinary incontinence (SUI) and evaluate the feasibility of muscle regeneration. The precise isolation, expansion, identification and transplantation the MPCs is complex. Within the setup of the GMP-compliant production, the transport of the biopsy material and the final product became the interface between the GMP and the good clinical practice (GCP) regulatory network and presented very pragmatic questions: What is the shelf life of the biopsy material and the final product? or How much time is available between the last production step and the injection for the release?

**Results:**
During the transport, responsibilities between GMP and GCP mingle. As within both parties several teams are involved in the release of the biopsy and the final product respectively the injection, timing is most crucial and quality of the material or product has to be ensured until further processing. The release of the biopsy for further manufacturing in GMP relies on clinical documentation provided straight from the OR. Only after successful release of the biopsy, it may be taken into the clean room. So, data was collected if the biopsy can be kept at 4°C for 24h. The full release of a patient batch production takes up to weeks and relies solely on the availability of analytical results from a certified company. A risk-based preliminary release of the final product needs to be established which respects the established shelf life of the final product. Hence, a stability study was performed to show how long the product meets the release requirements (cell viability >80%) to define this shelf life.A complex network of documentations and responsibilities is built which is the key stone for a smooth and compliant trial conduct.

**Conclusion:**
A careful navigation through already established regulations for GMP and GCP is necessary to lead this complex project for the application of MPCs as a novel cell-based therapy to a successful finish. All involved parties have different primary responsibilities which need to be taken into consideration while being compliant with the regulatory network on the way to a common goal: The improvement of the Quality of Life of the patients.

**284**

J. Barranco Garcia[1], R. Braun[1], S. Tanadini-Lang[1]

**On the Use of AI-based Diagnosis Tools in Dermatology**

*USZ[1]*

**Introduction:**
Artificial Intelligence (AI) have successfully demonstrated that it can be a powerful tool for skin lesion diagnosis. Recent published results showed that these algorithms are able to outperform board-certified dermatologists in certain classification tasks. However, these results did not consider real world datasets representing the situations encountered during routine dermatological consultation but rather prepared datasets of images from various sources. In order for these results to translate into trustful diagnosis-aid tools they should be designed and trained taking into consideration as much as possible of the diagnose procedure followed by experienced dermatologists.

**Methods:**
We will work with our own dataset of high quality polarized images acquired during routine consultations at the USZ Dermatology clinic. These images will cover large section of the patient's body surface allowing to be able to understand the lesion within its context. This is commonly overlooked in similar studies on this topic leading to lack of generalization of the models. Since some individuals can present hundreds of lesions distributed along all around the body an object detection algorithms have been developed and trained to localize such lesions and perform a first classification according to some clinical considerations. In a second stage, lesions selected as of interest will be classified using a CNN trained on a wider spectrum of skin lesions. This classifier is based in an ensemble learning scheme where different neural networks' results are combined to achieved an enhanced accuracy. Finally, we will introduce the concept of AI interpretability applied to our case at hand and explain how it is possible to extract human understandable concepts from these complex models.

**Results:**
We have shown how AI in its different applications can be used to design an end-to-end trustful diagnosis-aid tool which can contribute to maximize the efficiency of dermatology consultations. We have presented the different state-of-the-art AI architectures used to build our models and the steps to optimize their performance. We introduce and provide examples on how these interpetable algorithms can provide valuable high level information on the tasks that will allow the users to understand the logic behind the prediction. By supplying this option to the domain expert users it will be easier for them to provide valuable feedback on the algorithm's performance based on their expertise, as well as to maximize the clinical acceptance of these tools.

**Conclusion:**
AI algorithms are already known to be powerful diagnosis tools in dermatology, however they have been tested in certain generic circumstances. As the next step, it is necessary to include real world context as well as AI interpretability concept as main design drivers to ensure its acceptance and utility in the clinical practice.

**285**

S. Angori[1], H. Bolck[1], T. Karakulak[1], A. Kahraman[1], K. Mühlbauer[1], P. Schraml[1], H. Moch[1]

**Addressing the medical need for treatment of patients with papillary Renal Cell Carcinoma (pRCC)**

*Department of Pathology and Molecular Pathology, University Hospital Zurich, Zurich, Switzerland[1]*

**Introduction:**
Renal cell carcinoma (RCC) is the most prevalent urological cancer in adults. It affects nearly 300,000 patients worldwide and is responsible for approximately 100,000 deaths each year. Clear cell Renal Cell Carcinoma (ccRCC) is the predominant form of RCC, constituting 70% of them. Papillary renal cell carcinoma (pRCC) is an aggressive and highly lethal subtype accounting for 15 to 20% of RCCs. Importantly, pRCC is not a single disease but consists of at least two main subtypes: pRCC type 1 and type 2, often associated with a worse and more aggressive outcome. Since all RCC tumours are resistant to chemotherapy, current conventional treatment approaches include radiotherapy and resection. Besides, targeted therapies including tyrosine kinase and mTOR inhibitors have been developed. However, all of these systemic treatments have been designed based on the specific molecular aberrations that occur mainly in ccRCC tumours but less frequently in the other subtypes. Consequently, the response rates of the pRCC subtypes to these agents are often low. Recently, activation of the Nrf2-ARE pathway was also recognised as a tumour promoting mechanism responsible for pRCC. In cancer cells, Nrf2 over-activation promotes tumour progression and resistance to chemotherapeutics. As no effective targeted treatment exists for pRCC tumours to date, pharmacological inhibition of Nrf2 represents a promising therapeutic approach. For this reason, we want to investigate the molecular background of pRCC, by focusing on the aberrant activation of the Nrf2-ARE pathway.

**Methods:**
Comprehensive molecular characterization of 60 formalin-fixed, paraffin-embedded (FFPE) pRCC tumour samples by copy number (CN) analysis and Whole Exome Sequencing (WES) technology will allow us to identify grouped-cases based on their genetic background. Adequate cell models are essential to better understand the specific drug susceptibilities of pRCC tumours, potentially leading to the development of new agents and increased survival rates. To generate adequate in vitro tools, we developed patient-derived cell (PDC) models from human tissue using mouse embryonic fibroblasts as a feeder layer for supporting the growth of patient-derived cells in vitro. This has enabled us to generate cell models representative of pRCCs that closely resemble human tumours and that can be applied for pre-clinical drug profiling. To identify drugs or drug combinations that could effectively target cells with aberrations in the Nrf2-ARE pathway, we then performed a high-throughput drug screening on our established PDC cultures.

**Results:**
CN variation profiles reveal that pRCC samples are characterised by Chromosomal gains. pRCC type 1 show more frequent CN gains in Chr 7 and 17 than in pRCC type 2 while Chr 16 gain is more predominant in pRCC type 2. WES analysis confirms that pRCC tumours show different mutations in genes as CDKN2A, FH and c-MET. In addition, we find a subgroup of samples with mutations in genes involved in the Nrf2-ARE pathway. High-throughput drug screening shows different responses according to the molecular background of each PDC culture.

**Conclusion:**
With this approach, we want to further characterise the molecular background of pRCC tumours that have not been comprehensively studied to date. For the first time, we thus conduct a drug screen on pRCC PDC cultures and explore treatment option specific for pRCC patients that harbour a mutation in the Nrf2-ARE pathway. We envision that drugs or drug combinations that have emerged through high-throughput drug profiling could be further investigated in the patient-derived cell models we have developed. We anticipate that this will open up new possibilities for the clinical management of these patients, which are still treated with conventional RCC therapies.

**286**

M. Hilbers[4], F. Dimitriou[4], P. Lau[5], GA. McArthur[5], L. Zimmer[1], K. Kudura[2], CL. Gerard[3], O. Michielin[3], ML. Levesque[4], R. Dummer[4], J. Mangana[4], P. Cheng[4]

**Real-life data for first-line combination immune-checkpoint inhibition and targeted therapy in patients with melanoma brain metastases**

*Department of Dermatology University Hospital Essen[1], Department of Nuclear Medicine, University Hospital Zurich[2], Department of Oncology, CHUV[3], Dermatology Clinic University Hospital Zurich[4], Peter MacCallum Cancer Center[5]*

**Introduction:**
Recent data from clinical trials investigating combination immunotherapy (CombiIT: anti-PD1/anti-CTLA4) and targeted therapy (CombiTT: BRAF-/MEK-inhibitors) in patients with melanoma brain metastases (MBM) have proved clinical efficacy and durable responses. Systematic data studying the efficacy of these treatments beyond clinical trials is limited.

**Methods:**
Treatment-naïve MBM patients from four academic centers (Europe and Australia) with CombiIT or CombiTT within 3 months after MBM diagnosis between February 2014 and September 2018 were included. Endpoints of this study was progression-free survival (PFS) and overall survival (OS) in both groups.

**Results:**
Of the 116 included patients, 53 received CombiIT and 63 CombiTT. Median follow up was 32.3 months (range 3.44-79.4 months. Overall, CombiIT tripled mOS compared to CombiTT (44.8 vs 14.2, HR = 2.15, p = 0.0039), while the risk for progression was twice as high with CombiTT (5.9 versus 9.6 months, HR = 2.15, p=0.00093. In BRAF mutated patients, CombiIT first line resulted in substantial OS and PFS benefit compared to CombiIT (mOS not reached v10.9 months, HR = 3.02, p = 0.0042, PFS 6.5 vs 5.4 months, HR = 2.23, p = 0.0094). In patients with increased number of intracranial (>3) and exracranial metastases (>2) better outcome was achieved with CombiIT, while for elevated LDH or symptomatic versus asymptomatic MBM no significant PFS and OS difference was seen with either treatment. Interestingly, local therapy with surgery combined with stereotactic radiosurgery had the best benefit for OS (HR = 0.42 p = 0.035) and PFS (HR = 0.44, p = 0.021).

**Conclusion:**
Of the 116 included patients, 53 received CombiIT and 63 CombiTT. Median follow up was 32.3 months (range 3.44-79.4 months. Overall, CombiIT tripled mOS compared to CombiTT (44.8 vs 14.2, HR = 2.15, p = 0.0039), while the risk for progression was twice as high with CombiTT (5.9 versus 9.6 months, HR = 2.15, p=0.00093. In BRAF mutated patients, CombiIT first line resulted in substantial OS and PFS benefit compared to CombiIT (mOS not reached v10.9 months, HR = 3.02, p = 0.0042, PFS 6.5 vs 5.4 months, HR = 2.23, p = 0.0094). In patients with increased number of intracranial (>3) and exracranial metastases (>2) better outcome was achieved with CombiIT, while for elevated LDH or symptomatic versus asymptomatic MBM no significant PFS and OS difference was seen with either treatment. Interestingly, local therapy with surgery combined with stereotactic radiosurgery had the best benefit for OS (HR = 0.42 p = 0.035) and PFS (HR = 0.44, p = 0.021).

**287**

H. Lakshminarayanan[1], D. Rutishauser[1], S. Pfammatter[2], P. Schraml[1], H. Bolck[1], H. Moch[1]

**Liquid biopsy as a tool for disease monitoring in renal cell carcinoma**

*Department of Pathology and Molecular Pathology, University of Zurich and University Hospital Zurich, Zurich, Switzerland[1], Functional Genomics Center Zurich, Zurich, Switzerland[2]*

**Introduction:**
Clear cell renal cell carcinoma (ccRCC) is the most lethal urological malignancy. Currently, disease prognosis is mainly based on pathological characteristics such as tumor grade and stage. However, these often cannot correctly predict patient survival, which variably ranges from less than 6 months to over 5 years. To aid the clinical management of ccRCC patients, liquid biopsy could be a powerful tool since it enables the surveying of patient's biological fluids for molecular tumor biomarkers with minimal invasion. In this study, we seek to investigate patient plasma as a potential source of biomarkers for ccRCC monitoring.

**Methods:**
36 plasma samples from seven consenting ccRCC patients were used in this study. Samples collected before surgery and at several follow-up time points were investigated by LC-MS/MS analysis using tryptic cleavage following an SP3 assisted on-bead digestion protocol. The cleaved peptides were analyzed using Orbitrap FusionTM using a Data Dependent Acquisition (DDA) method. The sequenced peptides were queried with MaxQuant and discovered proteins were functionally annotated using DAVID and STRING.

**Results:**
A protein dataset was generated from these seven cases using the SP3 assisted on-bead digestion and Orbitrap mass analyzer. Specifically, 5145 peptides were identified at 1% false discovery rate, which were assembled into 407 proteins. A broad dynamic range of proteins was covered and representation of lower abundant proteins that could be associated with disease pathology was observed.

**Conclusion:**
Our first analysis shows that innovative proteomic analysis techniques enable the representation of lower abundant proteins from liquid biopsies potentially associated with pathologies. Thus, we can show that patient plasma can be used for the investigation of ccRCC-specific liquid biomarkers.

**288**

S. Ludwig[1], L. Schmid[1], A. Kahraman[2], M. Rechsteiner[2], M. Zoche[2], A. Curioni-Fontecedro[1], A. Siebenhüner[1], K. Dedes[3], M. Kiessling[1], R. Fritsch[1], A. Wicki[1], H. Moch[2], A. Weber[2], C. Britschgi[1]

**Impact of molecular testing and molecular tumor board decisions on clinical outcome of patients with solid tumors: A single center, retrospective analysis.**

*Department of Medical Oncology and Hematology, Comprehensive Cancer Center Zurich, University Hospital Zurich[1], Department of Pathology and Molecular Pathology, Comprehensive Cancer Center Zurich, University Hospital Zurich[2], Department of Gynecology, Comprehensive Cancer Center Zurich, University Hospital Zurich[3]*

**Introduction:**
Molecular testing plays a major role in patients with advanced and rare cancers with limited therapy options, allowing personalized therapeutical approaches. Beyond targeting well-established oncogenic alterations in single genes, such as EGFR or ALK in non-small cell lung cancer, or BRAF in melanoma, comprehensive genomic profiling (CGP) in unselected patients has also improved outcome by identifying targeted therapeutic alternatives in numerous studies. An interdisciplinary team is however crucial to approach CGP results for therapeutic recommendations. At the CCCZ, a Molecular Tumor Board (MTB) has been established with this intent. With the present study, we aimed to assess the impact of such a personalized approach on clinical outcomes by retrospectively analyzing molecular and clinical data of patients with CGP discussed at the MTB.

**Methods:**
The MTB is held weekly, moderated by senior physicians and researchers experienced in clinical trials research, genomics data, medical oncology and molecular pathology. Further participants are the responsible clinician, experienced medical oncologists, gynecological oncologists, (molecular) pathologists and bio-informaticians. Presentation of the clinical case includes presentation of histo-pathological and molecular characteristics using a dedicated software, the Molecular Tumor Profiling Pilot (MTP pilot). Main discussion points are clinical course, genomic alterations and biomarkers, actionability of such alterations and availability of targeted agents in or outside of a clinical trial with a documented consensus statement. As in all tumor boards of the CCCZ, consensus statement is a recommendation, but final therapeutic decision is made by the treating physician together with the patient. Included patients received CGP using at least one of several available platforms (mostly FoundationOneCDx®, FoundationOneHeme®, Oncomine Focus Assay™ or Oncomine Comprehensive Assay™) and were discussed at MTB between 1st of January 2018 and 31st of January 2020. All patients had a histologically confirmed solid tumor at a locally advanced or metastatic stage. Patients treated in curative intent were excluded from this analysis. Data on patient and tumor characteristics, treatments, MTB decision and clinical follow-up were collected from electronic medical records.

**Results:**
483 patients were included in this analysis. 506 molecular tests were performed. 55% of patients were male, median age was 64 years (range 20-90). The most represented cancer origin was lung (38%), followed by colo-rectal (11%), soft tissue and bone sarcomas (7%), biliary tract (7%), urogenital (6%), head and neck cancer (6%), pancreas (5%), breast (4%), gynecological (4%), gastro-esophageal (4%), skin (2%), thymus cancer (2%) and carcinoma of unknown primary (2%). At the time of MTB discussion, 72% of cases presented metastatic, 28% at locally advanced stage. The majority underwent one systemic therapy prior to MTB (42%). Median time from diagnosis to MTB was 14 months (range 0 - 347 months). Of 506 MTB decisions, a suggestion regarding a new therapy option based on CGP was made in 192 cases (38%). In 90 cases (18%), discussion at the MTB lead to a therapy change and in 10 cases (2%), patients were included in a clinical trial based on detected molecular aberrations. In case of MTB decision rejection, the majority was due to patient's wish (24%). Further analysis of clinical outcome parameters depending on MTB decision and molecular findings is currently ongoing and will be presented at the meeting.

**Conclusion:**

Within our cohort, molecular testing along with discussion at the MTB lead to application of a new systemic therapy in more than one fifth of patients. Therefore, we recommend CGP in locally advanced or metastatic solid tumors after standard of care and in rare cancers. Moreover, clearly defined molecular testing algorithms in the different tumor subtypes should be implemented.

**289**

C. Pellegrino[3], N. Favalli[1], S. Michael[1], L. Volta[3], G. Bassi[2], J. Millul[2], S. Cazzamalli[2], M. Matasci[2], A. Villa[2], R. Myburgh[3], M. Manz[3], D. Neri[2]

**Impact of Ligand Size and Conjugation Chemistry on the Performance of Universal Chimeric Antigen Receptor T-Cells for Tumor Killing**

*ETHZ[1], Philochem[2], USZ[3]*

**Introduction:**
Universal Chimeric Antigen Receptor T-cells (UniCAR T-cells) are T-cells that have been genetically engineered to recognize a unique tag. The tag can be conjugated to a vast range of binding molecules, conveying a universal targeting strategy towards virtually any tumour antigen of interest.

**Methods:**
In this study, we incorporated a sub-nano Molar affinity anti-Fluorescein binder into a second-generation CAR T-cell, to mediate a potent and selective tumour cell killing only in the presence of a fluorescein-tagged bispecific adaptor. For the bispecific adaptors, we employed well-established small organic ligands and different antibody formats specific against carbonic anhydrase IX. Carbonic anhydrase IX is a tumour-associated antigen expressed in 90% of patients suffering from renal cell carcinoma. We included multiple designs and conjugation strategies to assess whether the killing potential of UniCAR T-cells remained constant or altered.

**Results:**
Small molecule ligands and larger antibody fragments were potent in mediating tumour cell-line killing over a broad concentration range. Antibodies could be conveniently used both in IgG format and also as smaller diabody fragments. Importantly, the use of site-specific chemical modification strategies for the antibody coupling to fluorescein led to a substantial improvement of tumour cell killing performance, compared to the random modification of primary amino groups on the antibody surface.

**Conclusion:**
Small CAIX binders and antibody-based reagents could efficiently kill tumour cells in vitro, suggesting that the size of the adapter molecule did not substantially influence biocidal activity. By contrast, the use of site-specific modification strategies had a profound impact on cell killing performance. The stochastic modification of primary amino groups on antibody-based adapters led to a narrow therapeutic window, while molecularly defined adaptor molecules could kill tumours over a broad concentration range (i.e., between 1 µM and 1 pM). A low kinetic dissociation constant of the tumour binding moiety resulted in a durable saturation of cancer cells, leading to a decreased potency at high concentrations of fluorescein-labelled adapter molecules.

**290**

A. Kahraman[1, 2, 3], T. Karakulak[1, 2, 3], D. Szklarczyk[1, 3], C. von Mering[1, 3]

**Pathogenic impact of transcript isoform switching in 1209 cancer samples covering 27 cancer types using an isoform-specific interaction network**

*Swiss Institute of Bioinformatics[1], University Hospital Zurich[2], University of Zurich[3]*

**Introduction:**
Under normal conditions, cells of almost all tissue types express the same predominant canonical transcript isoform at each gene locus. In cancer, however, splicing regulation is often disturbed, leading to cancer-specific switches in the Most Dominant Transcripts (MDT).

**Methods:**
To address the pathogenic impact of these switches, we have analyzed isoform-specific protein–protein interaction disruptions in 1,209 cancer samples covering 27 different cancer types from the Pan-Cancer Analysis of Whole Genomes (PCAWG) project of the International Cancer Genomics Consortium (ICGC).

**Results:**
Our study revealed large variations in the number of cancer-specific MDT (cMDT) with the highest frequency in cancers of female reproductive organs. Interestingly, in contrast to the mutational load, cancers arising from the same primary tissue had a similar number of cMDT. Some cMDT were found in 100% of all samples in a cancer type, making them candidates for diagnostic biomarkers. cMDT tend to be located at densely populated network regions where they disrupted protein interactions in the proximity of pathogenic cancer genes. A gene ontology enrichment analysis showed that these disruptions occurred mostly in protein translation and RNA splicing pathways. Interestingly, samples with mutations in the spliceosomal complex tend to have higher number of cMDT, while other transcript expressions correlated with mutations in non-coding splice-site and promoter regions of their genes.

**Conclusion:**
This work demonstrates for the first time the large extent of cancer-specific alterations in alternative splicing for 27 different cancer types. It highlights distinct and common patterns of cMDT and suggests novel pathogenic transcripts and markers that induce large network disruptions in cancers.

**291**

L. Isenegger[1], P. Bode[2], C. Pauli[2], U. Camenisch[2], C. Matter[1], H. Moch[2], C. Britschgi[1]

**Phenotypic and Functional Validation of an in vitro Candidate Kinase Inhibitor Screen in Clear Cell Sarcoma**

*Department of Medical Oncology and Hematology, Comprehensive Cancer Center Zurich, University Hospital of Zurich, Switzerland[1], Department of Pathology and Molecular Pathology, Comprehensive Cancer Center Zurich, University Hospital of Zurich, Switzerland[2]*

**Introduction:**
Clear cell sarcoma (CCSA) is a rare aggressive soft tissue sarcoma. When localized it can be cured by surgery, however, local relapses and metastases develop frequently. CCSA is notoriously unresponsive to chemotherapy, targeted therapy or immune checkpoint inhibition, and consequently, novel therapies are desperately needed. We have performed a high-throughput small molecule screen using a candidate kinase modulator library on cultured CCSA cell lines to identify novel therapeutic approaches.

**Methods:**
The screen was performed in collaboration with NEXUS (ETH Zurich) using the ActiTarg-K library of 960 candidate kinase modulators. Two CCSA cell lines and one human fibroblast control cell line were plated on 384-well plates, cultured for 24 hrs, followed by robot-assisted addition of the library compounds in two concentrations. After 72 hrs of exposure, cell survival was assessed using a resazurin-based cell viability read-out. Methods for in vitro validation encompassed IC50 determination, long-term proliferation assays, Western blot analysis for apoptosis and autophagy markers, and fluorescent-activated cell sorting-based apoptosis assays. For target discovery, we performed an unbiased in vitro kinase screen using the KINOMEScan assay (Eurofins DiscoverX). Additionally, we performed experiments using the ProteomeProfiler Human Phospho-Kinase Array. In vivo validation is planned using CCSA xenograft models.

**Results:**
Using 960 compounds at two concentrations, we have screened six 384-well plates per cell line. Positive (doxorubicin and pazopanib) and negative controls (DMSO) were included. The Z-score was calculated as a quality control measure. This was above 0.6 on all the plates indicating very good assay quality. We performed a differential activity analysis and assigned each well a significance and effect size. Next, a cluster analysis of wells showing a significant and strong reduction of cell survival was performed in order to identify the candidate compounds with the desired therapeutic window; i.e. reduction of survival of CCSA cells, while sparing control cells. This stringent analysis workflow identified 14 compounds with the desired effect pattern, of which we have validated the 10 with the strongest effect using long-term proliferation assays. The more detailed in vitro validation was performed on 4 compounds. We determined the IC50 of the compounds using a resazurin-based readout. Apoptosis and autophagy experiments, however, did not lead to conclusive results, as the compounds did not generally induce either of the mechanisms of cell death. In parallel, we aimed at identifying the target(s) of the compounds using the KINOMEScan assay, but none on the kinases represented in the assay scored positive. On the other hand, the ProteomeProfiler Human Phospho-Kinase Array showed multiple up- and down regulated kinases pointing at multiple involved signaling pathways.

**Conclusion:**
We have successfully performed an unbiased high-throughput small molecule screen. We have validated the most promising compounds in vitro. Additionally, we have characterized the reduction of cell survival in apoptosis and autophagy assays. Next, we will validate the most promising candidate drugs in in vivo models. In parallel, we will proceed to investigate the targets by unbiased proteomics approaches. Those targets will then be validated on our collection of CCSA specimens, as well as on a dedicated CCSA tissue microarrays constructed by our international collaboration partners (Prof. Schöffski, UK Leuven and EORTC).

**292**

F. Dimitriou[2], R. Staeger[2], M. Ak[2], M. Maissen[2], K. Kudura[1], M. Barysch[2], M. Levesque[2], R. Dummer[2], J. Mangana[2], P. Cheng[2]

**Frequency, treatment and outcome of immune-related toxicities in patients with immune-checkpoint inhibitors for advanced melanoma: results form an institutional database analysis**

*Department of Nuclear Medicine, University Hospital Zurich[1], Dermatology Clinic University Hospital Zurich[2]*

**Introduction:**
Immune checkpoint inhibitors (ICI) such as anti-PD-1/PD-L1 or anti-CTLA-4 antibodies (Abs) have revolutionized the therapeutic landscape of metastatic melanoma. However, the resulting disinhibition of T-cell responses can lead to immune-related adverse events (irAEs). IrAEs are frequent and occur in up to 80% in patients treated with anti-CTLA-4 monotherapy or in combination with anti-PD-1 respectively and 60% of patients treated with anti-PD-1 or anti-PDL-1 monotherapy. Having grade 3 or 4 irAEs can lead to treatment pause or stop, thus management of these irAEs are highly crucial to patient health and treatment continuation.

**Methods:**
In this single-center retrospective cohort study, we included adult patients diagnosed with any subtype of melanoma that received ICI treatment in the adjuvant or metastatic setting (any line) in the Department of Dermatology of the University Hospital Zurich, Switzerland, from February 2011 to May 2020 with a follow-up period of at least 3 months. Date of onset, grade, irAE-directed treatment such as steroids and other immunomodulatory agents and resolution of irAEs were retrieved. Grading of irAEs was based on the Common Terminology Criteria for Adverse Events, version 5.0. In patients with an irAE, we defined the ICI treatment under which the first clinically, radiologically or histologically confirmed irAE was observed as the baseline. In patients without an irAE, the baseline was defined as the first ICI treatment.

**Results:**
A total of 257 patients, 192 (74.6%) in advanced/non-adjuvant and 65 (25.3%) in adjuvant setting with median age 63 years (range 25-92) were identified. Of these, 170 patients (66.4%) experienced some grade (1-4, CTCAEv5) of toxicity. Treatment-related toxicities were reported in fifty-four (79%%) patients with anti-PD1/anti-CTLA4, 76 (60%) with anti-PD1 and 40 (64%) with anti-CTLA4 alone. Median time to onset of irAEs was 52 days (range 0-1328). Overall, the most common treatment-related toxicities included thyroiditis (29.4%), colitis (27.6%), rash (24.7%), hepatitis (18.2%), arthritis (15.5%), hypophysitis (12.9%), pneumonitis (8.8%), vitiligo-like depigmentation (8.8%) and pancreatitis (7.6%). Other adverse events of special interest included cytokine release syndrome (CRS, 1.8%), type-1 diabetes (1.2%), encephalitis (0.6%), meningitis (0.6%), myocarditis (3.5%), myositis (0.6%), nephritis (0.6%) and uveitis (1.2%). Patients that presented with immune-related toxicities in the adjuvant setting showed no superior prognosis in regards to relapse-free survival (RFS) compared to the patients without toxicities, in the different treatment regimens ($p=0.43$ for anti-CTLA4 and $p=0.65$ for anti-PD1). Overall survival (OS) was similar between the two groups, but mOS was not reached. Nevertheless, in the non-adjuvant setting, patients with toxicities presented with more favorable PFS compared to non-toxicities in all treatment regimens ($p=0.0036$ for anti-CTLA4, $p=0.0022$ for anti-PD1 and $p<0.0001$ for anti-CTLA4/anti-PD1), which was also translated to survival benefit on OS rates. Of note, steroids and other anti-inflammatory drugs had no significant impact on survival (PFS & OS)

**Conclusion:**
In this study, patients in the non-adjuvant setting who experienced an irAE during ICI had significantly better PFS and OS compared to patients who did not. Application of steroids, anti-TNFalpha or anti-IL6 did not seem to have a negative effect on ICI efficacy. These data suggest that an irAE event could be a possible positive prognostic marker for ICI treatment.

**293**

V. Haunerdinger[2], M. Maria Domenica[3], L. Opitz[3], S. Vavassori[1], H. Dave[4], M. Hauri-Hohl[2]

**Comprehensive Identification and Quantitation of Human Thymic Epithelial Cells by Flow Cytometry.**

*Division of Immunology and Children's Research Center, University Children's Hospital, Pediatric Immunology, Zurich, Switzerland[1], Division of Stem Cell Transplantation and Children's Research Center, University Children's Hospital, Zurich, Switzerland[2], Functional Genomics Center Zurich, Swiss Federal Institute of Technology and University of Zurich, Zurich, Switzerland[3], University Children's Hospital, Division of Congenital Cardiovascular Surgery, Zurich, Switzerland[4]*

**Introduction:**
Thymic epithelial cells (TEC) are essential in supporting the lineage-commitment and proliferation of T-cell progenitors, guiding their differentiation and migration as well as providing the cues for positive and negative selection, ultimately ensuring the production of functional, self-tolerant T cells. While animal model systems have greatly aided in elucidating the contribution of stromal cells to these intricate processes, little is known about the situation in humans, mainly due to lack of suitable markers defining human TEC.

**Methods:**
Based on results from flow cytometry-based screening assays we identified and validated surface markers specific for human TEC subsets. Data from RNA-sequencing of bulk-sorted stromal cell populations was confirmed by immunofluorescence analysis. Thymi from 31 immunologically healthy children were subsequently used for quantitation of stromal cells and thymocytes.

**Results:**
We identified a panel of markers that allow the reliable and comprehensive identification and quantitation of human TEC subsets. Gene expression analysis of sorted cell populations confirmed the identity of cortical and medullary TECs and revealed their essential contribution to shaping the respective anatomical compartments with respect to structural and extracellular matrix components. In addition, quantifying TEC subsets in 31 immunologically healthy children we demonstrate gender-specific alterations of the TEC composition early in life, which impacts on the CD4-CD8-lineage choice of nascent T cells.

**Conclusion:**
The panel of markers developed in this study allows comprehensive identification, quantitation and isolation of human TECs. This will aid in assessing qualitative and numeric alterations or these essential stromal cells during development in human health and disease

**294**

F. Arnold[1], A. Kahraman[1], J. Hanimann[1], M. Nowak[1], C. Pauli[1, 2], B. Sobottka-Brillout[1], T. Karakulak[1, 2], D. Aguilera[1], H. Moch[1, 2], M. Zoche[1]

**MTPpilot: An Interactive Software-Tool for NGS Result Analyses for Molecular Tumor Boards**

*University Hospital Zurich[1], University of Zurich[2]*

**Introduction:**
Next-Generation Sequencing (NGS) cancer panels have become a key cornerstone for today's clinical decision making in oncology. In this context, NGS sequencing results are often discussed at molecular tumor boards, where amongst other oncologists, pathologists, bioinformaticians, and geneticists discuss these results to decide on the best treatment options for a patient. However, with the increasing size and complexity of NGS cancer panels, NGS results have become challenging to interpret, especially if presented merely in the form of a written report. Manual analysis of several mutations from a comprehensive NGS cancer panel is time-consuming and often incomplete.
To address these shortcomings, we developed the software Molecular Tumor Profiling Pilot (MTPpilot), which provides automated annotation, linking and interactive visualization to support the interpretation of NGS results at molecular tumor boards.

**Methods:**
MTPpilot is based on a Microsoft SQL database with a web-browser frontend implemented in PHP, HTML, and JavaScript. The SQL database holds tables for COSMIC, ClinVar, OnkoKB, ARUP and ExAC mutations to cross-check a patient's mutational profile against these databases. Metadata from UniProt, KEGG, Ensembl, GeneOntology, Protein Databank and the STRING database enrich the mutational profile with functional annotations. Target regions of most common gene panels are stored to check for concordance if multiple panels and gene tests have been run for the same patient. Optionally, MTPpilot can be connected to a local pathology database and NGS lab database to provide diagnostic pathology data and NGS history data for molecular tumor boards. To use MTPpilot in molecular tumor boards, it is sufficient to upload a patient's mutational profile in VCF or tab-delimited format to the database.

**Results:**
An overview of a patient's mutational profile is given via an ideogram, which gives a first glance of the distribution and type of alterations on human chromosomes. If provided, the values of the clinical biomarkers Microsatellite-Instability (MSI), Tumor Mutational Burden (TMB), Loss-Of-Hydrozyogcity (LOH) and Large-Scale-Transitions (LST) are provided next to the ideogram. A patient's mutational profile is separated into distinct tables for short variants, copy-number-alterations, and rearrangements. All tables provide indications for the existence of mutations in databases such as COSMIC, OncoKB, ARUP, etc. Mutations can be interactively visualized either on a SMART protein domain representation or on protein 3D structures using the MTP 3D viewer. MTPpilot also supplies an interactive fusion viewer to display gene structure and breaking points of fusion partners. Integrated with a local NGS lab database called MTPdb, MTPpilot offers an interactive tissue slide viewer for haematoxylin and eosin (H&E) stained tissue slides and a PatientMatcher to identify patients with a similar mutational profile for diagnosis, therapy and physician matching.

**Conclusion:**
Taken together, these and many other functions included in the MTPpilot software provide a user-optimized environment that aids best-informed decision makings at the weekly molecular tumor board of the USZ. This is particularly important for large comprehensive genome panels where the interactive and graphical tools allow for a deeper understanding of the patient's tumor profile.

**296**

D. Vuong[3], M. Bogowicz[3], J. Unkelbach[3], S. Hillinger[4], S. Thierstein[5], E.I. Eboulet[5], S. Peters[2], M. Pless[1], M. Guckenberger[3], S. Tanadini-Lang[3]

**A new voxel-based approach to study the relation of tumor location and overall survival in locally advanced NSCLC**

*Department of Medical Oncology, Kantonsspital Winterthur[1], Department of Oncology, Centre Hospitalier Universitaire Vaudois (CHUV)[2], Department of Radiation Oncology, University Hospital Zurich[3], Department of Thoracic Surgery, University Hospital Zurich[4], Swiss Group for Clinical Cancer Research (SAKK) Coordinating Center[5]*

**Introduction:**
The anatomical location and extension of the primary lung tumor (PT) has shown prognostic value for outcome prediction, however was often quantified manually. We present an exploratory analysis of a new voxel-based approach to predict overall survival (OS) using the PT location for locally advanced non-small cell lung cancer (NSCLC).

**Methods:**
In total, 130 NSCLC patients from a prospective Swiss multi-centric randomized trial (IIIA/N2, SAKK 16/00, neoadj. chemo- or radiochemotherapy prior to surgery) were included. Pre-treatment CT scans were registered to a reference patient CT using an ipsilateral lung contour-only based deformable image registration and the ipsilateral main bronchus as a landmark (MIM Vista, 6.9.2.). An in-house software was developed to transfer each PT to a reference patient lung while maintaining the original PT shape. Two maps were created: (1) Frequency map representing anatomical locations of the PTs and (2) frequency weighted cumulative status (fwCS) map where PT location was uni-labeled with 2 yrs OS patient status (control:-1/no control:1). Both maps were created on a second internal dataset (USZ, 28, IIIA/N2/IIIB NSCLC) to compare the cohorts. Nine anatomical non-overlapping lung regions were defined (2 cm from bronchi, heart, mediastinum and 1 cm from the chest wall divided into RL, AP and the rest lung region as peripheral). Mean fwCS values were calculated on those regions for both cohorts to identify risk areas. Additionally, from the PT regions of the internal cohort, 18 intensity features were calculated on the SAKK fwCS map. An univariate logistic regression was performed and the performance was quantified using the area under the roc curve (AUC) with the 2 yrs OS as an endpoint.

**Results:**
PT center of mass location from the in-house software agreed within +/- 3 mm Euclidean distance with the MIM software. The largest mean increase of fwCS value at 2 yrs and 5 yrs OS were observed at the heart and bronchi region for the SAKK cohort. The overlap of the maps for both cohorts is high (only 10% of PTs of the internal cohort were not covered by the SAKK cohort). At 2 yrs OS, the mean fwCS values indicate highest risk at the left-posterior chest wall for both cohorts and lowest risk for left anterior chest wall for the SAKK and heart region for the internal cohort. Univariate analysis to predict 2 yrs OS showed good performance, the best performing feature was robust mean absolute deviation (AUC = 0.75, p = 0.078).

**Conclusion:**
This explanatory analysis quantifies the value of primary tumor location for OS prediction. Additional data is needed to provide more conclusive results.

**298**

A. La Greca Saint-Esteven[2], M. Bogowicz[2], S. Tanadini-Lang[2], E. Konukoglu[1], J. van Timmeren[2]

**HPV Prediction in OPC patients by means of Deep Learning**

*Computer Vision Laboratory, ETH Zürich, Zurich, Switzerland[1], Department of Radiation Oncology, University Hospital Zurich and University of Zurich, Switzerland[2]*

**Introduction:**
Infection with human papillomavirus (HPV) is one of the most important prognostic determinants in oropharyngeal cancer (OPC). The inclusion of biomarkers such as HPV status in clinical decision-making allows for a more accurate and patient-tailored cancer treatment aimed to improve clinical outcome. Nonetheless, most biomarker assays are invasive, costly and/or time-consuming. Alternatively, radiomics constitutes a non-invasive tumor characterization tool under investigation in which high-throughput quantitative imaging features are extracted from regions of interest and posteriorly analyzed. More recently, deep learning (DL) has emerged as the state-of-the-art in many computer vision tasks including medical image classification. Convolutional Neural Networks (CNNs) are DL models capable of learning more and more abstract image patterns automatically from raw data. In the present study, we aimed to predict HPV status of advanced OPC patients using computer tomography (CT) images with a 2.5D CNN. We assessed model performance and compared it with an externally-validated radiomics model.

**Methods:**
CT images and clinical data from a total of 151 head-and-neck cancer patients (97/151 OPC patients) were retrospectively collected from our institution. Additionally, data from OPC patients from three different datasets publicly available at The Cancer Imaging Archive (TCIA) were collected. These amounted to a total of 431 subjects (OPC Radiomics collection), 68 subjects (HN1 collection) and 127 subjects (HNSCC collection). All patients had overall stage III or IV according to the AJCC 7th edition guidelines. The OPC Radiomics collection was employed together with our hospital dataset for model training (68.2% HPV+ and 31.8% HPV-), whereas the HN1 and HNSCC collections were used as independent test sets.
All CT scans and radiotherapy structure sets were resampled to the most frequent resolution in the training set (0.98 x 0.98 x 2 mm3) using cubic interpolation. A subvolume of size equal to the largest tumor in the dataset (106 x 106 x 56 voxels) was cropped on each scan, centered around the tumor. Then, 2.5D inputs were assembled by selecting the slice containing the largest tumor area per plane (axial, coronal and sagittal). The CNN consisted of the first 45 layers of the 2D Xception model, pre-trained on the ImageNet dataset. Ten-fold cross-validation (10-CV) was applied to evaluate model training performance by dividing the respective set into training (80%), validation (10%) and test (10%) sets in each fold. The model was trained using Adam optimizer with a starting learning rate of 0.001. The maximum number of epochs was set to 200. Early stopping was applied if the validation loss did not decrease during 50 epochs. On each epoch, the model was trained on a random subset of the training set to avoid over-fitting, in which minority class over-sampling was implemented to counteract class imbalance. Additionally, per epoch data augmentation (flipping in the L-R axis, small random rotations of up to ±5º, small elastic deformations, random scaling by a factor in the range of [0.9, 1.1]) was performed. At test time, soft majority voting was applied to predict HPV status.

**Results:**
The proposed model achieved a final area under receiver operating characteristic curve (AUC) of 0.81 (95%CI: 0.79 - 0.84) and accuracy of 0.77 (95%CI: 0.73 - 0.80) on the training dataset. After soft majority voting, AUC/PPV/NPV/accuracy values of 0.76/0.72/0.76/0.75 and 0.86/0.78/0.56/0.75 were achieved on the HN1 and HNSCC external test sets, respectively. Our model outperformed the radiomics model presented in (Bogowicz et al., 2020), which obtained an AUC of 0.82 (95%CI: 0.71 - 0.94) on the HNSCC dataset.

**Conclusion:**
DL was successfully applied to predict HPV status in CT of advanced OPC patients, with the proposed model achieving comparable and even superior performance to an externally validated radiomics model.

**299**

H. Gabrys[3], L. Basler[3], S. Hogan[1], M. Pavic[3], M. Bogowicz[3], D. Vuong[3], S. Tanadini-Lang[3], R. Förster[3], M. Huellner[2], R. Dummer[1], M. Guckenberger[3], M. Levesque[1]

**Radiomics for prediction of metastatic melanoma patient survival after immunotherapy**

*University Hospital Zurich, Department of Dermatology, Zurich, Switzerland[1], University Hospital Zurich, Department of Nuclear Medicine, Zurich, Switzerland[2], University Hospital Zurich, Department of Radiation Oncology, Zurich, Switzerland[3]*

**Introduction:**
Immune checkpoint inhibition achieved substantial improvements in survival of metastatic melanoma patients; however, reliable biomarkers for patient selection are lacking. This study aims to assess the predictive potential of PET/CT-based radiomics for modeling patient overall survival (OS) in metastatic melanoma patients receiving checkpoint inhibitors.

**Methods:**
A retrospective single-institution cohort of 112 patients with metastatic melanoma was the basis of this study. Patients were treated with either single-checkpoint-inhibition using anti-PD-1-antibodies or dual-checkpoint-inhibition in combination with anti-CTLA-4-antibodies. PET/CT imaging was done before the treatment (TP0) and at 3 months after the treatment initiation (TP1). All individual metastases (n=716) were segmented on all images for calculation of radiomic features (n=172) describing shape, intensity, and texture of the metastases. To perform the analysis on a patient level, radiomic features extracted from multiple lesions were aggregated via weighted arithmetic mean, where the weight corresponded to a lesion volume. Logistic regression models were built using the data available at TP0 and delta-radiomic features calculated between TP0 and TP1. The performance metric was the area under the receiver operating characteristic curve (AUC). The generalization performance of the models was estimated with a nested cross-validation (inner loop: 10-times-repeated 10-fold cross-validation, outer loop: 10-times-repeated 5-fold cross-validation). Model calibration was evaluated with calibration curves and the Brier score. The radiomic models were benchmarked against models based only on metastases volume.

**Results:**
The OS at 12 and 36 months was 84% and 55%, respectively. Prognostic models based on radiomic features achieved AUCs of 0.87 +/- 0.08 and 0.74 +/- 0.13 at 12 and 36 months, respectively. Volume-based models performed slightly worse with AUCs of 0.83 +/- 0.15 and 0.71 +/- 0.13, at 12 and 36 months, respectively. Furthermore, the radiomics models were more stable and better calibrated than the volume-based models. Inclusion of PET-based radiomic features did not improve performance of radiomic models in either of the investigated scenarios. Considering only the largest lesion instead of the weighted mean of all lesions resulted in AUC scores smaller by 0.16 on average.

**Conclusion:**
Radiomic features, considering all metastases in one patient from baseline imaging and follow-up imaging at 3 months, allow for accurate prediction of survival in metastatic melanoma patients at 12 and 36 months after treatment with immune checkpoint-inhibitors.

**300**

J. van Timmeren[1], M. Bogowicz[1], M. Chamberlain[1], S. Ehrbar[1], R. Dal Bello[1], H. Garcia Schüler[1], J. Krayenbuehl[1], L. Wilke[1], N. Andratschke[1], M. Guckenberger[1], S. Tanadini-Lang[1], P. Balermpas[1]

## Adaptive radiotherapy for head and neck cancer – evaluation of volume changes and migration of salivary glands

*University Hospital of Zurich and University of Zurich[1]*

**Introduction:**
The aim of this study was to evaluate volume changes and migration of parotid glands and submandibular glands in head-and-neck cancer (HNC) patients receiving magnetic resonance imaging (MRI)-guided adaptive radiotherapy.

**Methods:**
HNC patients receiving MRI-guided radiotherapy on the ViewRay MRIdian Linac were included. All patients received 35 fractions of 2 Gy daily, resulting in a total of 70 Gy to the macroscopic tumor, 60 Gy to the involved nodal levels and 50 Gy for elective nodal irradiation. Every week an offline plan-adaptation was performed based on the actual MR-treatment Image. The glands' volume and inter-gland distances were evaluated. Distances were calculated using the geometrical centers of the glands. Wilcoxon signed-rank test was used to evaluate the values with respect to baseline, and p-values below 0.05 were considered significant.

**Results:**
Ten patients were included into the analysis. The mean [range] change in parotid volume was -9.5% [-29.7 – 7.2] after one week of treatment ($p<0.0001$), and -32.4% [-47.5 - -14.5] after five weeks ($p<0.0001$). For the submandibular glands, this was -8.7% [-23.8 – 10.4] after one week ($p=0.0035$) and -26.4% [-49.4 – 9.3] after five weeks ($p=0.0003$). Linear regression showed an average decrease of 0.20 mL per day and 0.05 mL per day for parotids and submandibular glands, respectively. Inter-parotid distance changed on average by -4.9% [-8.1% - -1.0%] after five weeks ($p=0.0020$). The inter-submandibular gland distance did not change significantly.

**Conclusion:**
We observed significant volume reduction of parotid glands and submandibular glands during the course of radiotherapy, and significant migration of the parotids. This stresses the importance of plan adaptation during treatment. To this extend, weekly adaptation using MR-linac technology is a feasible approach to avoid excessive irradiation of these important salivary glands and the impact on xerostomia will be investigated in a future study.

# Information

**Wann**
Donnerstag, 15. April 2021
8.00 – 14.45 Uhr

**Kontakt**
Universitätsspital Zürich
Direktion Forschung und Lehre
Rämistrasse 100
8091 Zürich

+41 43 253 01 10
dfl@usz.ch
www.usz.ch

**Veranstalter**
Universitätsspital Zürich
Direktion Forschung und Lehre

**Anmeldung und Teilnahme**
Es ist keine Anmeldung nötig.
Die Teilnahme ist kostenlos.
Die Veranstaltung findet online statt.
Die Beiträge werden im Anschluss an die Veranstaltung online aufgeschaltet.

**Informationen und Abstracts**
Link

**Online-Link zur Teilnahme**
Link

Wir bedanken uns bei den Forschenden auf dem Titelblatt für die zur Verfügung gestellten Fotos.

Folgen Sie dem USZ unter

03.21